Bukti Publikasi Artikel di Theoretical Chemistry Accounts

Febdian Rusydi, S.T., M.Sc., Ph.D.
NIP. 19790206 200801 1 004

Daftar Bukti:

1. Dewan Editorial Jurnal
2. Daftar Isi Volume 140, Issue 7
3. Submit dan Draf Manuskrip
4. Review Manuskrip
    - Komentar Reviewer
    - Pertanyaan dan Jawaban
    - Revisi Draf Manuskrip
5. Manuskrip Diterima
6. Artikel Terbit
    - Persiapan Terbit
    - Persetujuan Terbit
    - Artikel

1. Dewan Editorial Jurnal

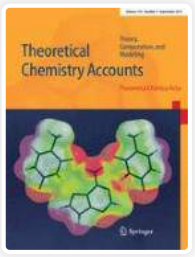

Theoretical Chemistry Accounts
Theory, Computation, and Modeling

Editors

Computational Biomedicine
Forschungszentrum Jülich
Jülich, Germany
p.carloni@fz-juelich.de

Mark E. Casida
Institut de Chimie Moleculaire de Grenoble
Université Joseph Fourier
Grenoble, France
mark.casida@ujf-grenoble.fr

Benoît Champagne
Facultés Université Notre Dame
de la Paix Namur
Namur, Belgium
benoit.champagne@fundp.ac.be

Henry Chermette
Institut des Sciences et Analytiques
Université Claude Bernard Lyon-1
Villeurbanne, France
cherm@ipnl.in2p3.fr

Michael A. Collins
Research School of Chemistry
Australian National University
Canberra, ACT, Australia
collins@rsc.anu.edu.au

Sonia Coriani
Università Degli Studi di Trieste
Department of Chemical and Pharmaceutical Sciences
Trieste, Italy
coriani@units.it

Clemence Corminboeuf
École Polytechnique Féderale de Lausanne
Laboratory for Computational Molecular Design
Lausanne, Switzerland
clemence.corminboeuf@epfl.ch

Gino A. DiLabio
National Institute for Nanotechnology
National Research Council
Edmonton, Alberta, Canada
Gino.DiLabio@nrc-cnrc.gc.ca

Masahiro Ehara
Institute for Molecular Science
Research Center for Computational Science
Okazaki, Japan
ehara@ims.ac.jp

Pedro Alexandrino Fernandes
Department of Chemistry and Biochemistry
University of Porto
Porto, Portugal
pafernan@fc.up.pt

Laura Gagliardi
University of Minnesota
Department of Chemistry
Minneapolis, MN, USA
gagliard@umn.edu

Leticia González
Institute of Theoretical Chemistry
University of Vienna
Vienna, Austria
leticia.gonzalez@univie.ac.at

Hua Guo
Department of Chemistry and Chemical Biology
University of New Mexico
Albuquerque, NM, USA
hguo@unm.edu

Jeremy Harvey
KU Leuven
Department of Chemistry
Heverlee, Belgium
jeremy.harvey@chem.kuleuven.be

So Hirata
Department of Chemistry
University of Illinois
at Urbana-Champaign
Urbana, IL, USA
sohirata@illinois.edu

Francesc Illas Riera
Departament de Quimica Fisica & IQTCUB
Universitat de Barcelona
Barcelona, Spain
francesc.illas@ub.edu

Annia Galano Jiménez
Departemento de Química
Universidad Autónoma Metropolitana
México, Mexico
agal@xanum.uam.mx

Erin Johnson
Department of Chemistry
Dalhousie University
Halifax, Canada
Erin.Johnson@Dal.Ca

Martin Kaupp
Technische Universität Berlin
Institut für Chemie
Berlin, Germany
martin.kaupp@tu-berlin.de

Carmay Lim
Institute of Biomedical Sciences
Academia Sinica
Taipei, Taiwan 11529
carmay@gate.sinica.edu.tw

José M. Lluch
Departamento de Química
Universitat Autònoma de Barcelona
Bellaterra (Barcelona), Spain
lluch@klingon.uab.es

F. Javier Luque
Unitat Fisicoquimica
Facultat de Farmacia
Universitat de Barcelona
Barcelona, Spain
fjluque@ub.edu

Neepa Maitra
Hunter College of the City University of New York
Dept. Of Physics and Astronomy
New York, USA
nmaitra@hunter.cuny.edu

Jan M.L. Martin
Department of Chemistry
Weizmann Institute of Science
Rehovot, Israel
gershom@Weizmann.ac.il

Benedetta Mennucci
Dipartimento di Chimica e Chimica Industriale
Università di Pisa
Pisa, Italy
bene@dcci.unipi.it

Fernando R. Ornellas
Universidade de São Paulo
Instituto de Química
Departmento de Química Fundamental
São Paulo, São Paulo, Brazil
frornell@usp.br

Gianfranco Pacchioni
Dipto. di Scienza dei Materiali
Università di Milano-Bicocca
Milano, Italy
gianfranco.pacchioni@unimib.it

Markus Reiher
ETH Zürich
Laboratory of Physical Chemistry
Zürich, Switzerland
markus.reiher@phys.chem.ethz.ch

Andreas Savin
Université Pierre et Marie Curie (Paris 6)
Paris, France
andreas.savin@lct.jussieu.fr

Zhigang Shuai
Department of Chemistry
Tsinghua University
Beijing, China
zgshuai@tsinghua.edu.cn

J. Ilja Siepmann
Department of Chemical Engineering
and Materials Science
University of Minnesota
Minneapolis, MN, USA
siepmann@umn.edu

Miquel Solà
Institute of Computational Chemistry and Catalysis
University of Girona
Girona, Spain
miquel.sola@udg.edu

Mark E. Tuckerman
Department of Chemistry and Courant
Institute of Mathematical Sciences
New York University
New York, NY, USA
mark.tuckerman@nyu.edu

Christoph van Wüllen
TU Kaiserslautern, FB Chemie
Kaiserslautern, Germany
vanwullen@chemie.uni-kl.de

Xin Xu
Fudan University
Dept. Of Chemistry
Shanghai, China
xxchem@fudan.edu.cn

Jinlong Yang
Department of Chemial Physics
University of Science and Technology of China
Hefei, Anhui, China
jlyang@ustc.edu.cn

Xiao Cheng Zeng
Department of Chemistry
University Nebraska-Lincoln
Lincoln, NE, USA
xzeng@unl.edu

Chang-Guo Zhan
College of Pharmacy
Dept. Pharmaceutical Sciences
University of Kentucky
Lexington, KY, USA
zhan@uky.edu

Explore

Volumes and issues

Collections

Sign up for alerts

Springer

Publish with us

Authors & Editors

Journal authors

Publishing ethics

Open Access & Springer

Discover content

SpringerLink

Books A-Z

Journals A-Z

Video

Other services

Instructors

Librarians (Springer Nature)

2. Daftar Isi Volume 140, Issue 7

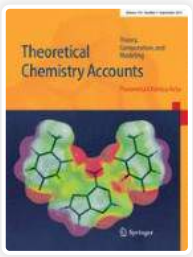

Theoretical Chemistry Accounts

Theory, Computation, and Modeling

Volume 140, issue 7, July 2021

22 articles in this issue

Recognition of the three-dimensional structure of small metal nanoparticles by a supervised artificial neural network

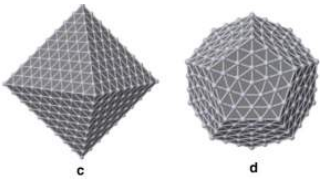

Timothée Fages, Franck Jolibois & Romuald Poteau

Regular Article | Published: 01 July 2021 | Article: 98

This is part of 2 collections

Ab initio calculation of the excited states of nitropyrenes

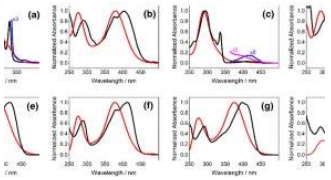

Qian Chen, Farhan Siddique ... Adelia J. A. Aquino

Regular Article | Published: 26 June 2021 | Article: 97

Perturbation approach to constrained electron transfer in density functional theory

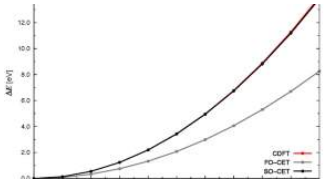

Javier Carmona-Espíndola & José L. Gázquez

Regular Article | Published: 25 June 2021 | Article: 96

This is part of 2 collections

Implementation of the parallel-tempering molecular dynamics method in deMon2k and application to the water hexamer

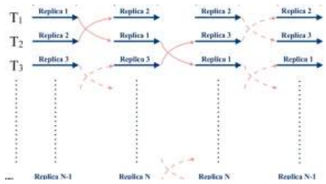

Fernand Louisnard, Gerald Geudtner ... Jérôme Cuny

Regular Article | Published: 24 June 2021 | Article: 95

This is part of 2 collections

O—H and C—H bond dissociations in non-phenyl and phenyl groups: A DFT study with dispersion and long-range corrections

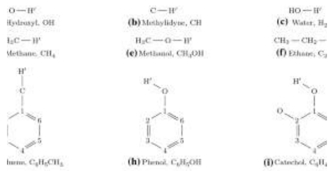

Lusia Silfia Pulo Boli, Febdian Rusydi ... Hermawan Kresno Dipojono

Regular Article | Published: 21 June 2021 | Article: 94

Intermediate complexes and activation energy for the Cl(^{2}P) + SiH_4 hydrogen abstraction reaction: a difficult case

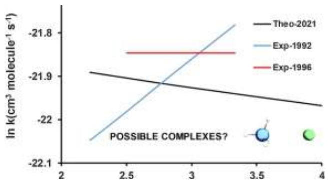

J. Espinosa-Garcia & J. C. Garcia-Bernaldez

Regular Article | Published: 19 June 2021 | Article: 93

Theoretical insight on the structural and electronic properties of $(PdH)_N$ (N = 10–35) clusters

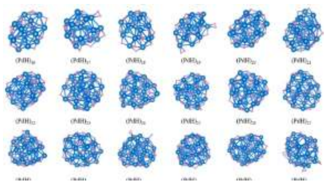

Qi Luo, Xiangyu Guo ... Shiping Huang

Regular Article | Published: 16 June 2021 | Article: 92

Optical properties of $Ag_{29}(BDT)_{12}(TPP)_4$ in the VIS and UV and influence of ligand modeling based on real-time electron dynamics

)

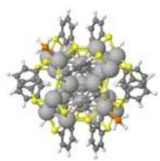

(2)

Rajarshi Sinha-Roy, Xóchitl López-Lozano ... Hans-Christian Weissker

Regular Article | Published: 15 June 2021 | Article: 91

This is part of 2 collections

Quantum chemical investigation of the ground- and excited-state acidities of a dihydroxyfuranoflavylium cation

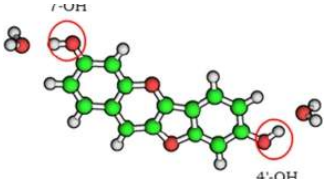

Jing Cui, Farhan Siddique ... Adelia J. A. Aquino

Regular Article | Published: 14 June 2021 | Article: 90

Radical cation transfer in a guanine pair: an insight to the G-quadruplex structure role using constrained DFT/MM

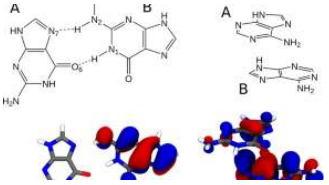

Ranjitha Ravindranath, Padmabati Mondal & Natacha Gillet

Regular Article | Published: 12 June 2021 | Article: 89

This is part of 2 collections

Correction to: Multiresolution non-covalent interaction analysis for ligand–protein promolecular electron density distributions

L. Leherte

Correction | Published: 12 June 2021 | Article: 88

Parallelization of deMon2k: an overview

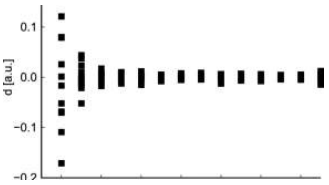

Gerald Geudtner

Regular Article | Published: 11 June 2021 | Article: 87

This is part of 2 collections

Effect of temperature on the structure of Pd_8 and Pd_7Au_1 clusters: an Ab initio molecular dynamics approach

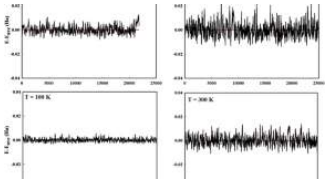

Analila Luna-Valenzuela, José Luis Cabellos & Alvaro Posada-Amarillas

Regular Article | Published: 10 June 2021 | Article: 86

This is part of 2 collections

Exploring energy landscapes at the DFTB quantum level using the threshold algorithm: the case of the anionic metal cluster Au_{20}^-

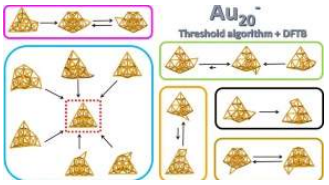

Mathias Rapacioli, J. Christian Schön & Nathalie Tarrat

Regular Article | Published: 10 June 2021 | Article: 85

This is part of 2 collections

Molecular dynamics simulations of sodium nanoparticle deposition on magnesium oxide

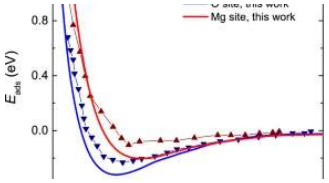

Yannick Fortouna, Pablo de Vera ... Andrey V. Solov'yov

Regular Article | Published: 10 June 2021 | Article: 84

This is part of 2 collections

A molecular electron density theory study of the [3 + 2] cycloaddition reaction of nitronic ester with methyl acrylate

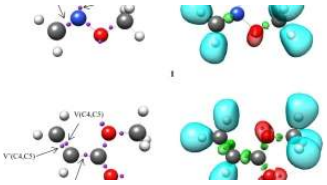

Haydar A. Mohammad-Salim

Regular Article | Published: 09 June 2021 | Article: 83

G_0W_0 based on time-dependent auxiliary density perturbation theory

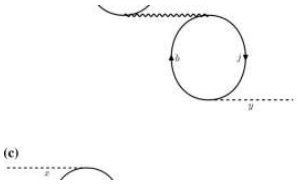

J. Villalobos-Castro, B. A. Zúñiga-Gutiérrez & R. Flores-Moreno

Regular Article | Published: 09 June 2021 | Article: 82

This is part of 2 collections

A comprehensive investigation of structural features, electron delocalization, optoelectronic and anti-corrosion characteristics in furan oligomers by DFT/TDDFT method

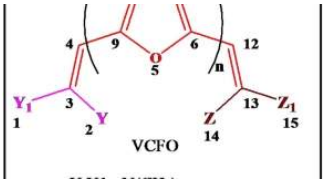

D. Gajalakshmi, V. Tamilmani & M. Jaccob

Regular Article | Published: 08 June 2021 | Article: 81

Which triel bond is stronger? TrHX···H_2Y versus TrH_2X···H_2Y (Tr = Ga, In; X = F, Cl, Br, I; Y = O, S)

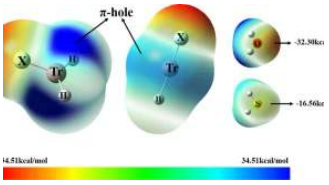

Xiaoting Wang, Yuchun Li ... Hongyan Wang

Regular Article | Published: 08 June 2021 | Article: 80

Growth of rare gases on coronene

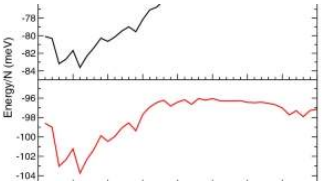

Esther García-Arroyo, Marta I. Hernández ... José Bretón

Regular Article | Published: 07 June 2021 | Article: 79

This is part of 2 collections

CO_2 electrochemical reduction to methane on transition metal porphyrin nitrogen-doped carbon material M@d-NC: theoretical insight

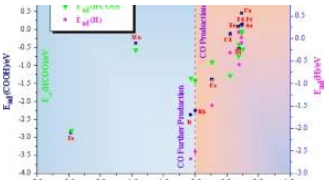

Sibei Guo

Regular Article | Published: 04 June 2021 | Article: 78

Femtosecond responses of hydrated DNA irradiated by ionizing rays focus on the sugar-phosphate part

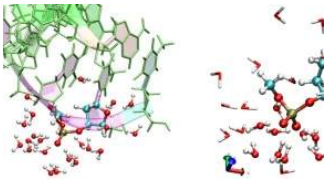

Aurélien de la Lande

Regular Article | Published: 03 June 2021 | Article: 77

This is part of 2 collections

You have access to our articles

For authors

Submission guidelines

Manuscript editing services

Ethics & disclosures

Open Access fees and funding

Contact the journal

Calls for papers

Submit manuscript

Working on a manuscript?

Avoid the most common mistakes and prepare your manuscript for journal editors.

Learn more →

Explore

Volumes and issues

Collections

Sign up for alerts

3. Submit dan Draf Manuskrip

Gmail Lusia silfia <lusiasilfia@gmail.com>

TCAC-D-20-00473 - Submission Notification to co-author - [EMID:5440ec9b531a5c8d]

Theoretical Chemistry Accounts (TCAC) <em@editorialmanager.com> 17 Desember 2020 18.30
Balas Ke: "Theoretical Chemistry Accounts (TCAC)" <saranya.sekar@springernature.com>
Kepada: Lusia Silfia Pulo Boli <lusiasilfia@gmail.com>

Re: "O-H and C-H bond dissociations in non-phenyl and phenyl groups: A DFT study with dispersion and long-range corrections"
Full author list: Lusia Silfia Pulo Boli, Master; Febdian Rusydi, Doctoral; Vera Khoirunisa, Master; Ira Puspitasari, Doctoral; Heni Rachmawati, Doctoral; Hermawan Kresno Dipojono, Doctoral

Dear Ms. Pulo Boli,

We have received the submission entitled: "O-H and C-H bond dissociations in non-phenyl and phenyl groups: A DFT study with dispersion and long-range corrections" for possible publication in Theoretical Chemistry Accounts, and you are listed as one of the co-authors.

The manuscript has been submitted to the journal by Dr. Mr. Febdian Rusydi who will be able to track the status of the paper through his/her login.

If you have any objections, please contact the editorial office as soon as possible. If we do not hear back from you, we will assume you agree with your co-authorship.

Thank you very much.

With kind regards,

Springer Journals Editorial Office
Theoretical Chemistry Accounts

Our flexible approach during the COVID-19 pandemic

If you need more time at any stage of the peer-review process, please do let us know. While our systems will continue to remind you of the original timelines, we aim to be as flexible as possible during the current pandemic.

This letter contains confidential information, is for your own use, and should not be forwarded to third parties.

Recipients of this email are registered users within the Editorial Manager database for this journal. We will keep your information on file to use in the process of submitting, evaluating and publishing a manuscript. For more information on how we use your personal details please see our privacy policy at https://www.springernature.com/production-privacy-policy. If you no longer wish to receive messages from this journal or you have questions regarding database management, please contact the Publication Office at the link below.

In compliance with data protection regulations, you may request that we remove your personal registration details at any time. (Use the following URL: https://www.editorialmanager.com/tcac/login.asp?a=r). Please contact the publication office if you have any questions.

Theoretical Chemistry Accounts

O-H and C-H bond dissociations in non-phenyl and phenyl groups: A DFT study with dispersion and long-range corrections

--Manuscript Draft--

Manuscript Number:	TCAC-D-20-00473
Full Title:	O-H and C-H bond dissociations in non-phenyl and phenyl groups: A DFT study with dispersion and long-range corrections
Article Type:	Regular Article
Keywords:	O—H and C—H dissociations; non-phenyl and phenyl groups; Density functional theory; dispersion correction; long-range correction
Corresponding Author:	Febdian Rusydi, Ph.D Universitas Airlangga Surabaya, Jawa Timur INDONESIA
Corresponding Author Secondary Information:	
Corresponding Author's Institution:	Universitas Airlangga
Corresponding Author's Secondary Institution:	
First Author:	Lusia Silfia Pulo Boli, Master
First Author Secondary Information:	
Order of Authors:	Lusia Silfia Pulo Boli, Master
	Febdian Rusydi, PhD
	Vera Khoirunisa, Master
	Ira Puspitasari, PhD
	Heni Rachmawati, PhD
	Hermawan Kresno Dipojono, PhD
Order of Authors Secondary Information:	
Funding Information:	
Abstract:	Hydrogen atom transfer is one important reaction in biological system, in industry, and in atmosphere. The reaction is preluded by hydrogen bond dissociation. To gain a comprehensive understanding on the reaction, it is necessary to investigate how the current computational methods model hydrogen bond dissociation. As the starting point, we utilized density functional theory-based calculations to identify the effect of dispersion and long-range corrections on O—H and C—H dissociation in non-phenyl and phenyl groups. We employed five different methods, namely B3LYP, CAM-B3LYP (long-range correction), M06-2X, and B3LYP and CAM-B3LYP with the D3 version of Grimme's dispersion. The results showed that for the case of O—H dissociation in two member of phenyl groups, namely phenol and catechol, the dispersion correction's effect is negligible but the long-range correction's effect is significant. The significant effect was shown by the increasing of the energy barrier and the shortening of O—H interatomic distance in the transition state. Therefore, we suggest one should consider the long-range correction in modeling hydrogen bond dissociation in phenolic compounds, namely phenol and catechol.
Suggested Reviewers:	Nadhratun Naiim Mobarak, PhD Senior Lecturer (Chemistry), Universiti Kebangsaan Malaysia nadhratunnaiim@ukm.edu.my She is an experimentalist. Her expertise is in polymer electrolyte. Thus, she can criticize this manuscript from experimental point of view.
	Allan Abraham Padama, PhD

	Head of Physics Division, University of the Philippines Los Banos abpadama@up.edu.ph His expertise is in first-principles study. Thus, he can give valuable critics to this manuscript.
	Yuji Kunisada, PhD Assistant Professor, Hokkaido University Faculty of Engineering kunisada@eng.hokudai.ac.jp His expertise is in first-principles study. Thus, he can give valuable critics to this manuscript.
	Ryo Kishida, PhD Assistant Professor, Kyushu University kishida@dent.kyushu-u.ac.jp His expertise is in first-principles study. Thus, he can give valuable critics to this manuscript.
	Tamio Oguchi, PhD Professor, Institute of Scientific and Industrial Research, Osaka University oguchi@sanken.osaka-u.ac.jp His expertise is Electron Theory of Condensed Matter System. Thus, he can give valuable critics to this manuscript.

Theoretical Chemistry Accounts manuscript No.
(will be inserted by the editor)

O—H and C—H bond dissociations in non-phenyl and phenyl groups: A DFT study with dispersion and long-range corrections

Lusia Silfia Pulo Boli[2,3] · **Febdian Rusydi**[1,2] · **Vera Khoirunisa**[2,4] · **Ira Puspitasari**[2,5] · **Heni Rachmawati**[6,7] · **Hermawan Kresno Dipojono**[3]

Received: date / Accepted: date

Abstract Hydrogen atom transfer is one important reaction in biological system, in industry, and in atmosphere. The reaction is preluded by hydrogen bond dissociation. To gain a comprehensive understanding on the reaction, it is necessary to investigate how the current computational methods model hydrogen bond dissociation. As the starting point, we utilized density functional theory-based calculations to identify the effect of dispersion and long-range corrections on O—H and C—H dissociation in non-phenyl and phenyl groups. We employed five different methods, namely B3LYP, CAM-B3LYP (with long-range correction), M06-2X, and B3LYP and CAM-B3LYP with the D3 version of Grimme's dispersion. The results showed that for the case of O—H dissociation in two member of phenyl groups, namely phenol and catechol, the dispersion correction's effect is negligible but the long-range correction's effect is significant. The significant effect was shown by the increasing of energy barrier and the shortening of O—H interatomic distance in the transition state. Therefore, we suggest one should consider the long-range correction in modeling hydrogen bond dissociation in phenolic compounds, namely phenol and catechol.

Keywords O—H and C—H dissociations · non-phenyl and phenyl groups · density functional theory · dispersion correction · long-range correction

✉Febdian Rusydi
rusydi@fst.unair.ac.id

[1] Department of Physics, Faculty of Science and Technology, Universitas Airlangga, Jl. Mulyorejo, Surabaya 60115, Indonesia.

[2] Research Center for Quantum Engineering Design, Faculty of Science and Technology, Universitas Airlangga, Jl. Mulyorejo, Surabaya 60115, Indonesia

[3] Department of Engineering Physics, Faculty of Industrial Engineering, Institut Teknologi Bandung, Bandung 40132, Indonesia

[4] Engineering Physics Study Program, Institut Teknologi Sumatera, Jl. Terusan Ryacudu, Lampung Selatan 35365, Indonesia

[5] Information System Study Program, Faculty of Science and Technology, Universitas Airlangga, Jl. Mulyorejo, Surabaya 60115, Indonesia

[6] School of Pharmacy, Institut Teknologi Bandung, Jl. Ganesha 10, Bandung 40132, Indonesia

[7] Research Center for Nanoscience and Nanotechnology, Institut Teknologi Bandung, Jl. Ganesha 10, Bandung 40132, Indonesia

1 Introduction

Hydrogen atom transfer is one important reaction that occurs in various environments: the biological systems, the atmosphere, and the industry. In biological systems, the reaction takes place in lipid peroxidation formation [1,2] and its prevention, [3–8] as well as in free radicals formation [9]. In the atmosphere, the reaction involves hydroxyl radical (OH) and organic or inorganic materials [10,11]. Meanwhile in industry, one way the reaction occurs is in the presence of a catalyst [12,13]. Overall, the reaction has been a subject of experimental and computational studies. However, there is still a need to understand how the current computational methods can model hydrogen bond dissociation. This understanding will help to achieve a comprehensive insight into the hydrogen atom transfer reaction.

Numerous publications have reported the usage of computational methods based on density functional the-

ory (DFT) to investigate hydrogen bond dissociation. One quantity describing the hydrogen bond dissociation is bond dissociation energy (BDE). In 1999, Barckholtz et al. reported the use of one DFT functional, B3LYP, to predict C−H BDE of small aromatics. The predictions were in agreement with the available experimental values [14]. In the following years, the functional was used to predict the BDE of various bonds in small and large molecules [15–17]. On the other hand, other publications showed that B3LYP has low accuracy [18–20] but is reliable to predict the substituent effect such as in alkyl and peroxyl radicals [18]. In 2008, Zhao and Truhlar introduced DFT functional from the Minnesota family, M06-2X. This functional has much-improved accuracy in predicting BDE [21]. M06-2X is reliable for various cases, such as predicting substituent effects on O−C and C−C BDE of lignin [22] and predicting BDE of polyphenols in various solvents [23]. The DFT used for the above prediction was unrestricted [15, 22]. In addition to B3LYP and M06-2X, Du et al. used CAM-B3LYP, which includes a long-range correction to B3LYP, in their calculations. They found that CAM-B3LYP underestimates O−CH_3 BDE relative to experimental values. However, this functional has better performance for aromatic molecules than for non-aromatic molecules [24]. Even though many references have reported the use of various DFT functionals for predicting BDE, there is still limited references reported about the path taken by hydrogen atom during the bond dissociation. The use of functionals to model the path is necessary to gain insight into the hydrogen atom transfer reactions. Thus, the present work investigates the effect of dispersion and long-range corrections in O−H and C−H bond dissociation. The corrections have been integrated into DFT functional. Therefore, it is necessary to use DFT to identify the effect of dispersion and long-range correction on O−H and C−H bond dissociation.

This work aims to study the effects of dispersion and long-range corrections on the O-H and C-H bond dissociation computationally. We utilize DFT with three functionals combined with the D3 version of Grimme's dispersion. The combination is five methods: B3LYP that has been used for chemical computation, CAM-B3LYP that includes a long-range correction, B3LYP-GD3 and CAM-B3LYP-GD3 which includes Grimme's dispersion, and M06-2X that has a good performance for noncovalent interactions [25–28]. The dissociation is designed to occur at O-H and C-H bonds of six non-phenyl and three phenyl groups. The phenyl groups containing O-H bonds are chosen to represent the phenolic compounds. To achieve the goal, we calculate bond dissociation energy and build hydrogen dissociation pathways using two techniques: a relaxed scan calculation and a geometry optimization in the ground and transition states. We have used these two techniques to study other chemical reactions [29–32]. This study will answer the following question: What are the effects of the dispersion and long-range corrections on the O-H and C-H dissociations of non-phenyl and phenyl groups?

2 Computational models

2.1 Reaction model

Scheme 1 presented our model for the hydrogen dissociation. The reactant was R−H′ possessing O−H, or C−H, bond; the products were R and a hydrogen atom. There were nine molecules of interest for R−H′, which were (a) hydroxyl, (b) methylidyne, (c) water, (d) methane, (e) methanol, (f) ethane, (g) toluene, (h) phenol, and (i) catechol. Figure 1 presented the Kekulé structure of these molecules.

$$\underset{\text{[in.]}}{\text{R}-\text{H}'} \longrightarrow \underset{\text{[fi.]}}{\text{R} + \text{H}'}$$

Scheme 1: The initial state [in.] and the final state [fi.] of the reaction model.

[Fig. 1 about here.]

2.2 DFT calculations

We performed computational techniques with the basis of DFT [33,34]. We used 6-311++G(d,p) basis set with three different XCs; they were (1) B3LYP, (2) CAM-B3LYP, and (3) M06-2X which were implemented in Gaussian 16 software [35]. The first XC has been a standard functional for a geometry structure study, while the second XC has improved the long-range interaction of the first XC. The third XC has been parameterized, such that noncovalent interactions take into account. We applied the D3 version of Grimme's dispersion to accommodate the dispersion effect along the dissociation pathways. We combined the XCs and the dispersion into five different methods, as shown in Table 1. In addition to DFT, we used Natural Bond Orbital (NBO) calculations for the natural hybrid orbital and charge population analysis [36].

[Table 1 about here.]

The procedure for DFT calculations is as follows. First, we validated that the three XCs were capable to

obtain the spin-state and the geometry in the ground state. For this purpose, we chose hydroxyl and phenol because they represented molecules with odd and even number of electrons and because their experimental results were available. Second, we performed a geometry optimization to obtain the geometry of all molecules of interest in the ground state using the five calculation methods. To obtain bond dissociation energy (BDE) of hydrogen, we coupled DFT with frequency calculations. It resulted in the total electronic energy with thermal correction to enthalpy at 298.15 K in the ground state. BDE was the enthalpy difference between the final and the initial states in Scheme 1. Third, we constructed the hydrogen dissociation pathways.

We employed two different computational techniques for the third DFT calculations procedure. The first technique was a relaxed scan calculation, where one hydrogen atom (with prime mark in Figure 1) left oxygen or carbon atom of R and let R relaxed. The increments were set to be 0.2 Å for all methods. The second one was based on the geometry optimization in the ground and transition states. We applied the first technique to the selected non-phenyl and phenyl groups. The value of BDE that was affected and was not affected by dispersion and/or long-range corrections became the restriction in selecting molecules in the first technique. The first technique resulted in potential energy curve (PEC) and the dissociation pathway was visualized using a polar coordinate. We emphasized that the pathway that led to other than hydrogen dissociation would not be discussed further. The PEC that was affected by dispersion and/or long-range corrections became the restriction to select molecules in the second technique. The second technique yielded a dissociation pathway in energy level diagrams (ELD). We have successfully applied both techniques in our previous studies for bigger molecules [29–32].

We excluded PEC results from M06-2X in the current study because it produced unreasonable results. We also noted that Mardirossian and Head-Gordon [37] reported a similar case, where M06-2X poorly predicted the bond length of krypton dimer and benzene-silane dimer through their potential energy curves.

3 Results and discussion

3.1 The ground state structures

Spin-state and geometry The geometry optimization using the three XCs obtained the doublet and singlet as the lowest in energy level for hydroxyl and phenol, respectively. On average, the doublet was 4.6 eV lower than the quartet (in hydroxyl); while the singlet was 4.2 eV lower than the triplet (in phenol). The doublet and the singlet were more stable compared to the quartet and the triplet. The results agree with the ground spin-states of hydroxyl and phenol reported in references [38, 39]. Furthermore, the selected geometrical parameters of hydroxyl and phenol in those spin-states were less than 0.017 Å and 1.4 degrees (see Table 2). The values were within the accuracy limit for DFT calculations [40]. Therefore, the three XCs were capable to obtain the correct ground state structure of the molecules with odd or even number of electrons. Based on these results, the same XCs were used to obtain the ground spin-state of other molecules with an odd and even numbers of electrons which were doublet and singlet, respectively.

[Table 2 about here.]

The dispersion and long-range corrections Table 3 presents O−H′ and C−H′ bond lengths of the obtained ground state geometry of all molecules of interest. The Cartesian coordinates of the ground state geometry were given in Table S1-S9 of Supplementary Information (SI). Calculation using the method with dispersion correction (M2 and M4) obtained the same bond length as the method without the correction (M1 and M3). The method with the long-range correction (M3) and the method parameterized with dispersion-like interaction (M5) obtained slightly shorter bond lengths (the negative values) than the method without the correction (M1). The results suggest the dispersion and the long-range corrections do not alter the ground state O−H′ and C−H′ bond lengths of our molecules of interest.

[Table 3 about here.]

3.2 The bond dissociation energy

Table 4 presents the discrepancy of D° between the calculated and experimental values. Among all methods, the M5 method obtained D° the closest to the experimental values for molecules with singlet spin-state. The results support the work of Zhao and Truhlar [21], which suggest using the M5 method for D° calculations of molecules with singlet spin-state. Therefore, M06-2X functional is suitable for dealing with the hydrogen dissociation energy of molecules with singlet spin-state.

[Table 4 about here.]

The discrepancy of D° obtained by each method varied compared to the discrepancy obtained by M1 method. In hydroxyl and methylidyne [Table 4(a) and (b)], M1, M2, M3, and M4 methods resulted in similar discrepancy of D°. It indicates that the dispersion

and the long-range corrections produce similar D° of molecules with doublet spin-state. In other molecules [Table 4(c)-(i)], results of M2 and M4 methods deviated on average of 1.1 and 0.8 kJ/mol, respectively higher than that of M1 method. While results of M3 method deviated on average of 4.4 kJ/mol higher than that of M1 method. The last deviation is significant, which implies that the long-range correction is the reason for the increasing in D° of molecules with singlet spin-state. Thus, the long-range correction plays a role in increasing D° of molecules with singlet spin-state but not the molecules with doublet spin-state.

Other variation was the increasing on the discrepancy of D° of O−H′ and C−H′ bonds obtained by M3 method relative to M1 method. In molecules with singlet spin-state, the average increasing on the discrepancy of O−H′ and C−H′ bonds were 5.7 kJ/mol and 2.8 kJ/mol, respectively. The increasing on the discrepancy of O−H′ bonds is significant. The increasing was not accompanied by the ground state O−H′ bond lengths alteration. However, the increasing was accompanied by a significant alteration of O−H′ bond orbitals, mainly in $(sp^\lambda)_O$ hybrid orbitals (see Table S10 of the SI). The NBO calculations showed, the average percentage of alteration at $(sp^\lambda)_O$ hybrid orbitals was 33 times more than that at $(sp^\lambda)_C$ hybrid orbitals. Therefore, the long-range correction plays a role in altering the electron density in the O−H′ bond orbitals; hence D° of O−H′ bond increases.

3.3 The potential energy curve

Figure 2 shows the PECs of four selected molecules together with their respective polar coordinates. All methods yielded two types of PEC profile. The first type was a PEC-like of dissociation diatomic molecules; region I described the dissociation process and region II described H′ was already a free atom. All methods agreed one to each other. Methane and toluene [Figure 2(a)left and Figure 2(b)left] were in this type of PEC profile, where there was no disagreement among the methods. The second type was somewhat challenging to explain since not all methods agreed. There was region III that contained barriers. Methanol had one barrier and phenol had at least three barriers [Figure 2(c)left and Figure 2(d)left]. On the other hand, the hydrogen dissociation pathways in the polar coordinates [Figure 2(a)right–Figure 2(d)right] showed that all methods only agreed for methane. It implies that the corrections (long-range and dispersion) significantly affect the pathway in real space rather than in the PEC profile.

[Fig. 2 about here.]

Overall, the PEC profiles of methanol and phenol in region III were explained as follows. For the case of methanol [Figure 2(c)left], the four calculation methods yielded two types of profile. The first type, with one barrier at 2.2 Å, was obtained by methods without long-range correction (M1 and M2). The second type, with six times higher barrier than that in the first type, was obtained by methods with long-range correction (M3 and M4). Thus, the dispersion correction (M2 and M4) did not alter the profile but the long-range correction did. However, this was not the case for phenol [Figure 2(d)left]. M1 and M2 obtained three barriers, while M3 and M4 obtained four barriers. At the first barrier, M3 and M4 obtained a barrier (**B1b**) at a shorter O−H′ distance than that in M1 and M2 (**B1a**). At the second barrier (labelled with **B2**), M3 obtained higher barrier than M1. At the third barrier (labelled with **B3**), M3 and M4 obtained almost similar barrier to M1 and M2. The results imply that the long-range correction plays a more significant role than dispersion correction in the PEC profiles of O−H′ dissociation.

In detail, the PEC profile of phenol was accompanied by the variation of dissociation pathways in polar coordinate [Figure 2(d)right]. The profile showed that the barriers were formed when the H′ atom dissociated from O−H′ bond and migrated to the next three consecutive carbon atoms (2, 3, and 4) before leaving the phenyl ring (see the illustration in Figure S1 of the SI). An exception occurred at the barrier between **B1a** and **B2**. Here, the H′ atom migrated toward a hydrogen atom instead of a carbon atom. Hence, there was a probability for the H−H′ to dissociate as a hydrogen molecule. At the O−H′ distances where the barriers formed, the polar coordinates showed various deviation in 2–1–O−H′ angle. This deviation caused the interatomic distances between H′ and its nearest atom vary. At **B1b**, **B2**, and **B3**, M3 and M4 obtained the O−H′, 2–H′, 3–H′ and 4–H′ interatomic distances in the range of 1.5–2.2 Å (Table S11 in the SI) which were in noncovalent region. Kamiya et al. [43] reported that in a system interacting through a noncovalent interactions (which was van der Waals interactions), XCs with long-range correction constantly obtained different profiles from XCs without correction. Thus, the different profiles obtained by the long-range correction (M3) may be due to the presence of noncovalent interactions, particularly at the region with barriers. Therefore, in line with its role in O−H′ BDE, the correction might play a role in energy barrier of O−H′ dissociation.

M1 and M3 obtained different interatomic distances along the pathways (see Table S11 of the SI). At **B1b**, M3 obtained the O−H′ interatomic distance of 2.0 Å or

0.4 Å shorter than M1 did. At **B2**, M3 obtained 2−H′ was shorter than 3−H′, while M1 obtained otherwise. Our results indicate that the long-range correction is the reason for the alteration of the O−H′ and C−H′ (where C is 2 or 3) interatomic distances. Therefore, the correction plays a role both in the energy barrier and the interatomic distances.

The alteration in the interatomic distances after the introduction of long-range correction was accompanied by the alteration in atomic charges. The NBO calculations showed that O, 2, and 3 were negatively charged while H′ was positively charged. At **B1b**, M3 obtained an increase of negative charge on O and the positive charge on H′ by 0.10 and 0.12 electrons, respectively. It implies that the Coulombic attraction between more negative O and more positive H′ is the reason for the shortening of the O−H′ interatomic distance. At **B2**, M3 obtained the charge of 2 was more negative than the charge of 3; while M1 obtained otherwise. It indicates that the Coulombic attraction between more negatively charged 2 and positively charged H′ is the reason for the shortening of the 2–H′. Therefore, the Coulombic interactions play a role in the interatomic distance alteration.

3.4 The dissociation pathway

Figure 3 shows the O−H′ dissociation pathways of two selected molecules, phenol and catechol, in an ELD. For the case of phenol [Figure 3(a)], each pathway had three transition states (TS) and three intermediate states (IS) as predicted earlier in Figure 2(d)left; while for the case of catechol [Figure 3(b)], each pathway had two TSs and two ISs. The experiment has observed the presence of IS1 in a photochemical reaction [44]. While a theoretical study reported IS1 and IS3 as two isomers of phenol [45]. Another theoretical study reported the first step in decomposition of catechol lead to IS4 [46]. The similarity between the molecules in the intermediate states with the previous studies indicate the possibility of hydrogen migration before O−H′ dissociation occurred.

[Fig. 3 about here.]

The dissociation pathways showed that in each TS, all methods obtained the same order of relative electronic energy for the case of phenol and catechol. The order for both cases from the lowest to the highest was M1 ≈ M2 < M3 ≈ M4 < M5. For the case of phenol, the average difference between the energy obtained by methods with long-range correction (M3 and M4) and methods without the correction (M1 and M2) was 0.16 eV. Similarly, for the case of catechol, the average difference was 0.14 eV. The differences are significant. It was aligned with the difference in the PEC profile [Figure 2(d)left], particularly at region with barriers, after the long-range correction was introduced. Since different profiles formed at region where the noncovalent interaction may be present, the results imply that the long-range correction predicts the dissociation is more difficult at this region. Therefore, the correction indeed plays a role in energy barrier of O−H′ dissociation.

Methods with long-range correction obtained shorter interatomic distance than the methods without the correction did in the TS structures. For the case of phenol, the O−H′ and 3−H′ interatomic distances shortened by 0.01 Å on average. The shortening was also similar for the case of catechol. The 0.01 Å was significant compared to the shortening in the O−H′ bond of the ground state phenol and catechol which was only 0.002 Å [Table 3(h) and (i)]. The shortening in the transition state structures confirmed the shortening of interatomic distance along the dissociation pathway discussed in Subsection 3.3. For this reason, the long-range correction indeed plays a role in the interatomic distance in the transition state.

Methods with the long-range correction (M3 and M4) obtained similar relative electronic energy to M5 in the TSs. The average differences of relative electronic energy obtained by those methods were 0.07 for phenol and 0.06 for catechol. These values are very small which indicate the similarity of transition state according to those methods. Therefore, CAM-B3LYP and M06-2X predicts comparable transition state of O−H′ dissociation.

Overall, all methods show consistent performances on the BDE calculations and O−H′ dissociation pathways prediction. For the BDE calculations, the methods obtained the O−H′ BDE of non-phenyl and phenyl groups which increase in the following order: M1 ≈ M2 < M3 ≈ M4 < M5. Compared to B3LYP (M1), the long-range correction in CAM-B3LYP (M3) increased BDE of the O−H′ bond. The increasing was in agreement with the study by Chan et al. [47] when using CAM-B3LYP to calculate O−H′ BDE of various small molecules. For the pathway prediction, the methods predicted different pathways in the case of O−H′ dissociation of phenyl groups, which are phenol and catechol. The different pathways were identified by different energy barriers and O−H′ interatomic distances. The methods obtained the energy barriers which increase in the same order as the increase of the O−H′ BDE. This result validates the study by Peach et al. [48] that showed the increasing of barrier height when using CAM-B3LYP compared to B3LYP. The increasing of energy barriers were accompanied by the shortening of the O−H′ interatomic distances as follow: M1 ≈ M2

> M3 ≈ M4. The shortening in the interatomic distance due to the long-range correction is in agreement with our previous study [31]. The results show the significance of this research, that is the use of long-range correction in CAM-B3LYP affects the O−H′ dissociation in two member of phenyl groups. On the other hand, the M06-2X used in this study predicted the highest BDE and energy barrier. The BDE was similar to the experimental observation. The M06-2X developer suggests the functional for applications involving main group thermochemistry, kinetics, and noncovalent interactions [21,28].

4 Conclusion

We have studied the effects of dispersion and long-range corrections on O−H and C−H dissociations of non-phenyl and phenyl groups. The effects were identified through bond dissociation energy and dissociation pathways. We summarized that the dispersion correction had negligible effects on the O−H and C−H bond dissociation energies as well as the dissociation pathways of non-phenyl and phenyl groups. While, the long-range correction in CAM-B3LYP had a minor effect on the O−H bond dissociation energy and a significant effect on theO−H dissociation pathways. We found that the long-range correction increased the bond dissociation energy of the O−H bond of non-phenyl and phenyl groups in their singlet states by 5.7 kJ/mol. We argued that the increasing was due to the alteration of electron density in the O−H bond orbitals. However, the dissociation energy was still far from the experimental results. The significant effects of the long-range correction on the O−H dissociation pathways occurred in two member of phenyl groups, namely phenol and catechol, were identified as follow. First, the correction shortened the O−H interatomic distances in the transition states. The shortening was 0.01 Å, on average, which was significant compared to the shortening of the O−H bond in the ground state due to the correction (only 0.002 Å, on average). Second, the correction increased the energy barrier by 0.16 eV for phenol and 0.14 eV for catechol, on average. Overall, our results support other theoretical studies on the increasing of energy barrier due to the long-range correction. Accordingly, we suggest that one should consider the long-range correction when studying hydrogen bond dissociation in phenolic compounds, such as phenol and catechol.

Acknowledgements Authors thank to Rizka Nur Fadilla from Research Center for Quantum Engineering Design (RCQED), Universitas Airlangga for the insightful discussions. LSPB is grateful for the doctoral scholarship by Lembaga Pengelola Dana Pendidikan (LPDP). All calculations using Gaussian 16 software are performed at Riven Cluster, the high performance computing facility in RCQED, Universitas Airlangga, Indonesia.

Declarations

Funding

No funding was received for conducting this study.

Conflict of Interest

The authors have no conflicts of interest to declare that are relevant to the content of this article.

Availability of Data and Materials

All data analysed during this study are included in this published article and its supplementary information file.

Code Availability

Not Applicable.

Authors Contribution

Conceptualization: F.R.; formal analysis: L.S.P.B, H.R., and I.P.; investigation: L.S.P.B and V.K.; methodology: F.R. and L.S.P.B; writing—original draft preparation: L.S.P.B; writing—review and editing: F.R. and H.K.D. All authors have read and agreed to the published version of the manuscript.

References

1. Zielinski ZAM and Pratt DA (2017) J Org Chem 82, 6, 2817–2825
2. Yin H and Porter NA (2011) Chem. Rev. 111, 10, 5944–5972
3. Shang Y, Zhou H, Li X, Zhou J, Chen K (2019) New J Chem 43: 15736-15742
4. Vo QV, Nam PC, Bay MV, Thong NM, Cuong ND, and Mechler A (2018) Sci Rep 8: 12361
5. Xue Y, Zheng Y, An L, Dou Y, Liu Y (2014) Food Chem 151: 198-206.
6. Iuga C, Alvarez-Idaboy JR, Russo N (2012) J Org Chem 12: 3868-3877.
7. Galano A, Alvarez-Diduk R, Ramirez-Silva MT, Alarcon-Angeles G, Rojas-Hernandez A (2009) Chem Phys 363: 13-23.
8. Jovanovic SV, Steenken S, Boone CW, Simic MG (1999) J Am Chem Soc 121:9677-9681.

9. Wang Y-N and Eriksson LA (2001) Theor Chem Acc 106:158-162
10. Mallick S, Sarkar S, Bandyopadhyay B, and Kumar P (2018) J Phys Chem A 122, 1, 350–363
11. Kumar M, Sinha A, and Francisco JS (2016) Acc Chem Res 49, 5, 877–883
12. Liang F, Zhong W, Xiang L, Mao L, Xu Q, Kirk SR, and Yin D (2019) J. Catal. 378:256-269
13. Asgari P, Hua Y, Bokka A, Thiamsiri C, Prasit-watcharakorn W, Karedath A, Chen X, Sardar S, Yum K, Leem G, Pierce BS, Nam K, Gao J, and Jeon J (2019) Nat Catal 2:164–173
14. Barckholtz C, Barckholtz TA, and Hadad CM (1999) J Am Chem Soc 121, 3, 491–500
15. Wang L, Yang F, Zhao X, and Li Y (2019) Food Chem 275: 339-345
16. Nantasenamat C, Isarankura-Na-Ayudhya C, Naenna T, Prachayasittikul V (2008) J Mol Graph Model 27:188-196
17. Zhang H-Y, Sun Y-M, and Wang X-L (2003)Chem Eur J 9:502-508
18. Brinck T, Lee H-N, Jonsson M (1999) J Phys Chem 103:7094-7104
19. Izgorodina EI, Coote ML, Radom L (2005) J Phys Chem A 109:7558-7566
20. Izgorodina EI, Brittain DRB, Hodgson JL, Krenske EH, Lin CY, Namazian M, and Coote ML (2007) J Phys Chem A 111: 10754-10768
21. Zhao Y and Truhlar DG (2008) J Phys Chem A 112: 1095-1099
22. Beste A and Buchanan III AC (2009) J Org Chem 74(7): 2837–2841
23. Zheng Y-Z, Fu Z-M, Deng G, Guo R, Chen D-F (2020) Phytochemistry 178: 112454
24. Du T, Quina FH, Tunega D, Zhang J, Aquino AJA (2020) Theor Chem Acc 139:75
25. Yanai T, Tew DP, Handy NC (2004) Chem Phys Lett 393: 51-57
26. Grimme S, Antony J, Ehrlich S, Krieg H (2010) J Chem Phys 132: 154104
27. Becke AD (1993) J Chem Phys 98: 5648
28. Zhao Y, Truhlar DG (2008) Theor Chem Acc 120: 215-241
29. Rusydi F, Madinah R, Puspitasari I, Mark-Lee WF, Ahmad A, Rusydi A (2020) Biochem Mol Biol Educ https://doi.org/10.1002/bmb.21433
30. Fadilla RN, Rusydi F, Aisyah ND, Khoirunisa V, Dipojono HK, Ahmad F, Mudasir, Puspitasari I (2020) Molecules 25: 670
31. Rusydi F, Aisyah ND, Fadilla RN, Dipojono HK, Ahmad F, Mudasir, Puspitasari I, Rusydi A (2019) Heliyon 5: e02409
32. Fadilla RN, Aisyah ND, Dipojono HK, Rusydi F (2017) Procedia Eng 170: 113-118
33. Hohenberg P, Kohn W (1964) Phys Rev 136: B864
34. Kohn W, Sham LJ (1965) Phys Rev 140: A1133
35. M. J. Frisch, G. W. Trucks, H. B. Schlegel, G. E. Scuseria, M. A. Robb, J. R. Cheeseman, G. Scalmani, V. Barone, G. A. Petersson, H. Nakatsuji, X. Li, M. Caricato, A. V. Marenich, J. Bloino, B. G. Janesko, R. Gomperts, B. Mennucci, H. P. Hratchian, J. V. Ortiz, A. F. Izmaylov, J. L. Sonnenberg, D. Williams-Young, F. Ding, F. Lipparini, F. Egidi, J. Goings, B. Peng, A. Petrone, T. Henderson, D. Ranasinghe, V. G. Zakrzewski, J. Gao, N. Rega, G. Zheng, W. Liang, M. Hada, M. Ehara, K. Toyota, R. Fukuda, J. Hasegawa, M. Ishida, T. Nakajima, Y. Honda, O. Kitao, H. Nakai, T. Vreven, K. Throssell, J. A. Montgomery, Jr., J. E. Peralta, F. Ogliaro, M. J. Bearpark, J. J. Heyd, E. N. Brothers, K. N. Kudin, V. N. Staroverov, T. A. Keith, R. Kobayashi, J. Normand, K. Raghavachari, A. P. Rendell, J. C. Burant, S. S. Iyengar, J. Tomasi, M. Cossi, J. M. Millam, M. Klene, C. Adamo, R. Cammi, J. W. Ochterski, R. L. Martin, K. Morokuma, O. Farkas, J. B. Foresman, and D. J. Fox (2013) Gaussian 16, Revision C.01, Gaussian, Inc., Wallingford CT
36. Glendening ED, Reed AE, Carpenter JE, Weinhold F Nbo version 3.1
37. Mardirossian N and Head-Gordon M (2016) J Chem Theory Comput 12: 4303-4325
38. Jones DB, da Silva GB, Neves RFC, Duque HV, Chiari L, de Oliveira EM, Lopes MCA, da Costa RF, Varella MTN, Bettega MHF, Lima MAP and Brunger MJ (2014) J Chem Phys 141: 074314
39. Huber KP and Herzberg G, Molecular Spectra and Moelcular Structure IV. Constants of Diatomic Molecules, Springer US, 1979, page 508
40. Young DC, Computational chemistry: A practical guide for applying techniques to real-world problems, John Wiley & Sons Inc., New York, 2001, Chp. 16, Page 138
41. Haynes WM, CRC Handbook of Chemistry and Physics, 95th ed., CRC Press, Boca Rotan, 2014, Chp.9
42. Lucarini M, Pedulli GF, Guerra M (2004) Chem Eur J 10: 933-939
43. Kamiya M, Tsuneda T and Hirao K (2002) J Chem Phys 117: 6010
44. Parker K and Davis SR (1999) J Am Chem Soc 121: 4271-4277
45. Zhu L and Bozzelli JW (2003) J Phys Chem A 107: 3696-3703
46. Altarawneh M, Dlugogorski BZ, Kennedy EM and Mackie J (2010) J Phys Chem A. 114: 1060-1067
47. Chan B, Morris M and Radom L (2011) Aust J Chem 64: 394-402
48. Peach MJG, Helgaker T, Salek P, Keal TW, Lutnæs OB, Tozer DJ and Handyd NC (2006) Phys Chem Chem Phys 8: 558-562

List of Figures

1 **Fig. 1** Kekulé structure of the molecule of interest. The primed H was the dissociated hydrogen atom. For clarity in molecules (g) – (i), only dissociated hydrogen atom were shown and carbon atoms were replaced by numbers 9

2 **Fig. 2** PECs of C−H′ and O−H′ bond dissociations with their respective polar coordinates. The I, II, and III represented three different regions based on the similarity of events at each region. Angles in the polar coordinate were H−C−H′ in methane, 2–1–C−H′ in toluene, H−C−O−H′ in methanol, and 2–1–O−H′ in phenol (see Figure 1). The initial angle was at zero degree, then deviated clockwise or counterclockwise. Particularly in methane, the clockwise represented inward deviation. **B1a**, **B1b**, **B2**, and **B3** in (d) represented first barrier obtained by M1 and M2, first barrier obtained by M3 and M4, Second barrier and third barrier obtained by all four methods, respectively 10

3 **Fig. 3** Energy level diagram for O−H′ dissociation pathways of two selected molecules. R1, R2, P1 and P2 represent phenol, catechol, product of phenol dissociation, and product of catechol dissociation. While TS and IS stand for transition state and intermediate state. The TSs were shown with the selected interactomic distances (unit in Å) 11

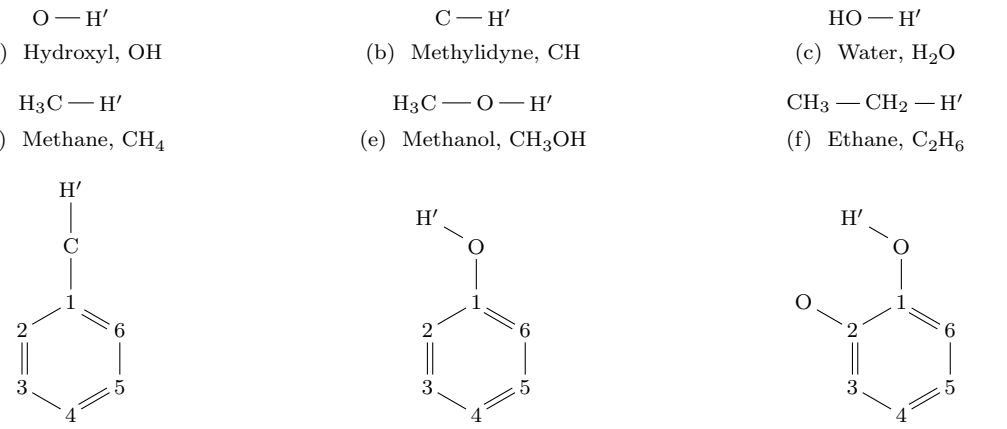

(a) Hydroxyl, OH (b) Methylidyne, CH (c) Water, H_2O

(d) Methane, CH_4 (e) Methanol, CH_3OH (f) Ethane, C_2H_6

(g) Toluene, $C_6H_5CH_3$ (h) Phenol, C_6H_5OH (i) Catechol, $C_6H_4(OH)_2$

Fig. 1 Kekulé structure of the molecule of interest. The primed H was the dissociated hydrogen atom. For clarity in molecules (g) – (i), only dissociated hydrogen atom were shown and carbon atoms were replaced by numbers

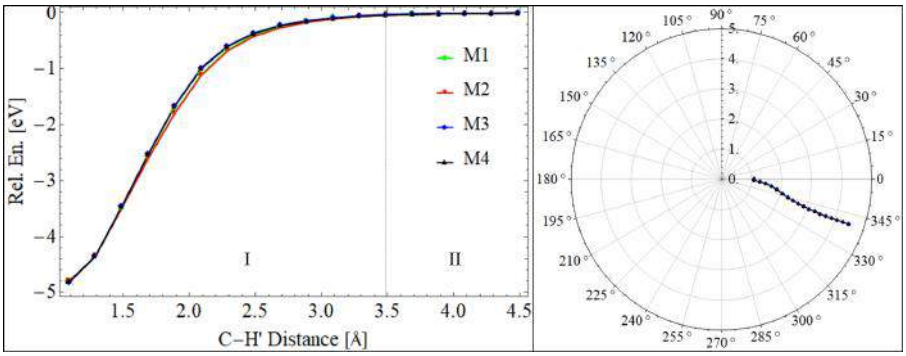

(a) PEC (left) and polar coordinate (right) of methane.

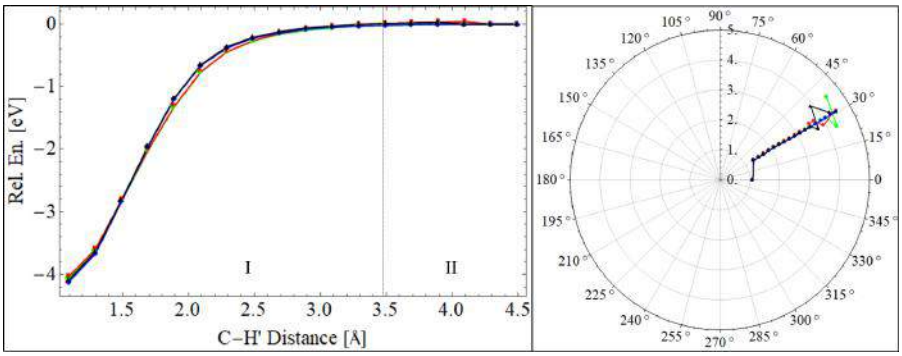

(b) PEC (left) and polar coordinate (right) of toluene.

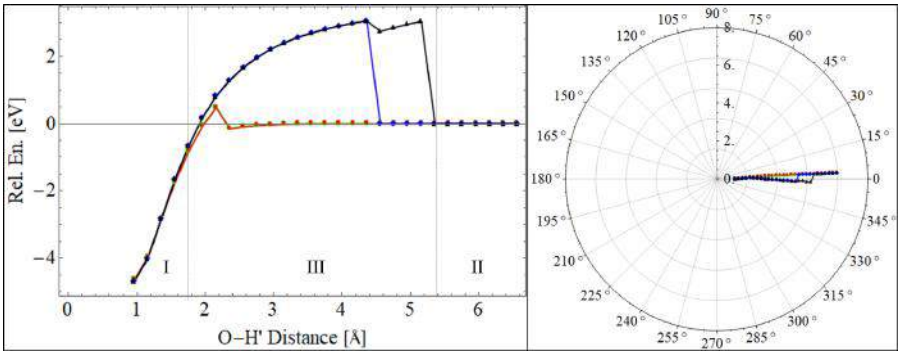

(c) PEC (left) and polar coordinate (right) of methanol.

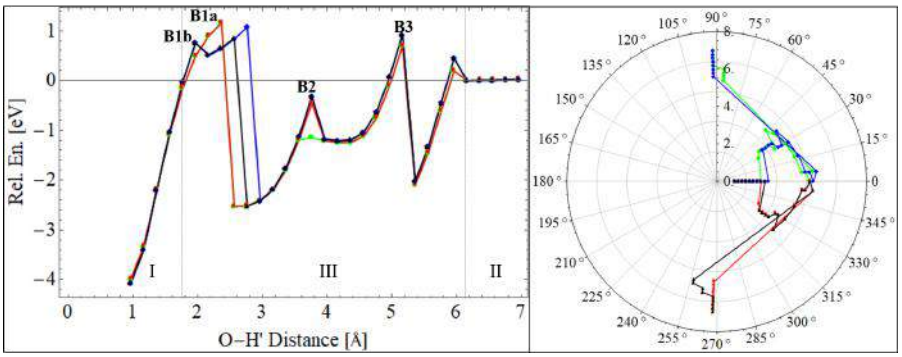

(d) PEC (left) and polar coordinate (right) of phenol.

Fig. 2 PECs of C−H′ and O−H′ bond dissociations with their respective polar coordinates. The I, II, and III represented three different regions based on the similarity of events at each region. Angles in the polar coordinate were H−C−H′ in methane, 2–1–C−H′ in toluene, H−C−O−H′ in methanol, and 2–1–O−H′ in phenol (see Figure 1). The initial angle was at zero degree, then deviated clockwise or counterclockwise. Particularly in methane, the clockwise represented inward deviation. **B1a**, **B1b**, **B2**, and **B3** in (d) represented first barrier obtained by M1 and M2, first barrier obtained by M3 and M4, Second barrier and third barrier obtained by all four methods, respectively

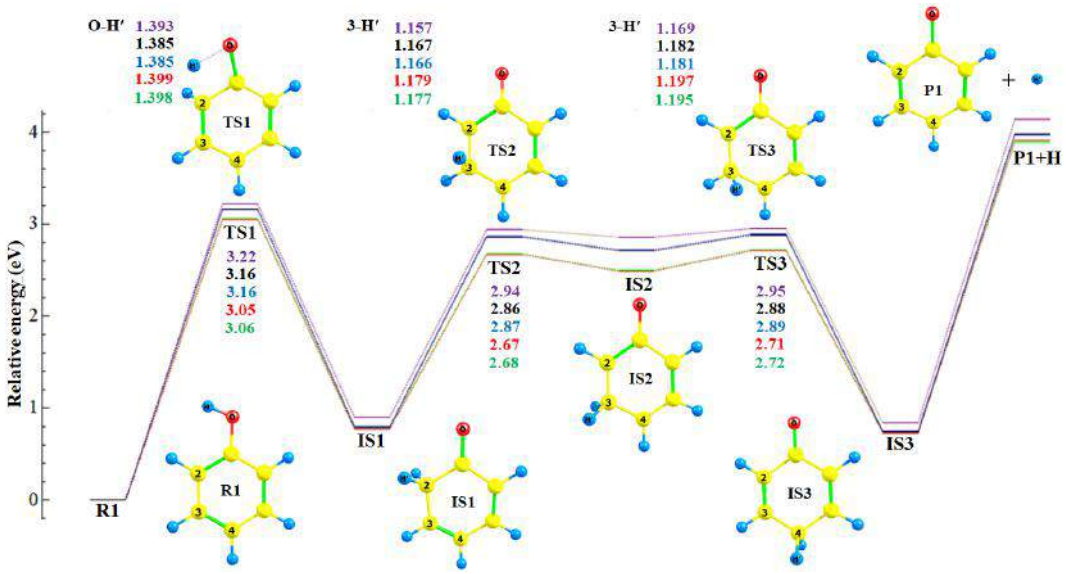

(a) O−H′ dissociation pathways of phenol

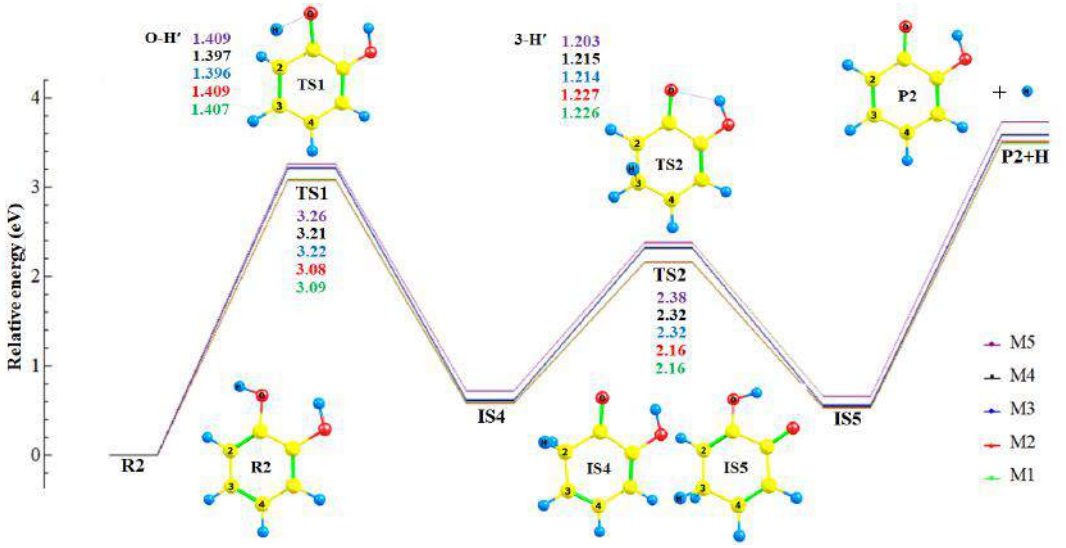

(b) O−H′ dissociation pathways of catechol

Fig. 3 Energy level diagram for O−H′ dissociation pathways of two selected molecules. R1, R2, P1 and P2 represent phenol, catechol, product of phenol dissociation, and product of catechol dissociation. While TS and IS stand for transition state and intermediate state. The TSs were shown with the selected interactomic distances (unit in Å)

List of Tables

1 **Table 1** List of methods used in the manuscript 13
2 **Table 2** The discrepancy of calculated geometrical parameters of hydroxyl and phenol by (1) B3LYP, (2) CAM-B3LYP, and (3) M06-2X with respect to the experimental values [41]. The parameters were bond length (R, in Å) and bond angle (A, in degree). The parameter in (i) belongs to hydroxyl; while others belong to phenol 14
3 **Table 3** The difference of calculated O−H′ and C−H′ bond lengths from M1 (Å). The label referred to Figure 1 15
4 **Table 4** The discrepancy of calculated D° with respect to the experimental values (kJ/mol) [41,42]. The label referred to Figure 1 16

Table 1 List of methods used in the manuscript

M1	B3LYP
M2	B3LYP + GD3
M3	CAM-B3LYP
M4	CAM-B3LYP + GD3
M5	M06-2X

Table 2 The discrepancy of calculated geometrical parameters of hydroxyl and phenol by (1) B3LYP, (2) CAM-B3LYP, and (3) M06-2X with respect to the experimental values [41]. The parameters were bond length (R, in Å) and bond angle (A, in degree). The parameter in (i) belongs to hydroxyl; while others belong to phenol

	Parameter	Expr.	(1)	(2)	(3)
(i)	R(O,H′)	0.970	+0.006	+0.005	+0.003
(ii)	R(O,H′)	0.956	+0.007	+0.005	+0.005
(iii)	R(C,C)av	1.397	-0.003	-0.009	-0.006
(iv)	R(1,O)	1.364	+0.006	0.000	-0.001
(v)	R(4,H)	1.082	+0.001	+0.001	0.000
(vi)	R(5,H)	1.076	+0.008	+0.008	+0.008
(vii)	R(6,H)	1.084	+0.002	+0.001	+0.002
(viii)	A(1,O,H′)	109.0	+0.8	+1.0	+0.8

Table 3 The difference of calculated O−H′ and C−H′ bond lengths from M1 (Å). The label referred to Figure 1

	Molecule	Bond	M1	M2	M3	M4	M5
(a)	Hydroxyl	O−H′	0.976	0.000	-0.002	-0.002	-0.004
(b)	Methylidyne	C−H′	1.127	0.000	-0.003	-0.003	-0.007
(c)	Water	O−H′	0.962	0.000	-0.001	-0.001	-0.003
(d)	Methane	C−H′	1.091	0.000	-0.001	-0.001	-0.002
(e)	Methanol	O−H′	0.961	0.000	-0.002	-0.002	-0.003
(f)	Ethane	C−H′	1.094	0.000	-0.001	-0.001	-0.002
(g)	Toluene	C−H′	1.094	0.000	-0.002	-0.002	-0.002
(h)	Phenol	O−H′	0.963	0.000	-0.002	-0.002	-0.002
(i)	Catechol	O−H′	0.962	0.000	-0.002	-0.002	-0.002

Table 4 The discrepancy of calculated D° with respect to the experimental values (kJ/mol) [41,42]. The label referred to Figure 1

	Molecule	Bond	Expr.	M1	M2	M3	M4	M5
(a)	Hydroxyl	O−H,	429.73	-1.1	-1.1	-0.8	-0.8	-9.2
(b)	Methylidyne	C−H,	338.4	+1.8	+1.8	-2.2	-2.2	-8.1
(c)	Water	O−H,	497.32	-17.1	-17.1	-14.0	-14.0	-11.7
(d)	Methane	C−H,	439.3	-8.3	-8.2	-7.1	-7.0	-6.1
(e)	Methanol	O−H,	440.2	-26.4	-25.2	-21.1	-20.3	-11.5
(f)	Ethane	C−H,	420.5	-8.9	-7.6	-6.8	-6.0	-3.4
(g)	Toluene	C−H,	375.5	-10.8	-9.1	-5.8	-4.7	+2.9
(h)	Phenol	O−H,	362.8	-16.0	-14.6	-9.6	-8.6	+6.7
(i)	Catechol	O−H,	342.3	-32.0	-29.9	-24.0	-22.5	-9.8

4. Review Manuskrip

- Komentar Reviewer
- Pertanyaan dan Jawaban
- Revisi Draf Manuskrip

Gmail

Lusia silfia <lusiasilfia@gmail.com>

Fwd: TCAC: Your manuscript entitled "O-H and C-H bond dissociations in non-phenyl and phenyl groups: A DFT study with dispersion and long-range corrections"

1 pesan

Febdian Rusydi <rusydi@fst.unair.ac.id> 8 Februari 2021 01.56
Kepada: "lusiasilfia@gmail.com" <lusiasilfia@gmail.com>

---------- Forwarded message ---------
From: **Dr. Ilaria Ciofini & Prof. Carlo Adamo** <em@editorialmanager.com>
Date: Sun, Feb 7, 2021 at 11:31 PM
Subject: TCAC: Your manuscript entitled "O-H and C-H bond dissociations in non-phenyl and phenyl groups: A DFT study with dispersion and long-range corrections"
To: Febdian Rusydi <rusydi@fst.unair.ac.id>

Manuscript Number: TCAC-D-20-00473
Article Title: O-H and C-H bond dissociations in non-phenyl and phenyl groups: A DFT study with dispersion and long-range corrections
Journal Title: Theoretical Chemistry Accounts

Dear Mr. Rusydi,

We have now received sufficient referee advice on your manuscript "O-H and C-H bond dissociations in non-phenyl and phenyl groups: A DFT study with dispersion and long-range corrections" which you submitted to "Theoretical Chemistry Accounts".

Based on the comments of the reviewer(s), you may elect to prepare a manuscript incorporating major revisions that address their criticisms.
Together with preparation of your revised manuscript, please assemble a list of responses to each point raised by the referee(s). Your revised manuscript will be likely to be subject to further review by one or more of the original reviewers and/or by new ones.

When you submit your revised MS, please also submit your response to the referee(s) as a separate submission item.

In order to submit your revised manuscript, please access the Editorial Manager website.

Your username is: FRusydi-768
If you forgot your password, you can click the 'Send Login Details' link on the EM Login page at
https://www.editorialmanager.com/tcac/

If you have forgotten your password, kindly use the Send Login Details link on the login page.

We look forward to receive your revised manuscript before 08 Apr 2021.

Thank you very much.

Best regards,

Dr. Ilaria Ciofini & Prof. Carlo Adamo
Editors-in-Chief
Theoretical Chemistry Accounts

COMMENTS TO THE AUTHOR:

Reviewer #1: The paper is interesting in general, but there are some deficiencies mainly related to the structure and the discussion.
1. It is not clear that exactly H' means. It is neutral atom, radical or positively charged particle?
2. Especially in the case of OH group dissociation also the simplest case - direct dissociation should be presented.
3. The discussion related to Figure 2 should be made more clear and reader friendly.
4. As seen from Table 4, the deviations from the experimentally determined values are larger in some of the cases for all used methods. Explanation is needed.
5. The text has to be corrected in respect of typos and jargons (for instance XCs in part 2.2).

—

--
Febdian Rusydi, Ph.D.

Head of Theoretical Physics Research Group
Department of Physics, Faculty of Science and Technology,
Universitas Airlangga, Surabaya, Indonesia

— Sent from my mobile phone

Theoretical Chemistry Accounts

O-H and C-H bond dissociations in non-phenyl and phenyl groups: A DFT study with dispersion and long-range corrections

--Manuscript Draft--

Manuscript Number:	TCAC-D-20-00473R1
Full Title:	O-H and C-H bond dissociations in non-phenyl and phenyl groups: A DFT study with dispersion and long-range corrections
Article Type:	Regular Article
Keywords:	O—H and C—H dissociations; non-phenyl and phenyl groups; Density functional theory; dispersion correction; long-range correction
Corresponding Author:	Febdian Rusydi, Ph.D Universitas Airlangga Surabaya, Jawa Timur INDONESIA
Corresponding Author Secondary Information:	
Corresponding Author's Institution:	Universitas Airlangga
Corresponding Author's Secondary Institution:	
First Author:	Lusia Silfia Pulo Boli, Master
First Author Secondary Information:	
Order of Authors:	Lusia Silfia Pulo Boli, Master
	Febdian Rusydi, PhD
	Vera Khoirunisa, Master
	Ira Puspitasari, PhD
	Heni Rachmawati, PhD
	Hermawan Kresno Dipojono, PhD
Order of Authors Secondary Information:	
Funding Information:	
Abstract:	Hydrogen atom transfer is one important reaction in biological system, in industry, and in atmosphere. The reaction is preluded by hydrogen bond dissociation. To gain a comprehensive understanding on the reaction, it is necessary to investigate how the current computational methods model hydrogen bond dissociation. As a starting point, we utilized density functional theory-based calculations to identify the effect of dispersion and long-range corrections on O—H and C—H dissociations in non-phenyl and phenyl groups. We employed five different methods, namely B3LYP, CAM-B3LYP (with long-range correction), M06-2X, and B3LYP and CAM-B3LYP with the D3 version of Grimme's dispersion. The results showed that for the case of O—H dissociation in two member of phenyl groups, namely phenol and catechol, the dispersion correction's effect was negligible but the long-range correction's effect was significant. The significant effect was shown by the increasing of energy barrier and the shortening of O—H interatomic distance in the transition state. Therefore, we suggest one should consider the long-range correction in modeling hydrogen bond dissociation in phenolic compounds, namely phenol and catechol.
Response to Reviewers:	We are grateful for the reviewer's constructive concerns about our manuscript. Here we respond to the reviewer's comments point by point. We revise the manuscript majorly to address the reviewer's concern. We use blue color for the revised and new sentences, while red color to emphasize our explanation. We hope that our revised manuscript meets the reviewer's expectations.

	Sincerely, on behalf of all authors Lusia Silfia Pulo Boli

BEGIN

Question 1

It is not clear that exactly H′ means. It is neutral atom, radical or positively charged particle?

We did address the explanation about what H′ was in the caption of Figure 1. The "prime sign" on the H is not the sign for radicalness or charge. It is to mark the H atom that goes under the dissociation.

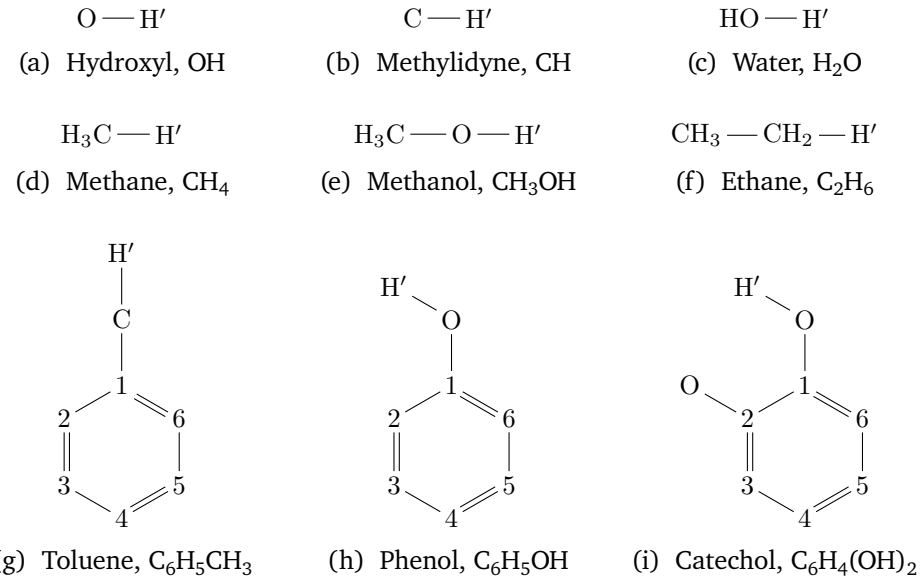

(a) Hydroxyl, OH (b) Methylidyne, CH (c) Water, H_2O

(d) Methane, CH_4 (e) Methanol, CH_3OH (f) Ethane, C_2H_6

(g) Toluene, $C_6H_5CH_3$ (h) Phenol, C_6H_5OH (i) Catechol, $C_6H_4(OH)_2$

Fig. 1 Kekulé structure of the molecule of interest. The primed H was the dissociated hydrogen atom. For clarity in molecules (g) – (i), only dissociated hydrogen atom was shown, and carbon atoms were replaced by numbers

Question 2

Especially in the case of O−H group dissociation also the simplest case - direct dissociation should be presented.

We appreciate the reviewer's suggestion. We have presented other direct dissociation cases, except catechol, in the form of a potential energy curve (PEC).

There are four other cases of O−H and C−H direct dissociation added to this manuscript. They are the dissociation in hydroxyl, methylidyne, water, and ethane. Their PECs are in Figure S1 of the Supporting Information (SI). It is because they are the supportive results for cases in Figure 2 in explaining two types of PEC. The case of catechol is excluded since its dissociation leads to a hydrogen molecule instead of a hydrogen atom as a product.

To accommodate the addition of Figure S1, we have revised the first paragraph of "3.3. The potential energy curve". The paragraph is now as follows.

In the manuscript

Figure 2 shows the PECs of four selected molecules together with their respective polar coordinates. All methods yielded two types of PEC profiles. The first type was a PEC-like of dissociation diatomic molecules [Figure 2(a)–(b) left]. Region I described the dissociation process, and region II described H′ was already a free atom. All methods agreed one to each other. The second type was somewhat challenging to explain since not all methods agreed [Figure 2(c)–(d) left]. There was region III that contained barriers. PEC profiles in methylidyne and ethane were supportive results to the first type, while PEC profiles in hydroxyl and water were supportive results to the second type. Hence, they were placed in Supporting Information [Figure S1(a)–(b) and S1(c)–(d) left]. On the other hand, the polar coordinates show that the hydrogen dissociation pathways in methane [Figure 2(a) right] are different from those in other molecules [Figure 2(b)–(d) right and Figure S1(c)–(d) right of the SI]. All methods were only agreed for methane. It implies that the corrections (long-range and dispersion) significantly affect the pathway in real space rather than in the PEC profile.

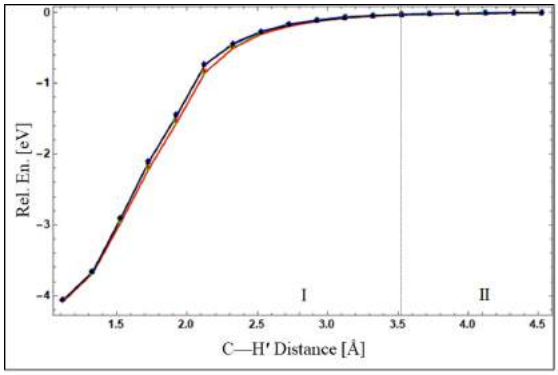

(a) PEC of methylidyne

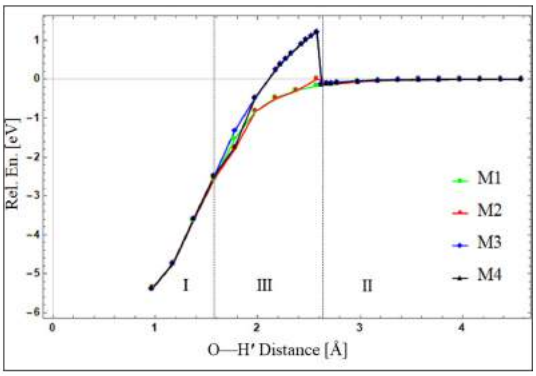

(b) PEC of hydroxyl

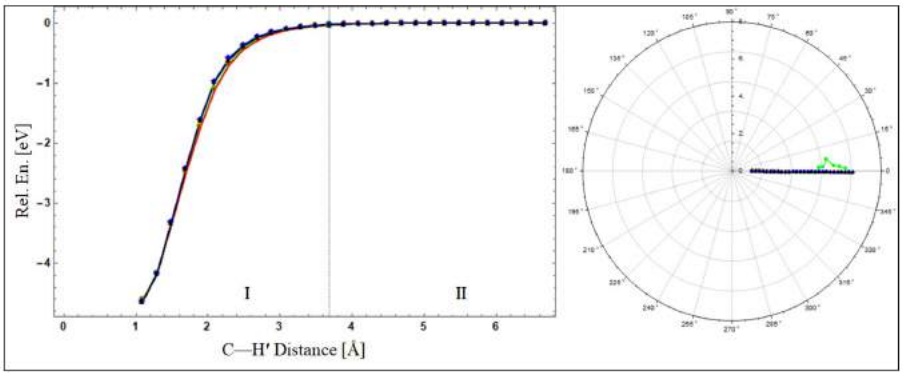

(c) PEC (left) and polar coordinate (right) of ethane

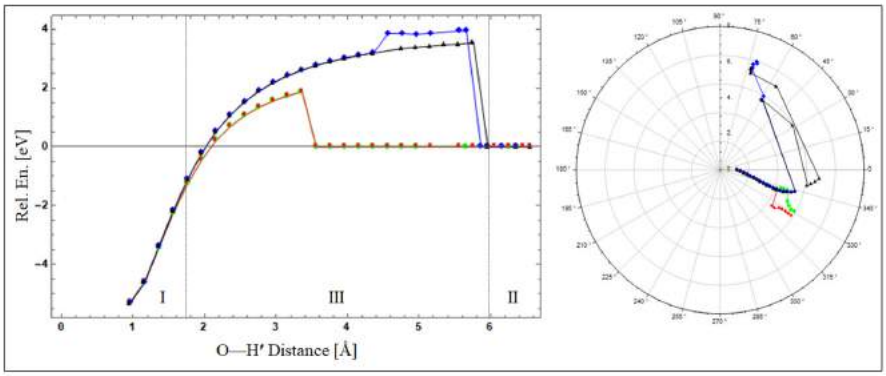

(d) PEC (left) and polar coordinate (right) of water

Figure S1 PECs of O−H′ (S1a and S1c) and C−H′ (S1b and S1d) bond dissociations. PECs in S1c and S1d were presented with their respective polar coordinates. The region I, II, and III in the PEC represented three different regions based on the similarity of events. Angle in the polar coordinate of water was H−O−H′ [see Figure 1(c) in the manuscript] that deviated inward or outward. Angles in the polar coordinate of ethane was H−C−C−H′ [see Figure 1(f) in the manuscript] that deviated clockwise or counterclockwise. The initial angle was at zero degree

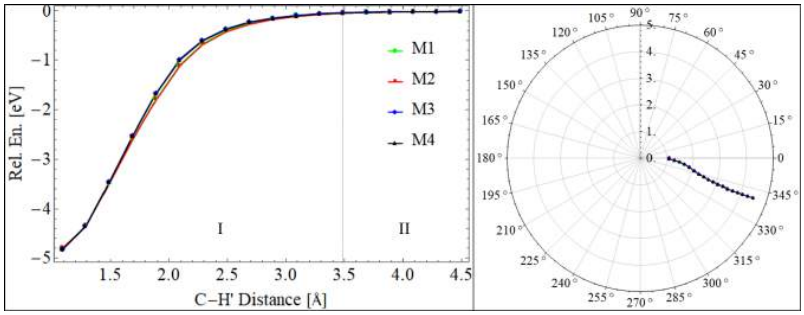

(a) PEC (left) and polar coordinate (right) of methane.

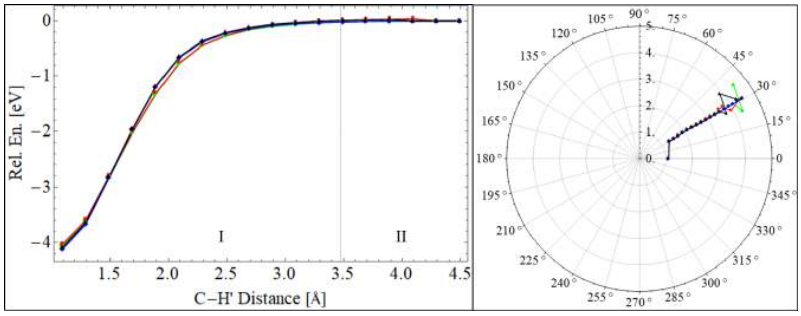

(b) PEC (left) and polar coordinate (right) of toluene.

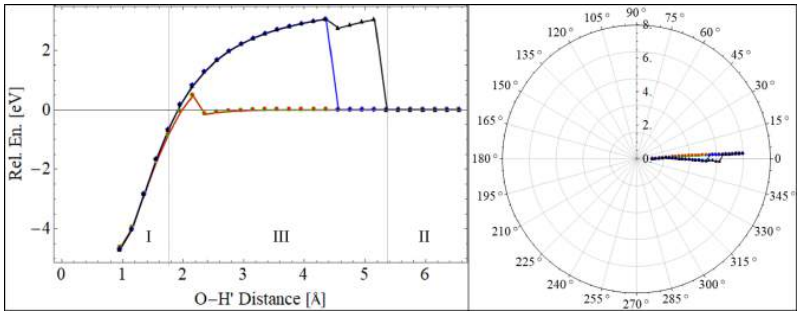

(c) PEC (left) and polar coordinate (right) of methanol.

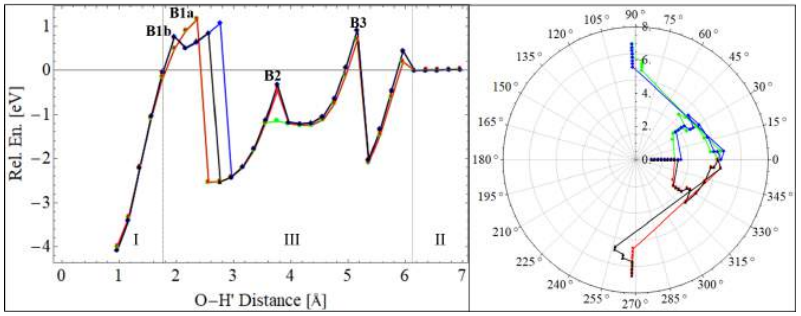

(d) PEC (left) and polar coordinate (right) of phenol.

Fig. 2 PECs of C−H′ and O−H′ bond dissociations with their respective polar coordinates. The I, II, and III represented three different regions based on the similarity of events at each region. Angles in the polar coordinate were H−C−H′ in methane, 2–1–C−H′ in toluene, H−C−O−H′ in methanol, and 2–1–O−H′ in phenol (see Figure 1). The initial angle was at zero degree, then deviated clockwise or counterclockwise. Particularly in methane, the clockwise represented inward deviation. **B1a**, **B1b**, **B2**, and **B3** in (d) represented first barrier obtained by M1 and M2, first barrier obtained by M3 and M4, second and third barrier obtained by all four methods, respectively

Question 3

The discussion related to Figure 2 should be made more clear and reader friendly.

We realize that our writing was unclear. To address this issue, we have revised all five paragraphs in section "3.3. The potential energy curve" subsection majorly. The first paragraph is as shown in our response to Question 2, while the other four paragraphs are now as follows.

In the manuscript

Overall, the PEC profiles of methanol and phenol [Figure 2(c)–2(d) left] were explained as follows. In region III, methanol and phenol had barriers; methanol had one, and phenol had at least three barriers. In both cases, M2 yielded a similar barrier height to M1 did. So did M4 and M3. It means the dispersion correction does not alter the PEC profile of O−H′ dissociation. However, in both cases, M3 yielded a different barrier height than M1 did. The results indicate that the long-range correction does alter the PEC profile of O−H′ dissociation. Therefore, the long-range correction plays a more significant role than the dispersion correction in the PEC profiles of O−H′ dissociation.

In detail, for phenol [Figure 2(d)], the variation of PEC profiles was accompanied by the variation of dissociation pathways in the polar coordinate. Both variations occurred only at a certain O−H′ distance ($r_{\mathrm{O-H'}}$) range. The PEC profile variation range was around 1.8–3 Å; while the pathway variation range was around 2–4 Å. In those ranges, M3 yielded a different profile and pathway than M1 did. Kamiya et al.[43] also obtained different profiles when using XCs with long-range correction in a system interacting through a van der Waals interaction (noncovalent interaction). Thus, the different profiles obtained by the long-range correction (M3) may be due to the presence of noncovalent interactions, particularly at a region with barriers. Therefore, in line with its role in O−H′ BDE, the long-range correction may play a role in the energy barrier of O−H′ dissociation.

In the manuscript

Along the phenol dissociation pathway, M1 and M3 obtained different r at B1a, B1b, and B2 (See Table S11 of the SI). At B1a and B1b, atom H$'$ was located around atom O [See Figure S2 of the SI]. Here, M3 obtained shorter $r_{\mathrm{O-H'}}$ at B1a than M1 did at B1b. Different than at B1a and B1b, at B2 atom H$'$ was located between atom 2 and atom 3. Here, M3 obtained shorter $r_{2-\mathrm{H'}}$ and longer $r_{3-\mathrm{H'}}$ than M1 did. The results indicate that the shortening and lengthening of r are due to the long-range correction.

The r alteration after the introduction of long-range correction was accompanied by atomic charges alteration. The NBO calculations showed that atoms O, 2, and 3 [See Figure 1(h)] were negatively charged while atom H$'$ was positively charged. At B1a, M3 yielded greater positive charge on atom H$'$ and greater negative charge on atom O than M1 did. It implies that the increasing coulombic attraction between atom O and H$'$ is the reason for the shortening of $r_{\mathrm{O-H'}}$ at B1a. At B2, M3 obtained lesser positive charge on atom H$'$ and greater negative charge on atom 2 than M1 did. It indicates that the increasing coulombic attraction between atom 2 and H$'$ is the reason for the shortening of the $r_{2-\mathrm{H'}}$. At this location, M3 obtained lesser negative charge on atom 3 than M1 did. It implies the increasing coulombic repulsion between atom 3 and H$'$ is the reason for the lengthening of the $r_{3-\mathrm{H'}}$. Therefore, the Coulombic interactions play a role in the alteration of r.

Following the revision in the "3.3. The potential energy curve" subsection, we also have rewritten some sentences in paragraph two and three of "3.4. The dissociation pathways" subsection,

In the manuscript

The dissociation pathways in phenol and catechol showed that all methods obtained the same relative electronic energy order in each TS. The order for both cases was M1 $\approx$ M2 $<$ M3 $\approx$ M4 $<$ M5. For the case of phenol, the average difference between the energy obtained by methods with long-range correction (M3 and M4) and methods without the correction (M1 and M2) was 0.16 eV. Similarly, for the case of catechol, the average difference was 0.14 eV. The differences are significant. It was aligned with the PEC profile difference [Figure 2(d)left] after the long-range correction was introduced, particularly at the region with barriers. The results imply that the long-range correction predicts the dissociation is more difficult at a region where the noncovalent interaction may be present. Therefore, the correction indeed plays a role in the energy barrier of O$-$H$'$ dissociation.

Methods with long-range correction (M3 and M4) obtained shorter r than methods without the correction did in the TS structures. For the case of phenol, the $r_{\mathrm{O-H'}}$ and $r_{3-\mathrm{H'}}$ shortened by 0.01 Å on average. The shortening was also similar to the case of catechol. The 0.01 Å is significant compared to the O$-$H$'$ bond length shortening in the ground state of phenol and catechol [Table 4(h) and (i)]. Thus, the shortening confirms the shortening of r along the dissociation pathway discussed in Subsection 3.3. For this reason, the long-range correction indeed plays a role in r in the transition state.

paragraph five of “3.4. The dissociation pathways” subsection,

In the manuscript

Overall, all methods showed consistent performances on the BDE calculations and O−H′ dissociation pathways prediction. For the BDE calculations, the methods obtained D° of O−H′ in all molecules increased in the following order: M1 ≈ M2 < M3 ≈ M4 < M5. The increase of D° after the presence of long-range correction in CAM-B3LYP (M3) was in agreement with the study by Chan et al. [47] For the pathways prediction, the methods obtained variation of pathways in phenol and catechol dissociation. The variations were identified by the alteration in energy barriers and $r_{\mathrm{O-H'}}$ in the TS. The energy barrier increased in the same order as the increase in D° of O−H′. This result validates the study by Peach et al. [48] that showed increasing barrier height when using CAM-B3LYP compared to B3LYP. The increasing energy barriers was accompanied by the shortening of $r_{\mathrm{O-H'}}$ as follows: M1 ≈ M2 > M3 ≈ M4. The shortening due to the long-range correction (M3) was in agreement with our previous study [31]. The results show the significance of this research: the use of long-range correction in CAM-B3LYP affects the $r_{\mathrm{O-H'}}$ in TS. On the other hand, the M06-2X used in this study predicted the highest D° and energy barrier. The D° was similar to the experimental observation. The M06-2X developer suggested the functional for applications involving main group thermochemistry, kinetics, and noncovalent interactions [21,28].

and section “4. Conclusion”.

In the manuscript

We have studied the effects of dispersion and long-range corrections on O−H and C−H dissociations of non-phenyl and phenyl groups. The effects were identified through bond dissociation energy and dissociation pathways. We summarized that the dispersion correction had negligible effects on the O−H and C−H bond dissociation energies and the non-phenyl and phenyl groups dissociation pathways. While the long-range correction in CAM-B3LYP had a minor effect on the O−H bond dissociation energy and a significant effect on the O−H dissociation pathways. We found that the long-range correction increased the bond dissociation energy of the O−H bond of non-phenyl and phenyl groups in their singlet states by 5.7 kJ/mol. We argued that the increase was due to the alteration of electron density in the O−H bond orbitals. However, the dissociation energy was still far from the experimental results. The significant effects of the long-range correction on the O−H dissociation pathways occurred in two members of phenyl groups, namely phenol and catechol. The effects were identified as follows. First, the correction shortened the O−H distances in the transition states by 0.01 Å, on average. Second, the correction increased the energy barrier by 0.16 eV (in phenol) and 0.14 eV (in catechol), on average. Overall, our results support other theoretical studies on the increasing energy barrier due to the long-range correction. Accordingly, we suggest that one should consider the long-range correction when studying hydrogen bond dissociation in phenolic compounds, such as phenol and catechol.

Question 4

As seen from Table 4, the deviations from the experimentally determined values are larger in some of the cases for all used methods. Explanation is needed.

Thank you for pointing out this issue. We purposely did not provide an explanation because it was not in line with the goal of this manuscript.

In Table 4 (now become Table 5), we do not compare the discrepancy (we use this term, instead of deviation, to refer to the difference between calculation and experimental results) to know how small or how large they are. Instead, we compare them

to determine their alteration among methods used. It is to achieve the manuscript's goal that we have stated in the first sentence of the last paragraph of the "1. Introduction" section.

However, we are aware that our discussion in the second and the third paragraphs of "3.2. The bond dissociation energy" subsection does not emphasize our goal clearly. Thus, we have rewritten the paragraphs and split the third paragraph into two. The subsection has four paragraphs now. The second to the fourth paragraphs are as follows.

In the manuscript

The discrepancy obtained by M2, M3, and M4 were varied compared to that obtained by M1. In all molecules [Table 5 (a)-(i)], M2 obtained 0.9 kJ/mol (in average) discrepancies higher than M1 did. Moreover, M4 obtained 0.6 kJ/mol (in average) discrepancies higher than M3 did. The results indicate that the dispersion correction does not alter the calculated D° of molecules with singlet and doublet spin-states. In hydroxyl and methylidyne [Table 5 (a) and (b)], M3 obtained 1.9 kJ/mol (on average) discrepancies lower than M1 did. Meanwhile, in other molecules [Table 5 (c)-(i)], M3 obtained 4.4 kJ/mol (in average) discrepancies higher than M1 did. The 4.4 kJ/mol is significant, which implies that the long-range correction is the reason for D° alteration of molecules with singlet spin-state. Thus, the long-range correction plays a role in altering D° of molecules with singlet spin-state but not the molecules with doublet spin-state.

Among seven molecules in Table 5 (c)-(i), the alteration of discrepancies from M1 to M3 on O$-$H$'$ bond differed from that on C$-$H$'$ bonds. The seven molecules were in their singlet spin-state. For four molecules with O$-$H$'$ bonds, the discrepancies increased by 5.7 kJ/mol (in average) from M1 to M3. However, for three molecules with C$-$H$'$ bonds, the discrepancies only increased by 2.8 kJ/mol (in average) from M1 to M3. The increase on O$-$H$'$ bonds is more significant than on C$-$H$'$ bonds. It indicates that the long-range correction alters the calculated D° on O$-$H$'$ bond more than that on C$-$H$'$ bond of molecules with singlet spin-state.

In the manuscript

The increase in the discrepancy on O−H′ bonds was not accompanied by bond length alteration but by O−H′ bond orbitals alteration. As discussed in section 3.1, from M1 to M3, the ground state O−H′ bond length only altered by 0.002 Å. However, from M1 to M3, the O−H′ bond orbitals altered mainly in $(sp^{\lambda})_O$ hybrid orbitals (see Table S10 of the SI). According to the NBO calculations, the average percentage of alteration at $(sp^{\lambda})_O$ hybrid orbitals was 33 times more than that at $(sp^{\lambda})_C$ hybrid orbitals. Therefore, the long-range correction plays a role in altering the electron density in the O−H′ bond orbitals; hence the calculated D° of O−H′ bond increases.

Question 5

The text has to be corrected in respect of (1) typos and (2) jargons (for instance XCs in part 2.2).

We apologize for this problem.

(1) We have corrected the typos as we revised questions 2 to 4. We also have corrected and added the missing verbs/noun/preposition.

(2) XC is not jargon. It is an acronym widely used.[1, 2]

To assist readers in getting familiar with the symbols and acronyms used throughout the manuscript, we have provided a list of symbols and acronyms in Table 2. We also corrected the sentences related to the acronyms and symbols.

To accommodate the addition of Table 2, we revised the last paragraph of "2.2. DFT Calculations" as follows.

In the manuscript

We excluded PEC results from M06-2X in the current study because it produced unreasonable results. We also noted that Mardirossian and Head-Gordon [37] reported a similar case. They highlighted that M06-2X poorly predicted the bond length of krypton dimer and benzene-silane dimer through their potential energy curves. We listed the symbols and acronyms in Table 2 to assist readers in getting familiar with them.

Table 2 List of symbols and acronyms used throughout the manuscript

Symbol/acronym	**Description**
D°	Bond dissociation energy
r	Distances between atoms
BDE	Bond dissociation energy
DFT	Density functional theory
ELD	Energy level diagram
IS	Intermediate state
NBO	Natural Bond Orbital
PEC	Potential energy curve
TS	Transition state
XC	Exchange-correlation

References

[1] M.J. Gillan, D. Alfel, and A. Michaelides, J. Chem. Phys.,Perspective: How good is DFT for water?, 144, 130901 (2016)

[2] E. Francisco, J. L. Casals-Sainz, Tomás Rocha-Rinza and A. Martín Pendás, Theor Chem Acc, Partitioning the DFT exchange-correlation energy in line with the interacting quantum atoms approach, 135, 170 (2016)

Theoretical Chemistry Accounts manuscript No.
(will be inserted by the editor)

O—H and C—H bond dissociations in non-phenyl and phenyl groups: A DFT study with dispersion and long-range corrections

Lusia Silfia Pulo Boli[2,3] · **Febdian Rusydi**[1,2] · **Vera Khoirunisa**[2,4] · **Ira Puspitasari**[2,5] · **Heni Rachmawati**[6,7] · **Hermawan Kresno Dipojono**[3]

Received: date / Accepted: date

Abstract Hydrogen atom transfer is one important reaction in biological system, in industry, and in atmosphere. The reaction is preluded by hydrogen bond dissociation. To gain a comprehensive understanding on the reaction, it is necessary to investigate how the current computational methods model hydrogen bond dissociation. As a starting point, we utilized density functional theory-based calculations to identify the effect of dispersion and long-range corrections on O—H and C—H dissociations in non-phenyl and phenyl groups. We employed five different methods, namely B3LYP, CAM-B3LYP (with long-range correction), M06-2X, and B3LYP and CAM-B3LYP with the D3 version of Grimme's dispersion. The results showed that for the case of O—H dissociation in two member of phenyl groups, namely phenol and catechol, the dispersion correction's effect was negligible but the long-range correction's effect was significant. The significant effect was shown by the increasing of energy barrier and the shortening of O—H interatomic distance in the transition state. Therefore, we suggest one should consider the long-range correction in modeling hydrogen bond dissociation in phenolic compounds, namely phenol and catechol.

Keywords O—H and C—H dissociations · non-phenyl and phenyl groups · density functional theory · dispersion correction · long-range correction

✉Febdian Rusydi
rusydi@fst.unair.ac.id

[1] Department of Physics, Faculty of Science and Technology, Universitas Airlangga, Jl. Mulyorejo, Surabaya 60115, Indonesia.

[2] Research Center for Quantum Engineering Design, Faculty of Science and Technology, Universitas Airlangga, Jl. Mulyorejo, Surabaya 60115, Indonesia

[3] Department of Engineering Physics, Faculty of Industrial Engineering, Institut Teknologi Bandung, Bandung 40132, Indonesia

[4] Engineering Physics Study Program, Institut Teknologi Sumatera, Jl. Terusan Ryacudu, Lampung Selatan 35365, Indonesia

[5] Information System Study Program, Faculty of Science and Technology, Universitas Airlangga, Jl. Mulyorejo, Surabaya 60115, Indonesia

[6] School of Pharmacy, Institut Teknologi Bandung, Jl. Ganesha 10, Bandung 40132, Indonesia

[7] Research Center for Nanoscience and Nanotechnology, Institut Teknologi Bandung, Jl. Ganesha 10, Bandung 40132, Indonesia

1 Introduction

Hydrogen atom transfer is one important reaction that occurs in various environments: the biological systems, the atmosphere, and the industry. In biological systems, the reaction takes place in lipid peroxidation formation [1,2] and its prevention, [3–8] as well as in free radicals formation [9]. In the atmosphere, the reaction involves hydroxyl radical (OH) and organic or inorganic materials [10,11]. Meanwhile in industry, one way the reaction occurs is in the presence of a catalyst [12,13]. Overall, the reaction has been a subject of experimental and computational studies. However, there is still a need to understand how the current computational methods can model hydrogen bond dissociation. This understanding will help to achieve a comprehensive insight into the hydrogen atom transfer reaction.

Numerous publications have reported the usage of computational methods based on density functional the-

ory (DFT) to investigate hydrogen bond dissociation. One quantity describing the hydrogen bond dissociation is bond dissociation energy (BDE). In 1999, Barckholtz et al. reported the use of one DFT exchange-correlation (XC) functional, B3LYP, to predict C−H BDE of small aromatics. The predictions were in agreement with the available experimental values [14]. In the following years, the XC was used to predict the BDE of various bonds in small and large molecules [15–17]. On the other hand, other publications showed that B3LYP has low accuracy [18–20] but is reliable to predict the substituent effect such as in alkyl and peroxyl radicals [18]. In 2008, Zhao and Truhlar introduced XC from the Minnesota family, M06-2X. This XC has much-improved accuracy in predicting BDE [21]. M06-2X is reliable for various cases, such as predicting substituent effects on O−C and C−C BDE of lignin [22] and predicting BDE of polyphenols in various solvents [23]. The DFT used for the above prediction was unrestricted [15,22]. In addition to B3LYP and M06-2X, Du et al. used CAM-B3LYP, which includes a long-range correction to B3LYP, in their calculations. They found that CAM-B3LYP underestimates O−CH_3 BDE relative to experimental values. However, this XC has better performance for aromatic molecules than for non-aromatic molecules [24]. Even though many references have reported the use of various DFT XCs for predicting BDE, there is still limited references reported about the path taken by hydrogen atom during the bond dissociation. The use of XCs to model the path is necessary to gain insight into the hydrogen atom transfer reactions. Thus, the present work investigates the effect of dispersion and long-range corrections in O−H and C−H bond dissociations. The corrections have been integrated into DFT XCs. Therefore, it is necessary to use DFT to identify the effect of dispersion and long-range correction on O−H and C−H bond dissociations.

This work aims to study the effects of dispersion and long-range corrections on the O-H and C-H bond dissociations computationally. We utilize DFT with three functionals combined with the D3 version of Grimme's dispersion. The combination is five methods: B3LYP that has been used for chemical computation, CAM-B3LYP that includes a long-range correction, B3LYP-GD3 and CAM-B3LYP-GD3 which includes Grimme's dispersion, and M06-2X that has a good performance for noncovalent interactions [25–28]. The dissociation is designed to occur at O-H and C-H bonds of six non-phenyl and three phenyl groups. The phenyl groups containing O-H bonds are chosen to represent the phenolic compounds. To achieve the goal, we calculate bond dissociation energy and build hydrogen dissociation pathways using two techniques: a relaxed scan calculation and a geometry optimization in the ground and transition states. We have used these two techniques to study other chemical reactions [29–32]. This study will answer the following question: What are the effects of the dispersion and long-range corrections on the O-H and C-H dissociations of non-phenyl and phenyl groups?

2 Computational models

2.1 Reaction model

Scheme 1 presents our model for the hydrogen dissociation. The reactant was R−H′ possessing O−H, or C−H, bond; the products were R and a hydrogen atom. There were nine molecules of interest for R−H′, which were (a) hydroxyl, (b) methylidyne, (c) water, (d) methane, (e) methanol, (f) ethane, (g) toluene, (h) phenol, and (i) catechol. Figure 1 presents the Kekulé structure of these molecules.

$$\underset{\text{[in.]}}{\text{R}-\text{H}'} \longrightarrow \underset{\text{[fi.]}}{\text{R} + \text{H}'}$$

Scheme 1: The initial state [in.] and the final state [fi.] of the reaction model.

[Fig. 1 about here.]

2.2 DFT calculations

We performed computational techniques with the basis of DFT [33,34]. We used 6-311++G(d,p) basis set with three different XCs; they were (1) B3LYP, (2) CAM-B3LYP, and (3) M06-2X which were implemented in Gaussian 16 software [35]. The first XC has become a standard functional for a geometry structure study, while the second XC has improved the long-range interaction of the first XC. The third XC has been parameterized, such that noncovalent interactions take into account. We applied the D3 version of Grimme's dispersion to accommodate the dispersion effect along the dissociation pathways. We combined the XCs and the dispersion into five different methods, as shown in Table 1. In addition to DFT, we used Natural Bond Orbital (NBO) calculations for the natural hybrid orbital and charge population analysis [36].

[Table 1 about here.]

The procedure for DFT calculations is as follows. First, we validated that the three XCs were capable to obtain the spin-state and the geometry in the ground

state. For this purpose, we chose hydroxyl and phenol because they represented molecules with odd and even number of electrons and because their experimental results were available. Second, we performed a geometry optimization to obtain the geometry of all molecules of interest in the ground state using the five calculation methods. To obtain BDE (D°) of hydrogen, we coupled DFT with frequency calculations. It resulted in the total electronic energy with thermal correction to enthalpy at 298.15 K in the ground state. D° was the enthalpy difference between the final and the initial states in Scheme 1. Third, we constructed the hydrogen dissociation pathways.

We employed two different computational techniques for the third DFT calculations procedure. The first technique was a relaxed scan calculation, where one hydrogen atom (with prime mark in Figure 1) left oxygen or carbon atom of R and let R relaxed. The increments were set to be 0.2 Å for all methods. The second one was based on the geometry optimization in the ground and transition states. We applied the first technique to the selected non-phenyl and phenyl groups. The value of D° that was affected and was not affected by dispersion and/or long-range corrections became the restriction in selecting molecules in the first technique. The first technique resulted in potential energy curve (PEC) and the dissociation pathway was visualized using a polar coordinate. We emphasized that the pathway that led to other than hydrogen dissociation would not be discussed further. The PEC that was affected by dispersion and/or long-range corrections became the restriction to select molecules in the second technique. The second technique yielded a dissociation pathway in energy level diagrams (ELD). We have successfully applied both techniques in our previous studies for bigger molecules [29–32].

We excluded PEC results from M06-2X in the current study because it produced unreasonable results. We also noted that Mardirossian and Head-Gordon [37] reported a similar case. They highlighted that M06-2X poorly predicted the bond length of krypton dimer and benzene-silane dimer through their potential energy curves. We listed the symbols and acronyms in Table 2 to assist readers in getting familiar with them.

[Table 2 about here.]

3 Results and discussion

3.1 The ground state structures

Spin-state and geometry The geometry optimization using the three XCs obtained the doublet and singlet as the lowest in energy level for hydroxyl and phenol, respectively. On average, the doublet was 4.6 eV lower than the quartet (in hydroxyl); while the singlet was 4.2 eV lower than the triplet (in phenol). The doublet and the singlet were more stable compared to the quartet and the triplet. The results agree with the ground spin-states of hydroxyl and phenol reported in references [38, 39]. Furthermore, the selected geometrical parameters of hydroxyl and phenol in those spin-states were less than 0.017 Å and 1.4 degrees (see Table 3). The values were within the accuracy limit for DFT calculations [40]. Therefore, the three XCs were capable to obtain the correct ground state structure of the molecules with odd or even number of electrons. Based on these results, the same XCs were used to obtain the ground spin-state of other molecules with an odd and even numbers of electrons which were doublet and singlet, respectively.

[Table 3 about here.]

The dispersion and long-range corrections Table 4 presents O−H′ and C−H′ bond lengths of the obtained ground state geometry of all molecules of interest. The Cartesian coordinates of the ground state geometry were given in Table S1-S9 of Supplementary Information (SI). Calculation using the method with dispersion correction (M2 and M4) obtained the same bond length as the method without the correction (M1 and M3). The method with the long-range correction (M3) and the method parameterized with dispersion-like interaction (M5) obtained slightly shorter bond lengths (the negative values) than the method without the correction (M1). The results suggest the dispersion and the long-range corrections do not alter the ground state O−H′ and C−H′ bond lengths of our molecules of interest.

[Table 4 about here.]

3.2 The bond dissociation energy

Table 5 presents the discrepancy of D° between the calculated and experimental values. Among all methods, the M5 method obtained D° the closest to the experimental values for molecules with singlet spin-state. The results supported the work of Zhao and Truhlar [21], which suggested using the M5 method for D° calculations of molecules with singlet spin-state. Therefore, M06-2X functional is suitable for dealing with the hydrogen dissociation energy of molecules with singlet spin-state.

[Table 5 about here.]

The discrepancies obtained by M2, M3, and M4 were varied compared to that obtained by M1. In all molecules [Table 5 (a)-(i)], M2 obtained 0.9 kJ/mol (in average) discrepancies higher than M1 did. Moreover, M4 obtained 0.6 kJ/mol (in average) discrepancies higher than M3 did. The results indicate that the dispersion correction does not alter the calculated D° of molecules with singlet and doublet spin-states. In hydroxyl and methylidyne [Table 5 (a) and (b)], M3 obtained 1.9 kJ/mol (in average) discrepancies lower than M1 did. Meanwhile, in other molecules [Table 5 (c)-(i)], M3 obtained 4.4 kJ/mol (in average) discrepancies higher than M1 did. The 4.4 kJ/mol is significant, which implies that the long-range correction is the reason for D° alteration of molecules with singlet spin-state. Thus, the long-range correction plays a role in altering D° of molecules with singlet spin-state but not the molecules with doublet spin-state.

Among seven molecules in Table 5 (c)-(i), the alteration of discrepancies from M1 to M3 on O−H′ bonds differed from that on C−H′ bonds. The seven molecules were in their singlet spin-state. For four molecules with O−H′ bonds, the discrepancies increased by 5.7 kJ/mol (on average) from M1 to M3. However, for three molecules with C−H′ bonds, the discrepancies only increased by 2.8 kJ/mol (in average) from M1 to M3. The increase on O−H′ bonds is more significant than on C−H′ bonds. It indicates that the long-range correction alters the calculated D° on O−H′ bond more than that on C−H′ bond of molecules with singlet spin-state.

The increase in the discrepancy on O−H′ bonds was not accompanied by bond length alteration but by O−H′ bond orbitals alteration. As discussed in section 3.1, from M1 to M3, the ground state O−H′ bond length only altered by 0.002 Å. However, from M1 to M3, the O−H′ bond orbitals altered mainly in $(sp^\lambda)_O$ hybrid orbitals (see Table S10 of the SI). According to the NBO calculations, the average percentage of alteration at $(sp^\lambda)_O$ hybrid orbitals was 33 times more than that at $(sp^\lambda)_C$ hybrid orbitals. Therefore, the long-range correction plays a role in altering the electron density in the O−H′ bond orbitals; hence the calculated D° of O−H′ bond increases.

3.3 The potential energy curve

Figure 2 shows the PECs of four selected molecules together with their respective polar coordinates. All methods yielded two types of PEC profiles. The first type was a PEC-like of dissociation diatomic molecules [Figure 2(a)–2(b) left]. Region I described the dissociation process, and region II described H′ was already a free atom. All methods agreed one to each other. The second type was somewhat challenging to explain since not all methods agreed [Figure 2(c)–2(d) left]. There was region III that contained barriers. PEC profiles in methylidyne and ethane were supportive results to the first type, while PEC profiles in hydroxyl and water were supportive results to the second type. Hence, they were placed in Supporting Information [Figure S1(a)–(b) and S1(c)–(d) left]. On the other hand, the polar coordinates show that the hydrogen dissociation pathways in methane [Figure 2(a) right] are different from those in other molecules [Figure 2(b)–2(d) right and Figure S1(c)–(d) right of the SI]. All methods were only agreed for methane. It implies that the corrections (long-range and dispersion) significantly affect the pathway in real space rather than in the PEC profile.

[Fig. 2 about here.]

Overall, the PEC profiles of methanol and phenol [Figure 2(c)–2(d) left] were explained as follows. In region III, methanol and phenol had barriers; methanol had one, and phenol had at least three barriers. In both cases, M2 yielded a similar barrier height to M1 did. So did M4 and M3. It means the dispersion correction does not alter the PEC profile of O−H′ dissociation. However, in both cases, M3 yielded a different barrier height than M1 did. The results indicate that the long-range correction does alter the PEC profile of O−H′ dissociation. Therefore, the long-range correction plays a more significant role than the dispersion correction in the PEC profiles of O−H′ dissociation.

In detail, for phenol [Figure 2(d)], the variation of PEC profiles was accompanied by the variation of dissociation pathways in the polar coordinate. Both variations occurred only at a certain O−H′ distance ($r_{\mathrm{O-H'}}$) range. The PEC profile variation range was around 1.8–3 Å; while the pathway variation range was around 2–4 Å. In those ranges, M3 yielded a different profile and pathway than M1 did. Kamiya et al.[43] also obtained different profiles when using XCs with long-range correction in a system interacting through a van der Waals interaction (noncovalent interaction). Thus, the different profiles obtained by the long-range correction (M3) may be due to the presence of noncovalent interactions, particularly at a region with barriers. Therefore, in line with its role in O−H′ BDE, the long-range correction may play a role in the energy barrier of O−H′ dissociation.

Along the phenol dissociation pathway, M1 and M3 obtained different r at B1a, B1b, and B2 (See Table S11 of the SI). At B1a and B1b, atom H′ was located around atom O [See Figure S2 of the SI]. Here, M3 obtained shorter $r_{\mathrm{O-H'}}$ at B1a than M1 did at B1b. Different than at B1a and B1b, at B2 atom H′ was located be-

tween atom 2 and atom 3. Here, M3 obtained shorter $r_{2-H'}$ and longer $r_{3-H'}$ than M1 did. The results indicate that the shortening and lengthening of r are due to the long-range correction.

The r alteration after the introduction of long-range correction was accompanied by atomic charges alteration. The NBO calculations showed that atom O, 2, and 3 [See Figure 1(h)] were negatively charged while atom H′ was positively charged. At B1a, M3 yielded greater positive charge on atom H′ and greater negative charge on atom O than M1 did. It implies that the increasing coulombic attraction between atom O and H′ is the reason for the shortening of $r_{O-H'}$ at B1a. At B2, M3 obtained lesser positive charge on atom H′ and greater negative charge on atom 2 than M1 did. It indicates that the increasing coulombic attraction between atom 2 and H′ is the reason for the shortening of the $r_{2-H'}$. At this location, M3 obtained lesser negative charge on atom 3 than M1 did. It implies the increasing coulombic repulsion between atom 3 and H′ is the reason for the lengthening of the $r_{3-H'}$. Therefore, the Coulombic interactions play a role in the alteration of r.

3.4 The dissociation pathway

Figure 3 shows the O−H′ dissociation pathways of two selected molecules, phenol and catechol, in an ELD. For the case of phenol [Figure 3(a)], each pathway had three transition states (TS) and three intermediate states (IS) as predicted earlier in Figure 2(d)left; while for the case of catechol [Figure 3(b)], each pathway had two TSs and two ISs. The experiment has observed the presence of IS1 in a photochemical reaction [44]. While a theoretical study reported IS1 and IS3 as two isomers of phenol [45]. Another theoretical study reported the first step in decomposition of catechol lead to IS4 [46]. The similarity between the molecules in the intermediate states with the previous studies indicate the possibility of hydrogen migration before O−H′ dissociation occurred.

[Fig. 3 about here.]

The dissociation pathways in phenol and catechol showed that all methods obtained the same relative electronic energy order in each TS. The order for both cases was M1 ≈ M2 < M3 ≈ M4 < M5. For the case of phenol, the average difference between the energy obtained by methods with long-range correction (M3 and M4) and methods without the correction (M1 and M2) was 0.16 eV. Similarly, for the case of catechol, the average difference was 0.14 eV. The differences are significant. It was aligned with the PEC profile difference [Figure 2(d)left] after the long-range correction was introduced, particularly at the region with barriers. The results imply that the long-range correction predicts the dissociation is more difficult at a region where the non-covalent interaction may be present. Therefore, the correction indeed plays a role in the energy barrier of O−H′ dissociation.

Methods with long-range correction (M3 and M4) obtained shorter r than methods without the correction did in the TS structures. For the case of phenol, the $r_{O-H'}$ and $r_{3-H'}$ shortened by 0.01 Å on average. The shortening was also similar to the case of catechol. The 0.01 Å is significant compared to the O−H′ bond length shortening in the ground state of phenol and catechol [Table 4(h) and (i)]. Thus, the shortening confirms the shortening of r along the dissociation pathway discussed in Subsection 3.3. For this reason, the long-range correction indeed plays a role in r in the transition state.

Methods with the long-range correction (M3 and M4) obtained similar relative electronic energy to M5 did in the TSs. The average differences of relative electronic energy obtained by those methods were 0.07 for phenol and 0.06 for catechol. These values are very small which indicate the similarity of transition state according to those methods. Therefore, CAM-B3LYP and M06-2X predicts comparable transition state of O−H′ dissociation.

Overall, all methods showed consistent performances on the BDE calculations and O−H′ dissociation pathways prediction. For the BDE calculations, the methods obtained the $D°$ of O−H′ bonds in all molecules increased in the following order: M1 ≈ M2 < M3 ≈ M4 < M5. The increase of $D°$ after the presence of long-range correction in CAM-B3LYP (M3) was in agreement with the study by Chan et al. [47] For the pathways prediction, the methods obtained variation of pathways in phenol and cathecol dissociation. The variations were identified by the alteration in energy barriers and $r_{O-H'}$ in the TS. The energy barrier increased in the same order as the increase in $D°$ of O−H′ bonds. This result validates the study by Peach et al. [48] that showed increasing barrier height when using CAM-B3LYP compared to B3LYP. The increasing energy barriers was accompanied by the shortening of $r_{O-H'}$ as follows: M1 ≈ M2 > M3 ≈ M4. The shortening due to the long-range correction (M3) was in agreement with our previous study [31]. The results show the significance of this research: the use of long-range correction in CAM-B3LYP affects the $r_{O-H'}$ in TS. On the other hand, the M06-2X used in this study predicted the highest $D°$ and energy barrier. The $D°$ was similar to the experimental observation. Its developer suggested the functional

for applications involving main group thermochemistry, kinetics, and noncovalent interactions [21,28].

4 Conclusion

We have studied the effects of dispersion and long-range corrections on O−H and C−H dissociations of non-phenyl and phenyl groups. The effects were identified through bond dissociation energy and dissociation pathways. We summarized that the dispersion correction had negligible effects on the O−H and C−H bond dissociation energies and the non-phenyl and phenyl groups dissociation pathways. While the long-range correction in CAM-B3LYP had a minor effect on the O−H bond dissociation energy and a significant effect on the O−H dissociation pathways. We found that the long-range correction increased the bond dissociation energy of the O−H bond of non-phenyl and phenyl groups in their singlet states by 5.7 kJ/mol. We argued that the increase was due to the alteration of electron density in the O−H bond orbitals. However, the dissociation energy was still far from the experimental results. The significant effects of the long-range correction on the O−H dissociation pathways occurred in two members of phenyl groups, namely phenol and catechol. The effects were identified as follows. First, the correction shortened the O−H distances in the transition states by 0.01 Å, on average. Second, the correction increased the energy barrier by 0.16 eV (in phenol) and 0.14 eV (in catechol), on average. Overall, our results support other theoretical studies on the increasing energy barrier due to the long-range correction. Accordingly, we suggest that one should consider the long-range correction when studying hydrogen bond dissociation in phenolic compounds, such as phenol and catechol.

Acknowledgements Authors thank to Rizka Nur Fadilla from Research Center for Quantum Engineering Design (RCQED), Universitas Airlangga for the insightful discussions. LSPB is grateful for the doctoral scholarship by Lembaga Pengelola Dana Pendidikan (LPDP). All calculations using Gaussian 16 software are performed at Riven Cluster, the high performance computing facility in RCQED, Universitas Airlangga, Indonesia.

Declarations

Funding

No funding was received for conducting this study.

Conflict of Interest

The authors have no conflicts of interest to declare that are relevant to the content of this article.

Availability of Data and Materials

All data analysed during this study are included in this published article and its supplementary information file.

Code Availability

Not Applicable.

Authors Contribution

Conceptualization: F.R.; formal analysis: L.S.P.B, H.R., and I.P.; investigation: L.S.P.B and V.K.; methodology: F.R. and L.S.P.B; writing—original draft preparation: L.S.P.B; writing—review and editing: F.R. and H.K.D. All authors have read and agreed to the published version of the manuscript.

References

1. Zielinski ZAM and Pratt DA (2017) J Org Chem 82, 6, 2817–2825
2. Yin H and Porter NA (2011) Chem. Rev. 111, 10, 5944–5972
3. Shang Y, Zhou H, Li X, Zhou J, Chen K (2019) New J Chem 43: 15736-15742
4. Vo QV, Nam PC, Bay MV, Thong NM, Cuong ND, and Mechler A (2018) Sci Rep 8: 12361
5. Xue Y, Zheng Y, An L, Dou Y, Liu Y (2014) Food Chem 151: 198-206.
6. Iuga C, Alvarez-Idaboy JR, Russo N (2012) J Org Chem 12: 3868-3877.
7. Galano A, Alvarez-Diduk R, Ramirez-Silva MT, Alarcon-Angeles G, Rojas-Hernandez A (2009) Chem Phys 363: 13-23.
8. Jovanovic SV, Steenken S, Boone CW, Simic MG (1999) J Am Chem Soc 121:9677-9681.
9. Wang Y-N and Eriksson LA (2001) Theor Chem Acc 106:158-162
10. Mallick S, Sarkar S, Bandyopadhyay B, and Kumar P (2018) J Phys Chem A 122, 1, 350–363
11. Kumar M, Sinha A, and Francisco JS (2016) Acc Chem Res 49, 5, 877–883
12. Liang F, Zhong W, Xiang L, Mao L, Xu Q, Kirk SR, and Yin D (2019) J. Catal. 378:256-269
13. Asgari P, Hua Y, Bokka A, Thiamsiri C, Prasit-watcharakorn W, Karedath A, Chen X, Sardar S, Yum K, Leem G, Pierce BS, Nam K, Gao J, and Jeon J (2019) Nat Catal 2:164–173
14. Barckholtz C, Barckholtz TA, and Hadad CM (1999) J Am Chem Soc 121, 3, 491–500

15. Wang L, Yang F, Zhao X, and Li Y (2019) Food Chem 275: 339-345
16. Nantasenamat C, Isarankura-Na-Ayudhya C, Naenna T, Prachayasittikul V (2008) J Mol Graph Model 27:188-196
17. Zhang H-Y, Sun Y-M, and Wang X-L (2003)Chem Eur J 9:502-508
18. Brinck T, Lee H-N, Jonsson M (1999) J Phys Chem 103:7094-7104
19. Izgorodina EI, Coote ML, Radom L (2005) J Phys Chem A 109:7558-7566
20. Izgorodina EI, Brittain DRB, Hodgson JL, Krenske EH, Lin CY, Namazian M, and Coote ML (2007) J Phys Chem A 111: 10754-10768
21. Zhao Y and Truhlar DG (2008) J Phys Chem A 112: 1095-1099
22. Beste A and Buchanan III AC (2009) J Org Chem 74(7): 2837–2841
23. Zheng Y-Z, Fu Z-M, Deng G, Guo R, Chen D-F (2020) Phytochemistry 178: 112454
24. Du T, Quina FH, Tunega D, Zhang J, Aquino AJA (2020) Theor Chem Acc 139:75
25. Yanai T, Tew DP, Handy NC (2004) Chem Phys Lett 393: 51-57
26. Grimme S, Antony J, Ehrlich S, Krieg H (2010) J Chem Phys 132: 154104
27. Becke AD (1993) J Chem Phys 98: 5648
28. Zhao Y, Truhlar DG (2008) Theor Chem Acc 120: 215-241
29. Rusydi F, Madinah R, Puspitasari I, Mark-Lee WF, Ahmad A, Rusydi A (2020) Biochem Mol Biol Educ https://doi.org/10.1002/bmb.21433
30. Fadilla RN, Rusydi F, Aisyah ND, Khoirunisa V, Dipojono HK, Ahmad F, Mudasir, Puspitasari I (2020) Molecules 25: 670
31. Rusydi F, Aisyah ND, Fadilla RN, Dipojono HK, Ahmad F, Mudasir, Puspitasari I, Rusydi A (2019) Heliyon 5: e02409
32. Fadilla RN, Aisyah ND, Dipojono HK, Rusydi F (2017) Procedia Eng 170: 113-118
33. Hohenberg P, Kohn W (1964) Phys Rev 136: B864
34. Kohn W, Sham LJ (1965) Phys Rev 140: A1133
35. M. J. Frisch, G. W. Trucks, H. B. Schlegel, G. E. Scuseria, M. A. Robb, J. R. Cheeseman, G. Scalmani, V. Barone, G. A. Petersson, H. Nakatsuji, X. Li, M. Caricato, A. V. Marenich, J. Bloino, B. G. Janesko, R. Gomperts, B. Mennucci, H. P. Hratchian, J. V. Ortiz, A. F. Izmaylov, J. L. Sonnenberg, D. Williams-Young, F. Ding, F. Lipparini, F. Egidi, J. Goings, B. Peng, A. Petrone, T. Henderson, D. Ranasinghe, V. G. Zakrzewski, J. Gao, N. Rega, G. Zheng, W. Liang, M. Hada, M. Ehara, K. Toyota, R. Fukuda, J. Hasegawa, M. Ishida, T. Nakajima, Y. Honda, O. Kitao, H. Nakai, T. Vreven, K. Throssell, J. A. Montgomery, Jr., J. E. Peralta, F. Ogliaro, M. J. Bearpark, J. J. Heyd, E. N. Brothers, K. N. Kudin, V. N. Staroverov, T. A. Keith, R. Kobayashi, J. Normand, K. Raghavachari, A. P. Rendell, J. C. Burant, S. S. Iyengar, J. Tomasi, M. Cossi, J. M. Millam, M. Klene, C. Adamo, R. Cammi, J. W. Ochterski, R. L. Martin, K. Morokuma, O. Farkas, J. B. Foresman, and D. J. Fox (2013) Gaussian 16, Revision C.01, Gaussian, Inc., Wallingford CT
36. Glendening ED, Reed AE, Carpenter JE, Weinhold F Nbo version 3.1
37. Mardirossian N and Head-Gordon M (2016) J Chem Theory Comput 12: 4303-4325
38. Jones DB, da Silva GB, Neves RFC, Duque HV, Chiari L, de Oliveira EM, Lopes MCA, da Costa RF, Varella MTN, Bettega MHF, Lima MAP and Brunger MJ (2014) J Chem Phys 141: 074314
39. Huber KP and Herzberg G, Molecular Spectra and Moelcular Structure IV. Constants of Diatomic Molecules, Springer US, 1979, page 508
40. Young DC, Computational chemistry: A practical guide for applying techniques to real-world problems, John Wiley & Sons Inc., New York, 2001, Chp. 16, Page 138
41. Haynes WM, CRC Handbook of Chemistry and Physics, 95th ed., CRC Press, Boca Rotan, 2014, Chp.9
42. Lucarini M, Pedulli GF, Guerra M (2004) Chem Eur J 10: 933-939
43. Kamiya M, Tsuneda T and Hirao K (2002) J Chem Phys 117: 6010
44. Parker K and Davis SR (1999) J Am Chem Soc 121: 4271-4277
45. Zhu L and Bozzelli JW (2003) J Phys Chem A 107: 3696-3703
46. Altarawneh M, Dlugogorski BZ, Kennedy EM and Mackie J (2010) J Phys Chem A. 114: 1060-1067
47. Chan B, Morris M and Radom L (2011) Aust J Chem 64: 394-402
48. Peach MJG, Helgaker T, Salek P, Keal TW, Lutnæs OB, Tozer DJ and Handyd NC (2006) Phys Chem Chem Phys 8: 558-562

List of Figures

1 **Fig. 1** Kekulé structure of the molecule of interest. The primed H was the dissociated hydrogen atom. For clarity in molecules (g) – (i), only dissociated hydrogen atom was shown, and carbon atoms were replaced by numbers 9

2 **Fig. 2** PECs of C−H′ and O−H′ bond dissociations with their respective polar coordinates. The I, II, and III represented three different regions based on the similarity of events at each region. Angles in the polar coordinate were H−C−H′ in methane, 2–1–C−H′ in toluene, H−C−O−H′ in methanol, and 2–1–O−H′ in phenol (see Figure 1). The initial angle was at zero degree, then deviated clockwise or counterclockwise. Particularly in methane, the clockwise represented inward deviation. **B1a**, **B1b**, **B2**, and **B3** in (d) represented first barrier obtained by M1 and M2, first barrier obtained by M3 and M4, second and third barrier obtained by all four methods, respectively 10

3 **Fig. 3** Energy level diagram for O−H′ dissociation pathways of two selected molecules. R1, R2, P1, and P2 represent phenol, catechol, product of phenol dissociation, and product of catechol dissociation. While TS and IS stand for transition state and intermediate state. The TSs were shown with the selected interactomic distances (unit in Å) 11

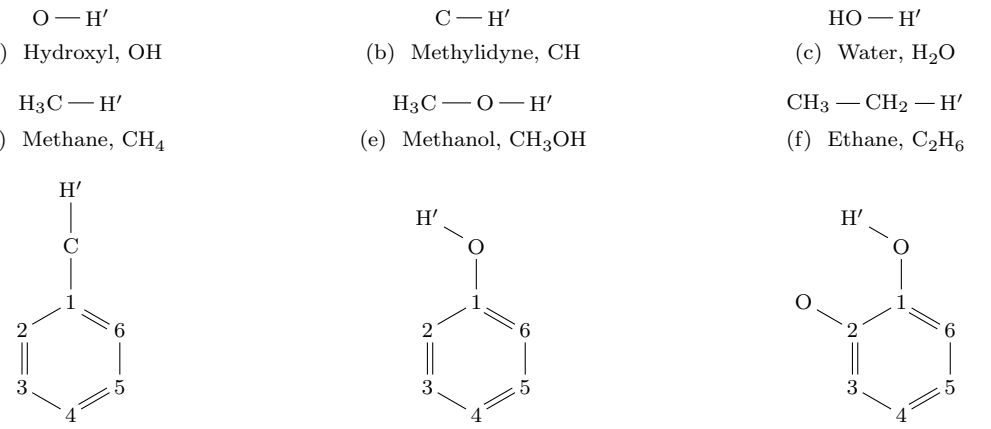

(a) Hydroxyl, OH (b) Methylidyne, CH (c) Water, H_2O

(d) Methane, CH_4 (e) Methanol, CH_3OH (f) Ethane, C_2H_6

(g) Toluene, $C_6H_5CH_3$ (h) Phenol, C_6H_5OH (i) Catechol, $C_6H_4(OH)_2$

Fig. 1 Kekulé structure of the molecule of interest. The primed H was the dissociated hydrogen atom. For clarity in molecules (g) – (i), only dissociated hydrogen atom was shown, and carbon atoms were replaced by numbers

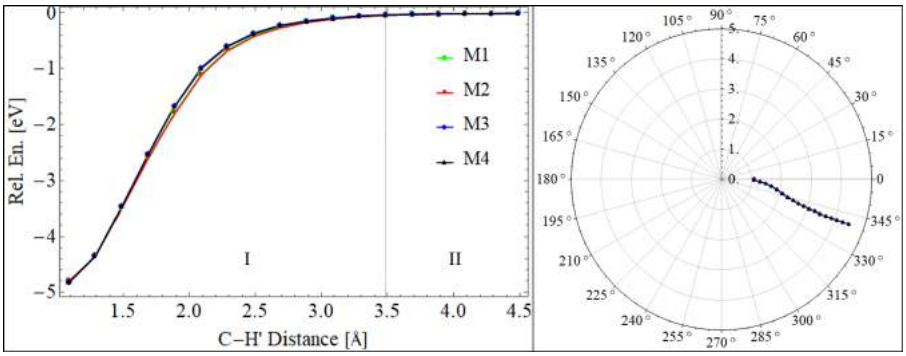

(a) PEC (left) and polar coordinate (right) of methane.

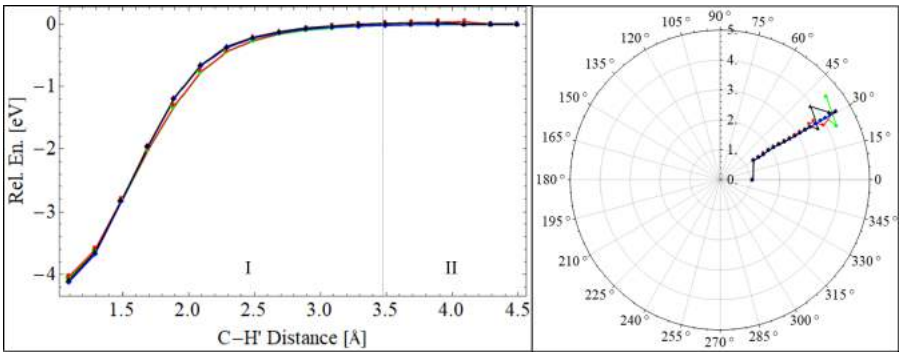

(b) PEC (left) and polar coordinate (right) of toluene.

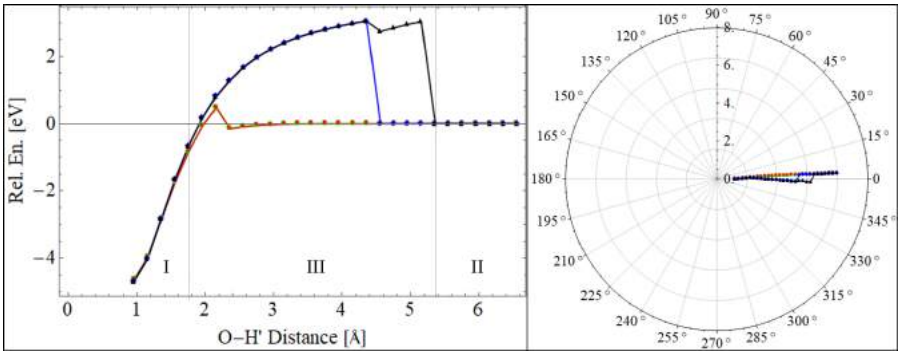

(c) PEC (left) and polar coordinate (right) of methanol.

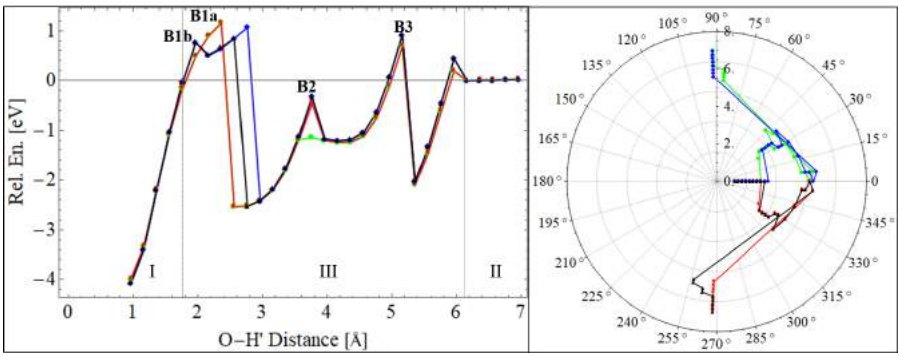

(d) PEC (left) and polar coordinate (right) of phenol.

Fig. 2 PECs of C−H′ and O−H′ bond dissociations with their respective polar coordinates. The I, II, and III represented three different regions based on the similarity of events at each region. Angles in the polar coordinate were H−C−H′ in methane, 2–1–C−H′ in toluene, H−C−O−H′ in methanol, and 2–1–O−H′ in phenol (see Figure 1). The initial angle was at zero degree, then deviated clockwise or counterclockwise. Particularly in methane, the clockwise represented inward deviation. **B1a**, **B1b**, **B2**, and **B3** in (d) represented first barrier obtained by M1 and M2, first barrier obtained by M3 and M4, second and third barrier obtained by all four methods, respectively

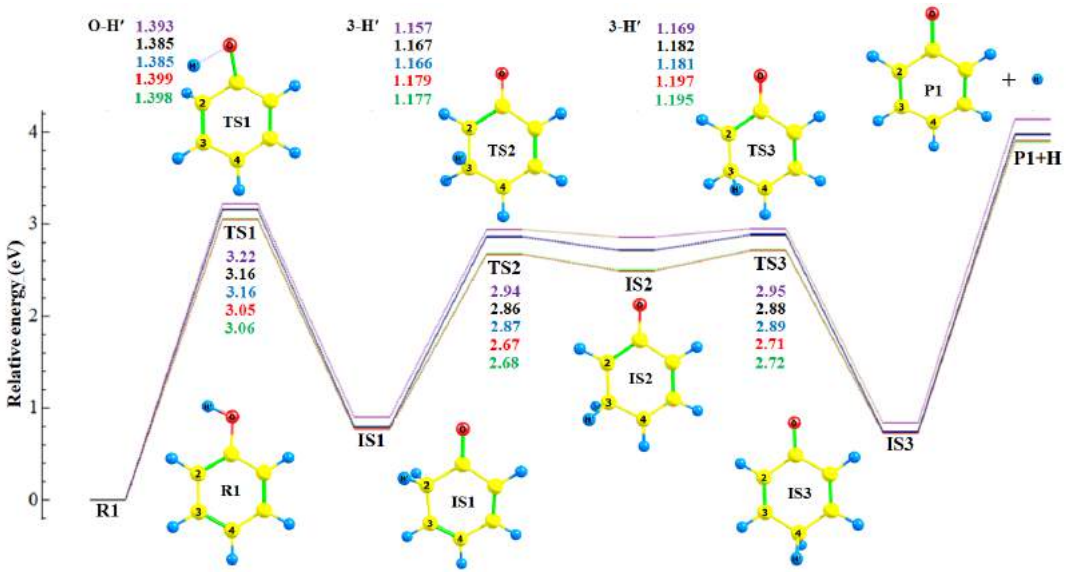

(a) O−H′ dissociation pathways of phenol

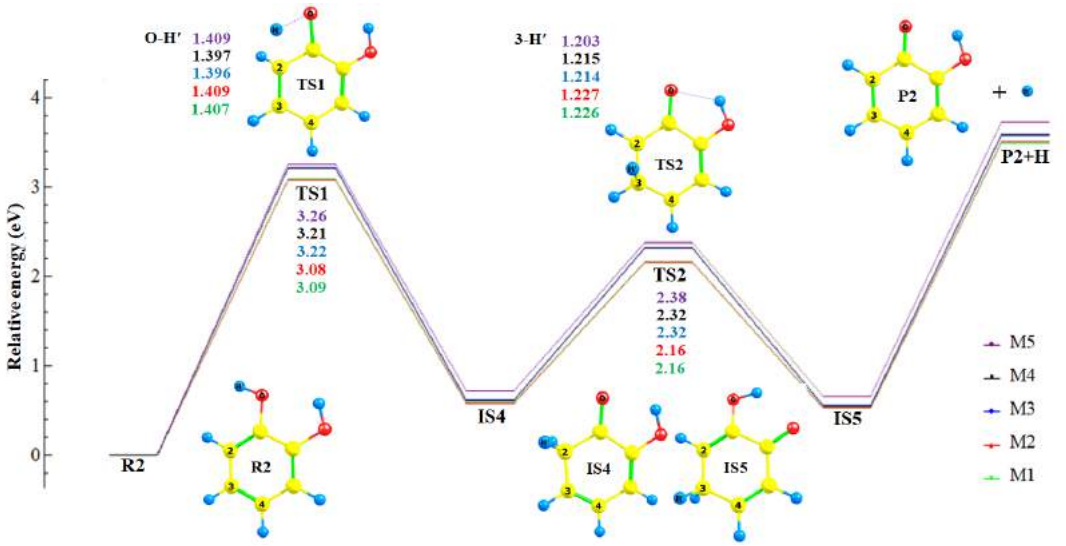

(b) O−H′ dissociation pathways of catechol

Fig. 3 Energy level diagram for O−H′ dissociation pathways of two selected molecules. R1, R2, P1, and P2 represent phenol, catechol, product of phenol dissociation, and product of catechol dissociation. While TS and IS stand for transition state and intermediate state. The TSs were shown with the selected interactomic distances (unit in Å)

List of Tables

1 **Table 1** List of methods used in the manuscript 13
2 **Table 2** List of symbols and acronyms used throughout the manuscript 14
3 **Table 3** The discrepancy of calculated geometrical parameters of hydroxyl and phenol by (1) B3LYP, (2) CAM-B3LYP, and (3) M06-2X with respect to the experimental values [41]. The parameters were bond length (R, in Å) and bond angle (A, in degree). The parameter in (i) belongs to hydroxyl; while others belong to phenol 15
4 **Table 4** The difference of calculated O−H′ and C−H′ bond lengths from M1 (Å). The label referred to Figure 1 16
5 **Table 5** The discrepancy of calculated D° with respect to the experimental values (kJ/mol) [41,42]. The label referred to Figure 1 17

Table 1 List of methods used in the manuscript

M1	B3LYP
M2	B3LYP + GD3
M3	CAM-B3LYP
M4	CAM-B3LYP + GD3
M5	M06-2X

Table 2 List of symbols and acronyms used throughout the manuscript

Symbol/acronym	**Description**
D°	Bond dissociation energy
r	Distances between atoms
BDE	Bond dissociation energy
DFT	Density functional theory
ELD	Energy level diagram
IS	Intermediate state
NBO	Natural Bond Orbital
PEC	Potential energy curve
TS	Transition state
XC	Exchange-correlation

Table 3 The discrepancy of calculated geometrical parameters of hydroxyl and phenol by (1) B3LYP, (2) CAM-B3LYP, and (3) M06-2X with respect to the experimental values [41]. The parameters were bond length (R, in Å) and bond angle (A, in degree). The parameter in (i) belongs to hydroxyl; while others belong to phenol

	Parameter	Expr.	(1)	(2)	(3)
(i)	R(O,H′)	0.970	+0.006	+0.005	+0.003
(ii)	R(O,H′)	0.956	+0.007	+0.005	+0.005
(iii)	R(C,C)av	1.397	-0.003	-0.009	-0.006
(iv)	R(1,O)	1.364	+0.006	0.000	-0.001
(v)	R(4,H)	1.082	+0.001	+0.001	0.000
(vi)	R(5,H)	1.076	+0.008	+0.008	+0.008
(vii)	R(6,H)	1.084	+0.002	+0.001	+0.002
(viii)	A(1,O,H′)	109.0	+0.8	+1.0	+0.8

Table 4 The difference of calculated O−H′ and C−H′ bond lengths from M1 (Å). The label referred to Figure 1

	Molecule	Bond	M1	M2	M3	M4	M5
(a)	Hydroxyl	O−H′	0.976	0.000	-0.002	-0.002	-0.004
(b)	Methylidyne	C−H′	1.127	0.000	-0.003	-0.003	-0.007
(c)	Water	O−H′	0.962	0.000	-0.001	-0.001	-0.003
(d)	Methane	C−H′	1.091	0.000	-0.001	-0.001	-0.002
(e)	Methanol	O−H′	0.961	0.000	-0.002	-0.002	-0.003
(f)	Ethane	C−H′	1.094	0.000	-0.001	-0.001	-0.002
(g)	Toluene	C−H′	1.094	0.000	-0.002	-0.002	-0.002
(h)	Phenol	O−H′	0.963	0.000	-0.002	-0.002	-0.002
(i)	Catechol	O−H′	0.962	0.000	-0.002	-0.002	-0.002

Table 5 The discrepancy of calculated D° with respect to the experimental values (kJ/mol) [41,42]. The label referred to Figure 1

	Molecule	Bond	Expr.	M1	M2	M3	M4	M5
(a)	Hydroxyl	O−H,	429.73	-1.1	-1.1	-0.8	-0.8	-9.2
(b)	Methylidyne	C−H,	338.4	+1.8	+1.8	-2.2	-2.2	-8.1
(c)	Water	O−H,	497.32	-17.1	-17.1	-14.0	-14.0	-11.7
(d)	Methane	C−H,	439.3	-8.3	-8.2	-7.1	-7.0	-6.1
(e)	Methanol	O−H,	440.2	-26.4	-25.2	-21.1	-20.3	-11.5
(f)	Ethane	C−H,	420.5	-8.9	-7.6	-6.8	-6.0	-3.4
(g)	Toluene	C−H,	375.5	-10.8	-9.1	-5.8	-4.7	+2.9
(h)	Phenol	O−H,	362.8	-16.0	-14.6	-9.6	-8.6	+6.7
(i)	Catechol	O−H,	342.3	-32.0	-29.9	-24.0	-22.5	-9.8

Theoretical Chemistry Accounts

O-H and C-H bond dissociations in non-phenyl and phenyl groups: A DFT study with dispersion and long-range corrections

--Manuscript Draft--

Manuscript Number:	TCAC-D-20-00473R2
Full Title:	O-H and C-H bond dissociations in non-phenyl and phenyl groups: A DFT study with dispersion and long-range corrections
Article Type:	Regular Article
Keywords:	density functional theory; dispersion correction; energy; long-range correction; non-phenyl and phenyl groups; O—H and C—H dissociations
Corresponding Author:	Febdian Rusydi, Ph.D Universitas Airlangga Surabaya, Jawa Timur INDONESIA
Corresponding Author Secondary Information:	
Corresponding Author's Institution:	Universitas Airlangga
Corresponding Author's Secondary Institution:	
First Author:	Lusia Silfia Pulo Boli, Master
First Author Secondary Information:	
Order of Authors:	Lusia Silfia Pulo Boli, Master
	Febdian Rusydi, PhD
	Vera Khoirunisa, Master
	Ira Puspitasari, PhD
	Heni Rachmawati, PhD
	Hermawan Kresno Dipojono, PhD
Order of Authors Secondary Information:	
Funding Information:	Universitas Airlangga (1148/UN3.14/LT/2019) — Dr Febdian Rusydi
	Kementerian Riset Teknologi Dan Pendidikan Tinggi Republik Indonesia (1288r/I1.C06/PL/2020) — Prof. Hermawan Kresno Dipojono
Abstract:	Hydrogen atom transfer is one important reaction in biological system, in industry, and in atmosphere. The reaction is preluded by hydrogen bond dissociation. To gain a comprehensive understanding on the reaction, it is necessary to investigate how the current computational methods model hydrogen bond dissociation. As a starting point, we utilized density functional theory-based calculations to identify the effect of dispersion and long-range corrections on O—H and C—H dissociations in non-phenyl and phenyl groups. We employed five different methods, namely B3LYP, CAM-B3LYP (with long-range correction), M06-2X, and B3LYP and CAM-B3LYP with the D3 version of Grimme's dispersion. The results showed that for the case of O—H dissociation in two member of phenyl groups, namely phenol and catechol, the dispersion correction's effect was negligible but the long-range correction's effect was significant. The significant effect was shown by the increasing of energy barrier and the shortening of O—H interatomic distance in the transition state. Therefore, we suggest one should consider the long-range correction in modeling hydrogen bond dissociation in phenolic compounds, namely phenol and catechol.
Response to Reviewers:	We are grateful for the reviewer's constructive concerns about our manuscript. Here we respond to the reviewer's comments point by point and revise the manuscript (marked by blue color) according to the comments.

	We hope that our revised manuscript meets the reviewer's expectations. Sincerely, on behalf of all authors Lusia Silfia Pulo Boli

BEGIN

Question 1

The most of the questions are answered in the revised form. However, it is still not clear what kind of dissociation is modelled. The Scheme 1 in the present form is wrong. It should be either $R{-}H' \longrightarrow R^{\bullet} + H^{\bullet\prime}$ or $R{-}H' \longrightarrow R^{-} + H^{+\prime}$ depending on what kind of dissociation is presented – homolytic or heterolytic.

We realize that (1) our explanation about the type of dissociation modelled was unclear and (2) the reaction modelled in Scheme 1 was wrong.

To address these issues:

(1) we revise the first paragraph of "2.1. Reaction model" as follows.

In the manuscript

Scheme 1 presents our model for the homolytic hydrogen dissociation. The reactant was $R{-}H'$ possessing O−H, or C−H, bond; the products were $R^{\bullet}$ and a hydrogen atom ($H'^{\bullet}$). There were nine molecules of interest for $R{-}H'$, which were (a) hydroxyl, (b) methylidyne, (c) water, (d) methane, (e) methanol, (f) ethane, (g) toluene, (h) phenol, and (i) catechol. Figure 1 presents the Kekulé structure of these molecules.

We also revise the writing of $R^{\bullet}$ and $H'^{\bullet}$ throughout the manuscript.

(2) we revise Scheme 1 as follows.

$$\underset{\text{[in.]}}{R{-}H'} \longrightarrow \underset{\text{[fi.]}}{R^{\bullet} + H'^{\bullet}}$$

Scheme 1: The initial state [in.] and the final state [fi.] of the reaction model.

The superscripts in $H'^{\bullet}$ is written according to [1].

References

[1] Carey FA and Sundberg RJ (2007) Advanced Organic Chemistry Part A: Structure and Mechanisms, Fifth Ed., Springer Science+Business Media.

Theoretical Chemistry Accounts manuscript No.
(will be inserted by the editor)

O—H and C—H bond dissociations in non-phenyl and phenyl groups: A DFT study with dispersion and long-range corrections

Lusia Silfia Pulo Boli[2,3] · **Febdian Rusydi**[1,2] · **Vera Khoirunisa**[2,4] · **Ira Puspitasari**[2,5] · **Heni Rachmawati**[6,7] · **Hermawan Kresno Dipojono**[3]

Received: date / Accepted: date

Abstract Hydrogen atom transfer is one important reaction in biological system, in industry, and in atmosphere. The reaction is preluded by hydrogen bond dissociation. To gain a comprehensive understanding on the reaction, it is necessary to investigate how the current computational methods model hydrogen bond dissociation. As a starting point, we utilized density functional theory-based calculations to identify the effect of dispersion and long-range corrections on O—H and C—H dissociations in non-phenyl and phenyl groups. We employed five different methods, namely B3LYP, CAM-B3LYP (with long-range correction), M06-2X, and B3LYP and CAM-B3LYP with the D3 version of Grimme's dispersion. The results showed that for the case of O—H dissociation in two member of phenyl groups, namely phenol and catechol, the dispersion correction's effect was negligible but the long-range correction's effect was significant. The significant effect was shown by the increasing of energy barrier and the shortening of O—H interatomic distance in the transition state. Therefore, we suggest one should consider the long-range correction in modeling hydrogen bond dissociation in phenolic compounds, namely phenol and catechol.

Keywords density functional theory · dispersion correction · energy · long-range correction · non-phenyl and phenyl groups · O—H and C—H dissociations

✉Febdian Rusydi
rusydi@fst.unair.ac.id

[1] Department of Physics, Faculty of Science and Technology, Universitas Airlangga, Jl. Mulyorejo, Surabaya 60115, Indonesia.

[2] Research Center for Quantum Engineering Design, Faculty of Science and Technology, Universitas Airlangga, Jl. Mulyorejo, Surabaya 60115, Indonesia

[3] Department of Engineering Physics, Faculty of Industrial Engineering, Institut Teknologi Bandung, Bandung 40132, Indonesia

[4] Engineering Physics Study Program, Institut Teknologi Sumatera, Jl. Terusan Ryacudu, Lampung Selatan 35365, Indonesia

[5] Information System Study Program, Faculty of Science and Technology, Universitas Airlangga, Jl. Mulyorejo, Surabaya 60115, Indonesia

[6] School of Pharmacy, Institut Teknologi Bandung, Jl. Ganesha 10, Bandung 40132, Indonesia

[7] Research Center for Nanoscience and Nanotechnology, Institut Teknologi Bandung, Jl. Ganesha 10, Bandung 40132, Indonesia

1 Introduction

Hydrogen atom transfer is one important reaction that occurs in various environments: the biological systems, the atmosphere, and the industry. In biological systems, the reaction takes place in lipid peroxidation formation [1,2] and its prevention, [3–8] as well as in free radicals formation [9]. In the atmosphere, the reaction involves hydroxyl radical (OH) and organic or inorganic materials [10,11]. Meanwhile in industry, one way the reaction occurs is in the presence of a catalyst [12,13]. Overall, the reaction has been a subject of experimental and computational studies. However, there is still a need to understand how the current computational methods can model hydrogen bond dissociation. This understanding will help to achieve a comprehensive insight into the hydrogen atom transfer reaction.

Numerous publications have reported the usage of computational methods based on density functional the-

ory (DFT) to investigate hydrogen bond dissociation. One quantity describing the hydrogen bond dissociation is bond dissociation energy (BDE). In 1999, Barckholtz et al. reported the use of one DFT exchange-correlation (XC) functional, B3LYP, to predict C−H BDE of small aromatics. The predictions were in agreement with the available experimental values [14]. In the following years, the XC was used to predict the BDE of various bonds in small and large molecules [15–17]. On the other hand, other publications showed that B3LYP has low accuracy [18–20] but is reliable to predict the substituent effect such as in alkyl and peroxyl radicals [18]. In 2008, Zhao and Truhlar introduced XC from the Minnesota family, M06-2X. This XC has much-improved accuracy in predicting BDE [21]. M06-2X is reliable for various cases, such as predicting substituent effects on O−C and C−C BDE of lignin [22] and predicting BDE of polyphenols in various solvents [23]. The DFT used for the above prediction was unrestricted [15,22]. In addition to B3LYP and M06-2X, Du et al. used CAM-B3LYP, which includes a long-range correction to B3LYP, in their calculations. They found that CAM-B3LYP underestimates O−CH_3 BDE relative to experimental values. However, this XC has better performance for aromatic molecules than for non-aromatic molecules [24]. Even though many references have reported the use of various DFT XCs for predicting BDE, there is still limited references reported about the path taken by hydrogen atom during the bond dissociation. The use of XCs to model the path is necessary to gain insight into the hydrogen atom transfer reactions. Thus, the present work investigates the effect of dispersion and long-range corrections in O−H and C−H bond dissociations. The corrections have been integrated into DFT XCs. Therefore, it is necessary to use DFT to identify the effect of dispersion and long-range correction on O−H and C−H bond dissociations.

This work aims to study the effects of dispersion and long-range corrections on the O-H and C-H bond dissociations computationally. We utilize DFT with three functionals combined with the D3 version of Grimme's dispersion. The combination is five methods: B3LYP that has been used for chemical computation, CAM-B3LYP that includes a long-range correction, B3LYP-GD3 and CAM-B3LYP-GD3 which includes Grimme's dispersion, and M06-2X that has a good performance for noncovalent interactions [25–28]. The dissociation is designed to occur at O-H and C-H bonds of six non-phenyl and three phenyl groups. The phenyl groups containing O-H bonds are chosen to represent the phenolic compounds. To achieve the goal, we calculate bond dissociation energy and build hydrogen dissociation pathways using two techniques: a relaxed scan calculation and a geometry optimization in the ground and transition states. We have used these two techniques to study other chemical reactions [29–32]. This study will answer the following question: What are the effects of the dispersion and long-range corrections on the O-H and C-H dissociations of non-phenyl and phenyl groups?

2 Computational models

2.1 Reaction model

Scheme 1 presents our model for the homolytic hydrogen dissociation. The reactant was R−H′ possessing O−H, or C−H, bond; the products were R$^\bullet$ and a hydrogen atom (H′$^\bullet$). There were nine molecules of interest for R−H′, which were (a) hydroxyl, (b) methylidyne, (c) water, (d) methane, (e) methanol, (f) ethane, (g) toluene, (h) phenol, and (i) catechol. Figure 1 presents the Kekulé structure of these molecules.

$$\underset{\text{[in.]}}{\text{R}-\text{H}'} \longrightarrow \underset{\text{[fi.]}}{\text{R}^\bullet + \text{H}'^\bullet}$$

Scheme 1: The initial state [in.] and the final state [fi.] of the reaction model.

[Fig. 1 about here.]

2.2 DFT calculations

We performed computational techniques with the basis of DFT [33,34]. We used 6-311++G(d,p) basis set with three different XCs; they were (1) B3LYP, (2) CAM-B3LYP, and (3) M06-2X which were implemented in Gaussian 16 software [35]. The first XC has become a standard functional for a geometry structure study, while the second XC has improved the long-range interaction of the first XC. The third XC has been parameterized, such that noncovalent interactions take into account. We applied the D3 version of Grimme's dispersion to accommodate the dispersion effect along the dissociation pathways. We combined the XCs and the dispersion into five different methods, as shown in Table 1. In addition to DFT, we used Natural Bond Orbital (NBO) calculations for the natural hybrid orbital and charge population analysis [36].

[Table 1 about here.]

The procedure for DFT calculations is as follows. First, we validated that the three XCs were capable to obtain the spin-state and the geometry in the ground

state. For this purpose, we chose hydroxyl and phenol because they represented molecules with odd and even number of electrons and because their experimental results were available. Second, we performed a geometry optimization to obtain the geometry of all molecules of interest in the ground state using the five calculation methods. To obtain BDE (D°) of hydrogen, we coupled DFT with frequency calculations. It resulted in the total electronic energy with thermal correction to enthalpy at 298.15 K in the ground state. D° was the enthalpy difference between the final and the initial states in Scheme 1. Third, we constructed the hydrogen dissociation pathways.

We employed two different computational techniques for the third DFT calculations procedure. The first technique was a relaxed scan calculation, where one hydrogen atom (with prime mark in Figure 1) left oxygen or carbon atom of R$^\bullet$ and let R$^\bullet$ relaxed. The increments were set to be 0.2 Å for all methods. The second one was based on the geometry optimization in the ground and transition states. We applied the first technique to the selected non-phenyl and phenyl groups. The value of D° that was affected and was not affected by dispersion and/or long-range corrections became the restriction in selecting molecules in the first technique. The first technique resulted in potential energy curve (PEC) and the dissociation pathway was visualized using a polar coordinate. We emphasized that the pathway that led to other than hydrogen dissociation would not be discussed further. The PEC that was affected by dispersion and/or long-range corrections became the restriction to select molecules in the second technique. The second technique yielded a dissociation pathway in energy level diagrams (ELD). We have successfully applied both techniques in our previous studies for bigger molecules [29–32].

We excluded PEC results from M06-2X in the current study because it produced unreasonable results. We also noted that Mardirossian and Head-Gordon [37] reported a similar case. They highlighted that M06-2X poorly predicted the bond length of krypton dimer and benzene-silane dimer through their potential energy curves. We listed the symbols and acronyms in Table 2 to assist readers in getting familiar with them.

[Table 2 about here.]

3 Results and discussion

3.1 The ground state structures

Spin-state and geometry The geometry optimization using the three XCs obtained the doublet and singlet as the lowest in energy level for hydroxyl and phenol, respectively. On average, the doublet was 4.6 eV lower than the quartet (in hydroxyl); while the singlet was 4.2 eV lower than the triplet (in phenol). The doublet and the singlet were more stable compared to the quartet and the triplet. The results agree with the ground spin-states of hydroxyl and phenol reported in references [38, 39]. Furthermore, the selected geometrical parameters of hydroxyl and phenol in those spin-states were less than 0.017 Å and 1.4 degrees (see Table 3). The values were within the accuracy limit for DFT calculations [40]. Therefore, the three XCs were capable to obtain the correct ground state structure of the molecules with odd or even number of electrons. Based on these results, the same XCs were used to obtain the ground spin-state of other molecules with an odd and even numbers of electrons which were doublet and singlet, respectively.

[Table 3 about here.]

The dispersion and long-range corrections Table 4 presents O−H′ and C−H′ bond lengths of the obtained ground state geometry of all molecules of interest. The Cartesian coordinates of the ground state geometry were given in Table S1-S9 of Supplementary Information (SI). Calculation using the method with dispersion correction (M2 and M4) obtained the same bond length as the method without the correction (M1 and M3). The method with the long-range correction (M3) and the method parameterized with dispersion-like interaction (M5) obtained slightly shorter bond lengths (the negative values) than the method without the correction (M1). The results suggest the dispersion and the long-range corrections do not alter the ground state O−H′ and C−H′ bond lengths of our molecules of interest.

[Table 4 about here.]

3.2 The bond dissociation energy

Table 5 presents the discrepancy of D° between the calculated and experimental values. Among all methods, the M5 method obtained D° the closest to the experimental values for molecules with singlet spin-state. The results supported the work of Zhao and Truhlar [21], which suggested using the M5 method for D° calculations of molecules with singlet spin-state. Therefore, M06-2X functional is suitable for dealing with the hydrogen dissociation energy of molecules with singlet spin-state.

[Table 5 about here.]

The discrepancies obtained by M2, M3, and M4 were varied compared to that obtained by M1. In all molecules [Table 5 (a)-(i)], M2 obtained 0.9 kJ/mol (in average) discrepancies higher than M1 did. Moreover, M4 obtained 0.6 kJ/mol (in average) discrepancies higher than M3 did. The results indicate that the dispersion correction does not alter the calculated D° of molecules with singlet and doublet spin-states. In hydroxyl and methylidyne [Table 5 (a) and (b)], M3 obtained 1.9 kJ/mol (in average) discrepancies lower than M1 did. Meanwhile, in other molecules [Table 5 (c)-(i)], M3 obtained 4.4 kJ/mol (in average) discrepancies higher than M1 did. The 4.4 kJ/mol is significant, which implies that the long-range correction is the reason for D° alteration of molecules with singlet spin-state. Thus, the long-range correction plays a role in altering D° of molecules with singlet spin-state but not the molecules with doublet spin-state.

Among seven molecules in Table 5 (c)-(i), the alteration of discrepancies from M1 to M3 on O−H′ bonds differed from that on C−H′ bonds. The seven molecules were in their singlet spin-state. For four molecules with O−H′ bonds, the discrepancies increased by 5.7 kJ/mol (on average) from M1 to M3. However, for three molecules with C−H′ bonds, the discrepancies only increased by 2.8 kJ/mol (in average) from M1 to M3. The increase on O−H′ bonds is more significant than on C−H′ bonds. It indicates that the long-range correction alters the calculated D° on O−H′ bond more than that on C−H′ bond of molecules with singlet spin-state.

The increase in the discrepancy on O−H′ bonds was not accompanied by bond length alteration but by O−H′ bond orbitals alteration. As discussed in section 3.1, from M1 to M3, the ground state O−H′ bond length only altered by 0.002 Å. However, from M1 to M3, the O−H′ bond orbitals altered mainly in $(sp^\lambda)_O$ hybrid orbitals (see Table S10 of the SI). According to the NBO calculations, the average percentage of alteration at $(sp^\lambda)_O$ hybrid orbitals was 33 times more than that at $(sp^\lambda)_C$ hybrid orbitals. Therefore, the long-range correction plays a role in altering the electron density in the O−H′ bond orbitals; hence the calculated D° of O−H′ bond increases.

3.3 The potential energy curve

Figure 2 shows the PECs of four selected molecules together with their respective polar coordinates. All methods yielded two types of PEC profiles. The first type was a PEC-like of dissociation diatomic molecules [Figure 2(a)–2(b) left]. Region I described the dissociation process, and region II described H′• was already a free atom. All methods agreed one to each other. The second type was somewhat challenging to explain since not all methods agreed [Figure 2(c)–2(d) left]. There was region III that contained barriers. PEC profiles in methylidyne and ethane were supportive results to the first type, while PEC profiles in hydroxyl and water were supportive results to the second type. Hence, they were placed in Supporting Information [Figure S1(a)–(b) and S1(c)–(d) left]. On the other hand, the polar coordinates show that the hydrogen dissociation pathways in methane [Figure 2(a) right] are different from those in other molecules [Figure 2(b)–2(d) right and Figure S1(c)–(d) right of the SI]. All methods were only agreed for methane. It implies that the corrections (long-range and dispersion) significantly affect the pathway in real space rather than in the PEC profile.

[Fig. 2 about here.]

Overall, the PEC profiles of methanol and phenol [Figure 2(c)–2(d) left] were explained as follows. In region III, methanol and phenol had barriers; methanol had one, and phenol had at least three barriers. In both cases, M2 yielded a similar barrier height to M1 did. So did M4 and M3. It means the dispersion correction does not alter the PEC profile of O−H′ dissociation. However, in both cases, M3 yielded a different barrier height than M1 did. The results indicate that the long-range correction does alter the PEC profile of O−H′ dissociation. Therefore, the long-range correction plays a more significant role than the dispersion correction in the PEC profiles of O−H′ dissociation.

In detail, for phenol [Figure 2(d)], the variation of PEC profiles was accompanied by the variation of dissociation pathways in the polar coordinate. Both variations occurred only at a certain O−H′ distance ($r_{\mathrm{O-H'}}$) range. The PEC profile variation range was around 1.8–3 Å; while the pathway variation range was around 2–4 Å. In those ranges, M3 yielded a different profile and pathway than M1 did. Kamiya et al.[43] also obtained different profiles when using XCs with long-range correction in a system interacting through a van der Waals interaction (noncovalent interaction). Thus, the different profiles obtained by the long-range correction (M3) may be due to the presence of noncovalent interactions, particularly at a region with barriers. Therefore, in line with its role in O−H′ BDE, the long-range correction may play a role in the energy barrier of O−H′ dissociation.

Along the phenol dissociation pathway, M1 and M3 obtained different r at B1a, B1b, and B2 (See Table S11 of the SI). At B1a and B1b, atom H′• was located around atom O [See Figure S2 of the SI]. Here, M3 obtained shorter $r_{\mathrm{O-H'}}$ at B1a than M1 did at B1b. Different than at B1a and B1b, at B2 atom H′• was lo-

cated between atom 2 and atom 3. Here, M3 obtained shorter $r_{2-H'}$ and longer $r_{3-H'}$ than M1 did. The results indicate that the shortening and lengthening of r are due to the long-range correction.

The r alteration after the introduction of long-range correction was accompanied by atomic charges alteration. The NBO calculations showed that atom O, 2, and 3 [See Figure 1(h)] were negatively charged while atom $H'^{\bullet}$ was positively charged. At B1a, M3 yielded greater positive charge on atom $H'^{\bullet}$ and greater negative charge on atom O than M1 did. It implies that the increasing coulombic attraction between atom O and $H'^{\bullet}$ is the reason for the shortening of $r_{O-H'}$ at B1a. At B2, M3 obtained lesser positive charge on atom $H'^{\bullet}$ and greater negative charge on atom 2 than M1 did. It indicates that the increasing coulombic attraction between atom 2 and $H'^{\bullet}$ is the reason for the shortening of the $r_{2-H'}$. At this location, M3 obtained lesser negative charge on atom 3 than M1 did. It implies the increasing coulombic repulsion between atom 3 and $H'^{\bullet}$ is the reason for the lengthening of the $r_{3-H'}$. Therefore, the Coulombic interactions play a role in the alteration of r.

3.4 The dissociation pathway

Figure 3 shows the O−H′ dissociation pathways of two selected molecules, phenol and catechol, in an ELD. For the case of phenol [Figure 3(a)], each pathway had three transition states (TS) and three intermediate states (IS) as predicted earlier in Figure 2(d)left; while for the case of catechol [Figure 3(b)], each pathway had two TSs and two ISs. The experiment has observed the presence of IS1 in a photochemical reaction [44]. While a theoretical study reported IS1 and IS3 as two isomers of phenol [45]. Another theoretical study reported the first step in decomposition of catechol lead to IS4 [46]. The similarity between the molecules in the intermediate states with the previous studies indicate the possibility of hydrogen migration before O−H′ dissociation occurred.

[Fig. 3 about here.]

The dissociation pathways in phenol and catechol showed that all methods obtained the same relative electronic energy order in each TS. The order for both cases was M1 ≈ M2 < M3 ≈ M4 < M5. For the case of phenol, the average difference between the energy obtained by methods with long-range correction (M3 and M4) and methods without the correction (M1 and M2) was 0.16 eV. Similarly, for the case of catechol, the average difference was 0.14 eV. The differences are significant. It was aligned with the PEC profile difference [Figure 2(d)left] after the long-range correction was introduced, particularly at the region with barriers. The results imply that the long-range correction predicts the dissociation is more difficult at a region where the non-covalent interaction may be present. Therefore, the correction indeed plays a role in the energy barrier of O−H′ dissociation.

Methods with long-range correction (M3 and M4) obtained shorter r than methods without the correction did in the TS structures. For the case of phenol, the $r_{O-H'}$ and $r_{3-H'}$ shortened by 0.01 Å on average. The shortening was also similar to the case of catechol. The 0.01 Å is significant compared to the O−H′ bond length shortening in the ground state of phenol and catechol [Table 4(h) and (i)]. Thus, the shortening confirms the shortening of r along the dissociation pathway discussed in Subsection 3.3. For this reason, the long-range correction indeed plays a role in r in the transition state.

Methods with the long-range correction (M3 and M4) obtained similar relative electronic energy to M5 did in the TSs. The average differences of relative electronic energy obtained by those methods were 0.07 for phenol and 0.06 for catechol. These values are very small which indicate the similarity of transition state according to those methods. Therefore, CAM-B3LYP and M06-2X predicts comparable transition state of O−H′ dissociation.

Overall, all methods showed consistent performances on the BDE calculations and O−H′ dissociation pathways prediction. For the BDE calculations, the methods obtained the D° of O−H′ bonds in all molecules increased in the following order: M1 ≈ M2 < M3 ≈ M4 < M5. The increase of D° after the presence of long-range correction in CAM-B3LYP (M3) was in agreement with the study by Chan et al. [47] For the pathways prediction, the methods obtained variation of pathways in phenol and cathecol dissociation. The variations were identified by the alteration in energy barriers and $r_{O-H'}$ in the TS. The energy barrier increased in the same order as the increase in D° of O−H′ bonds. This result validates the study by Peach et al. [48] that showed increasing barrier height when using CAM-B3LYP compared to B3LYP. The increasing energy barriers was accompanied by the shortening of $r_{O-H'}$ as follows: M1 ≈ M2 > M3 ≈ M4. The shortening due to the long-range correction (M3) was in agreement with our previous study [31]. The results show the significance of this research: the use of long-range correction in CAM-B3LYP affects the $r_{O-H'}$ in TS. On the other hand, the M06-2X used in this study predicted the highest D° and energy barrier. The D° was similar to the experimental observation. Its developer suggested the functional

for applications involving main group thermochemistry, kinetics, and noncovalent interactions [21,28].

4 Conclusion

We have studied the effects of dispersion and long-range corrections on O−H and C−H dissociations of non-phenyl and phenyl groups. The effects were identified through bond dissociation energy and dissociation pathways. We summarized that the dispersion correction had negligible effects on the O−H and C−H bond dissociation energies and the non-phenyl and phenyl groups dissociation pathways. While the long-range correction in CAM-B3LYP had a minor effect on the O−H bond dissociation energy and a significant effect on the O−H dissociation pathways. We found that the long-range correction increased the bond dissociation energy of the O−H bond of non-phenyl and phenyl groups in their singlet states by 5.7 kJ/mol. We argued that the increase was due to the alteration of electron density in the O−H bond orbitals. However, the dissociation energy was still far from the experimental results. The significant effects of the long-range correction on the O−H dissociation pathways occurred in two members of phenyl groups, namely phenol and catechol. The effects were identified as follows. First, the correction shortened the O−H distances in the transition states by 0.01 Å, on average. Second, the correction increased the energy barrier by 0.16 eV (in phenol) and 0.14 eV (in catechol), on average. Overall, our results support other theoretical studies on the increasing energy barrier due to the long-range correction. Accordingly, we suggest that one should consider the long-range correction when studying hydrogen bond dissociation in phenolic compounds, such as phenol and catechol.

Acknowledgements Authors thank to Rizka Nur Fadilla (Universitas Airlangga, Indonesia) and Prof. Azizan Ahmad (University Kebangsaan Malaysia, Malaysia) for the insightful discussions. LSPB is grateful for the doctoral scholarship by Lembaga Pengelola Dana Pendidikan (LPDP). All calculations using Gaussian 16 software are performed at Riven Cluster, the high performance computing facility in Research Center for Quantum Engineering Design, Universitas Airlangga, Indonesia.

Declarations

Funding

This work was supported by Universitas Airlangga under grant scheme Riset Kolaborasi Mitra Luar Negeri 2019 no. 1148/UN3.14/LT/2019 and by Direktorat Riset dan Pengabdian Masyarakat, Deputi Bidang Penguatan Riset dan Pengembangan Kementerian Riset dan Teknologi/Badan Riset dan Inovasi Nasional, Republik Indonesia under grant scheme Penelitian Dasar Unggulan Perguruan Tinggi (PDUPT) 2020 no. 1288r/I1.C06/PL/2020.

Conflict of Interest

The authors have no conflicts of interest to declare that are relevant to the content of this article.

Availability of Data and Materials

All data analysed during this study are included in this published article and its supplementary information file.

Code Availability

Not Applicable.

Authors Contribution

Conceptualization: F.R.; formal analysis: L.S.P.B, H.R., and I.P.; investigation: L.S.P.B and V.K.; methodology: F.R. and L.S.P.B; resources: I.P.; writing—original draft preparation: L.S.P.B; writing—review and editing: F.R. and H.K.D. All authors have read and agreed to the published version of the manuscript.

References

1. Zielinski ZAM and Pratt DA (2017) J Org Chem 82, 6, 2817–2825
2. Yin H and Porter NA (2011) Chem. Rev. 111, 10, 5944–5972
3. Shang Y, Zhou H, Li X, Zhou J, Chen K (2019) New J Chem 43: 15736-15742
4. Vo QV, Nam PC, Bay MV, Thong NM, Cuong ND, and Mechler A (2018) Sci Rep 8: 12361
5. Xue Y, Zheng Y, An L, Dou Y, Liu Y (2014) Food Chem 151: 198-206.
6. Iuga C, Alvarez-Idaboy JR, Russo N (2012) J Org Chem 12: 3868-3877.
7. Galano A, Alvarez-Diduk R, Ramirez-Silva MT, Alarcon-Angeles G, Rojas-Hernandez A (2009) Chem Phys 363: 13-23.
8. Jovanovic SV, Steenken S, Boone CW, Simic MG (1999) J Am Chem Soc 121:9677-9681.
9. Wang Y-N and Eriksson LA (2001) Theor Chem Acc 106:158-162
10. Mallick S, Sarkar S, Bandyopadhyay B, and Kumar P (2018) J Phys Chem A 122, 1, 350–363
11. Kumar M, Sinha A, and Francisco JS (2016) Acc Chem Res 49, 5, 877–883

12. Liang F, Zhong W, Xiang L, Mao L, Xu Q, Kirk SR, and Yin D (2019) J. Catal. 378:256-269
13. Asgari P, Hua Y, Bokka A, Thiamsiri C, Prasit-watcharakorn W, Karedath A, Chen X, Sardar S, Yum K, Leem G, Pierce BS, Nam K, Gao J, and Jeon J (2019) Nat Catal 2:164–173
14. Barckholtz C, Barckholtz TA, and Hadad CM (1999) J Am Chem Soc 121, 3, 491–500
15. Wang L, Yang F, Zhao X, and Li Y (2019) Food Chem 275: 339-345
16. Nantasenamat C, Isarankura-Na-Ayudhya C, Naenna T, Prachayasittikul V (2008) J Mol Graph Model 27:188-196
17. Zhang H-Y, Sun Y-M, and Wang X-L (2003)Chem Eur J 9:502-508
18. Brinck T, Lee H-N, Jonsson M (1999) J Phys Chem 103:7094-7104
19. Izgorodina EI, Coote ML, Radom L (2005) J Phys Chem A 109:7558-7566
20. Izgorodina EI, Brittain DRB, Hodgson JL, Krenske EH, Lin CY, Namazian M, and Coote ML (2007) J Phys Chem A 111: 10754-10768
21. Zhao Y and Truhlar DG (2008) J Phys Chem A 112: 1095-1099
22. Beste A and Buchanan III AC (2009) J Org Chem 74(7): 2837–2841
23. Zheng Y-Z, Fu Z-M, Deng G, Guo R, Chen D-F (2020) Phytochemistry 178: 112454
24. Du T, Quina FH, Tunega D, Zhang J, Aquino AJA (2020) Theor Chem Acc 139:75
25. Yanai T, Tew DP, Handy NC (2004) Chem Phys Lett 393: 51-57
26. Grimme S, Antony J, Ehrlich S, Krieg H (2010) J Chem Phys 132: 154104
27. Becke AD (1993) J Chem Phys 98: 5648
28. Zhao Y, Truhlar DG (2008) Theor Chem Acc 120: 215-241
29. Rusydi F, Madinah R, Puspitasari I, Mark-Lee WF, Ahmad A, Rusydi A (2020) Biochem Mol Biol Educ https://doi.org/10.1002/bmb.21433
30. Fadilla RN, Rusydi F, Aisyah ND, Khoirunisa V, Dipojono HK, Ahmad F, Mudasir, Puspitasari I (2020) Molecules 25: 670
31. Rusydi F, Aisyah ND, Fadilla RN, Dipojono HK, Ahmad F, Mudasir, Puspitasari I, Rusydi A (2019) Heliyon 5: e02409
32. Fadilla RN, Aisyah ND, Dipojono HK, Rusydi F (2017) Procedia Eng 170: 113-118
33. Hohenberg P, Kohn W (1964) Phys Rev 136: B864
34. Kohn W, Sham LJ (1965) Phys Rev 140: A1133
35. M. J. Frisch, G. W. Trucks, H. B. Schlegel, G. E. Scuseria, M. A. Robb, J. R. Cheeseman, G. Scalmani, V. Barone, G. A. Petersson, H. Nakatsuji, X. Li, M. Caricato, A. V. Marenich, J. Bloino, B. G. Janesko, R. Gomperts, B. Mennucci, H. P. Hratchian, J. V. Ortiz, A. F. Izmaylov, J. L. Sonnenberg, D. Williams-Young, F. Ding, F. Lipparini, F. Egidi, J. Goings, B. Peng, A. Petrone, T. Henderson, D. Ranasinghe, V. G. Zakrzewski, J. Gao, N. Rega, G. Zheng, W. Liang, M. Hada, M. Ehara, K. Toyota, R. Fukuda, J. Hasegawa, M. Ishida, T. Nakajima, Y. Honda, O. Kitao, H. Nakai, T. Vreven, K. Throssell, J. A. Montgomery, Jr., J. E. Peralta, F. Ogliaro, M. J. Bearpark, J. J. Heyd, E. N. Brothers, K. N. Kudin, V. N. Staroverov, T. A. Keith, R. Kobayashi, J. Normand, K. Raghavachari, A. P. Rendell, J. C. Burant, S. S. Iyengar, J. Tomasi, M. Cossi, J. M. Millam, M. Klene, C. Adamo, R. Cammi, J. W. Ochterski, R. L. Martin, K. Morokuma, O. Farkas, J. B. Foresman, and D. J. Fox (2013) Gaussian 16, Revision C.01, Gaussian, Inc., Wallingford CT
36. Glendening ED, Reed AE, Carpenter JE, Weinhold F Nbo version 3.1
37. Mardirossian N and Head-Gordon M (2016) J Chem Theory Comput 12: 4303-4325
38. Jones DB, da Silva GB, Neves RFC, Duque HV, Chiari L, de Oliveira EM, Lopes MCA, da Costa RF, Varella MTN, Bettega MHF, Lima MAP and Brunger MJ (2014) J Chem Phys 141: 074314
39. Huber KP and Herzberg G, Molecular Spectra and Moelcular Structure IV. Constants of Diatomic Molecules, Springer US, 1979, page 508
40. Young DC, Computational chemistry: A practical guide for applying techniques to real-world problems, John Wiley & Sons Inc., New York, 2001, Chp. 16, Page 138
41. Haynes WM, CRC Handbook of Chemistry and Physics, 95th ed., CRC Press, Boca Rotan, 2014, Chp.9
42. Lucarini M, Pedulli GF, Guerra M (2004) Chem Eur J 10: 933-939
43. Kamiya M, Tsuneda T and Hirao K (2002) J Chem Phys 117: 6010
44. Parker K and Davis SR (1999) J Am Chem Soc 121: 4271-4277
45. Zhu L and Bozzelli JW (2003) J Phys Chem A 107: 3696-3703
46. Altarawneh M, Dlugogorski BZ, Kennedy EM and Mackie J (2010) J Phys Chem A. 114: 1060-1067
47. Chan B, Morris M and Radom L (2011) Aust J Chem 64: 394-402
48. Peach MJG, Helgaker T, Salek P, Keal TW, Lutnæs OB, Tozer DJ and Handyd NC (2006) Phys Chem Chem Phys 8: 558-562

List of Figures

1 **Fig. 1** Kekulé structure of the molecule of interest. The primed H was the dissociated hydrogen atom. For clarity in molecules (g) – (i), only dissociated hydrogen atom was shown, and carbon atoms were replaced by numbers 9

2 **Fig. 2** PECs of C−H′ and O−H′ bond dissociations with their respective polar coordinates. The I, II, and III represented three different regions based on the similarity of events at each region. Angles in the polar coordinate were H−C−H′ in methane, 2–1–C−H′ in toluene, H−C−O−H′ in methanol, and 2–1–O−H′ in phenol (see Figure 1). The initial angle was at zero degree, then deviated clockwise or counterclockwise. Particularly in methane, the clockwise represented inward deviation. **B1a**, **B1b**, **B2**, and **B3** in (d) represented first barrier obtained by M1 and M2, first barrier obtained by M3 and M4, second and third barrier obtained by all four methods, respectively 10

3 **Fig. 3** Energy level diagram for O−H′ dissociation pathways of two selected molecules. R1, R2, P1, and P2 represent phenol, catechol, product of phenol dissociation, and product of catechol dissociation. While TS and IS stand for transition state and intermediate state. The TSs were shown with the selected interactomic distances (unit in Å) 11

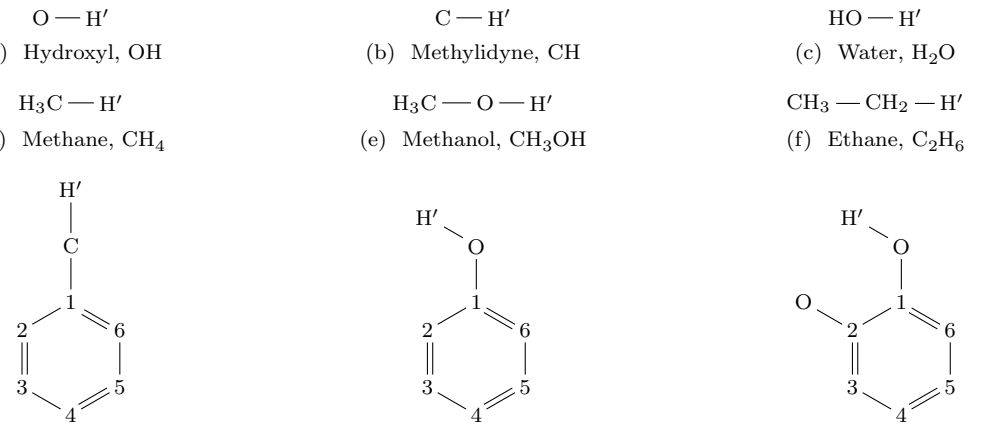

(a) Hydroxyl, OH (b) Methylidyne, CH (c) Water, H_2O

(d) Methane, CH_4 (e) Methanol, CH_3OH (f) Ethane, C_2H_6

(g) Toluene, $C_6H_5CH_3$ (h) Phenol, C_6H_5OH (i) Catechol, $C_6H_4(OH)_2$

Fig. 1 Kekulé structure of the molecule of interest. The primed H was the dissociated hydrogen atom. For clarity in molecules (g) – (i), only dissociated hydrogen atom was shown, and carbon atoms were replaced by numbers

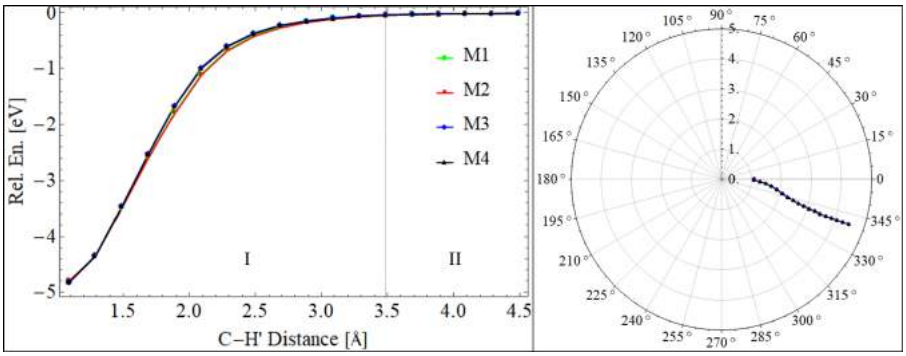

(a) PEC (left) and polar coordinate (right) of methane.

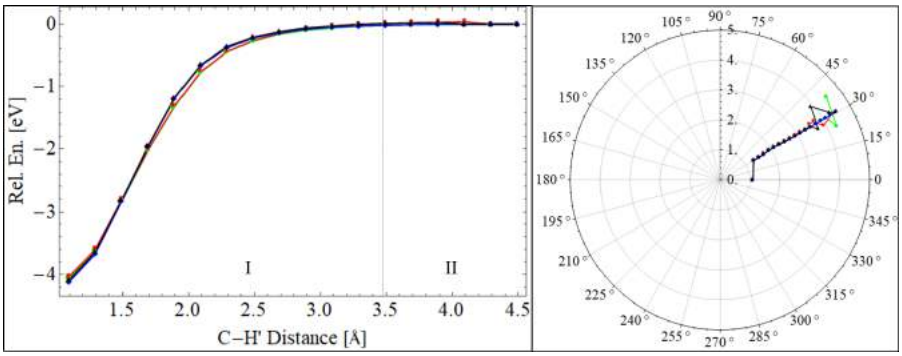

(b) PEC (left) and polar coordinate (right) of toluene.

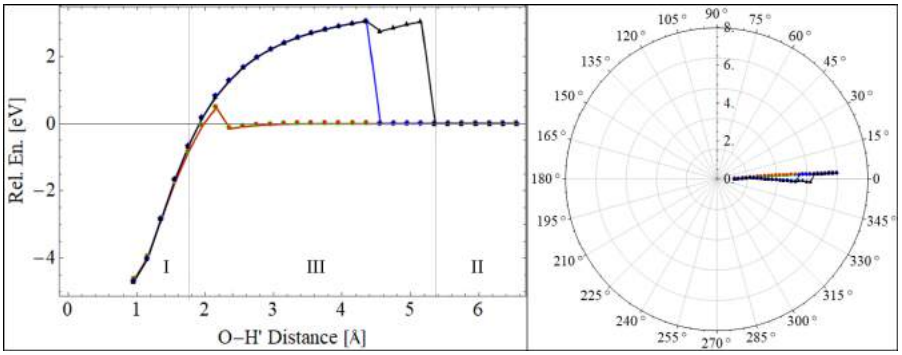

(c) PEC (left) and polar coordinate (right) of methanol.

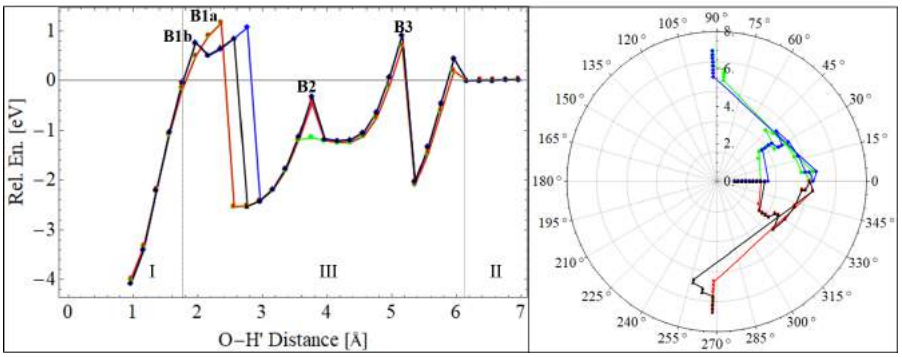

(d) PEC (left) and polar coordinate (right) of phenol.

Fig. 2 PECs of C−H′ and O−H′ bond dissociations with their respective polar coordinates. The I, II, and III represented three different regions based on the similarity of events at each region. Angles in the polar coordinate were H−C−H′ in methane, 2–1–C−H′ in toluene, H−C−O−H′ in methanol, and 2–1–O−H′ in phenol (see Figure 1). The initial angle was at zero degree, then deviated clockwise or counterclockwise. Particularly in methane, the clockwise represented inward deviation. **B1a**, **B1b**, **B2**, and **B3** in (d) represented first barrier obtained by M1 and M2, first barrier obtained by M3 and M4, second and third barrier obtained by all four methods, respectively

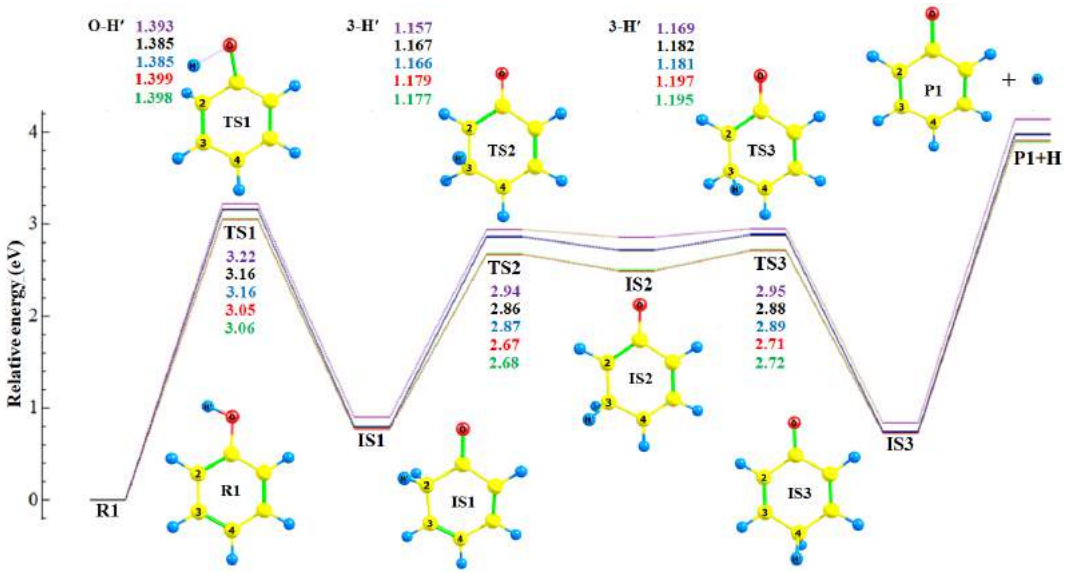

(a) O−H′ dissociation pathways of phenol

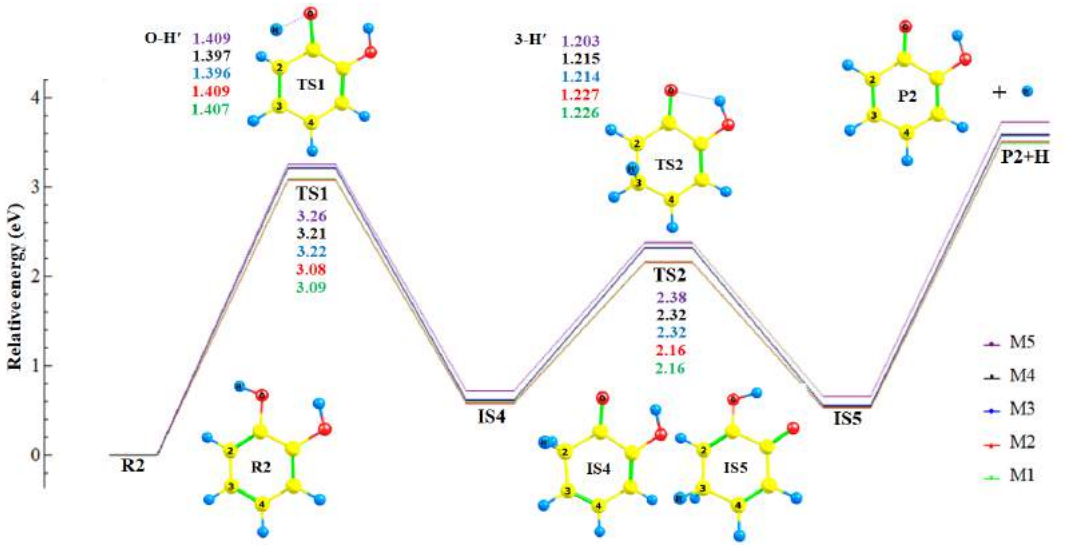

(b) O−H′ dissociation pathways of catechol

Fig. 3 Energy level diagram for O−H′ dissociation pathways of two selected molecules. R1, R2, P1, and P2 represent phenol, catechol, product of phenol dissociation, and product of catechol dissociation. While TS and IS stand for transition state and intermediate state. The TSs were shown with the selected interactomic distances (unit in Å)

List of Tables

1 **Table 1** List of methods used in the manuscript 13
2 **Table 2** List of symbols and acronyms used throughout the manuscript 14
3 **Table 3** The discrepancy of calculated geometrical parameters of hydroxyl and phenol by (1) B3LYP, (2) CAM-B3LYP, and (3) M06-2X with respect to the experimental values [41]. The parameters were bond length (R, in Å) and bond angle (A, in degree). The parameter in (i) belongs to hydroxyl; while others belong to phenol 15
4 **Table 4** The difference of calculated O−H′ and C−H′ bond lengths from M1 (Å). The label referred to Figure 1 16
5 **Table 5** The discrepancy of calculated D° with respect to the experimental values (kJ/mol) [41,42]. The label referred to Figure 1 17

Table 1 List of methods used in the manuscript

M1	B3LYP
M2	B3LYP + GD3
M3	CAM-B3LYP
M4	CAM-B3LYP + GD3
M5	M06-2X

Table 2 List of symbols and acronyms used throughout the manuscript

Symbol/acronym	**Description**
D°	Bond dissociation energy
r	Distances between atoms
BDE	Bond dissociation energy
DFT	Density functional theory
ELD	Energy level diagram
IS	Intermediate state
NBO	Natural Bond Orbital
PEC	Potential energy curve
TS	Transition state
XC	Exchange-correlation

Table 3 The discrepancy of calculated geometrical parameters of hydroxyl and phenol by (1) B3LYP, (2) CAM-B3LYP, and (3) M06-2X with respect to the experimental values [41]. The parameters were bond length (R, in Å) and bond angle (A, in degree). The parameter in (i) belongs to hydroxyl; while others belong to phenol

	Parameter	Expr.	(1)	(2)	(3)
(i)	R(O,H′)	0.970	+0.006	+0.005	+0.003
(ii)	R(O,H′)	0.956	+0.007	+0.005	+0.005
(iii)	R(C,C)av	1.397	-0.003	-0.009	-0.006
(iv)	R(1,O)	1.364	+0.006	0.000	-0.001
(v)	R(4,H)	1.082	+0.001	+0.001	0.000
(vi)	R(5,H)	1.076	+0.008	+0.008	+0.008
(vii)	R(6,H)	1.084	+0.002	+0.001	+0.002
(viii)	A(1,O,H′)	109.0	+0.8	+1.0	+0.8

Table 4 The difference of calculated O−H′ and C−H′ bond lengths from M1 (Å). The label referred to Figure 1

	Molecule	Bond	M1	M2	M3	M4	M5
(a)	Hydroxyl	O−H′	0.976	0.000	-0.002	-0.002	-0.004
(b)	Methylidyne	C−H′	1.127	0.000	-0.003	-0.003	-0.007
(c)	Water	O−H′	0.962	0.000	-0.001	-0.001	-0.003
(d)	Methane	C−H′	1.091	0.000	-0.001	-0.001	-0.002
(e)	Methanol	O−H′	0.961	0.000	-0.002	-0.002	-0.003
(f)	Ethane	C−H′	1.094	0.000	-0.001	-0.001	-0.002
(g)	Toluene	C−H′	1.094	0.000	-0.002	-0.002	-0.002
(h)	Phenol	O−H′	0.963	0.000	-0.002	-0.002	-0.002
(i)	Catechol	O−H′	0.962	0.000	-0.002	-0.002	-0.002

Table 5 The discrepancy of calculated D° with respect to the experimental values (kJ/mol) [41,42]. The label referred to Figure 1

	Molecule	Bond	Expr.	M1	M2	M3	M4	M5
(a)	Hydroxyl	O−H,	429.73	-1.1	-1.1	-0.8	-0.8	-9.2
(b)	Methylidyne	C−H,	338.4	+1.8	+1.8	-2.2	-2.2	-8.1
(c)	Water	O−H,	497.32	-17.1	-17.1	-14.0	-14.0	-11.7
(d)	Methane	C−H,	439.3	-8.3	-8.2	-7.1	-7.0	-6.1
(e)	Methanol	O−H,	440.2	-26.4	-25.2	-21.1	-20.3	-11.5
(f)	Ethane	C−H,	420.5	-8.9	-7.6	-6.8	-6.0	-3.4
(g)	Toluene	C−H,	375.5	-10.8	-9.1	-5.8	-4.7	+2.9
(h)	Phenol	O−H,	362.8	-16.0	-14.6	-9.6	-8.6	+6.7
(i)	Catechol	O−H,	342.3	-32.0	-29.9	-24.0	-22.5	-9.8

5. Manuskrip Diterima

Date:	15 May 2021
To:	"Febdian Rusydi" rusydi@fst.unair.ac.id;febdian@gmail.com
From:	"Dr. Ilaria Ciofini & Prof. Carlo Adamo" 'Ilaria.ciofini@chimie-paristech.fr';'carlo.adamo@chimie-paristech.fr';tca@chimie-paristech.fr
Subject:	TCAC: Your manuscript entitled O-H and C-H bond dissociations in non-phenyl and phenyl groups: A DFT study with dispersion and long-range corrections

Ref.:
Ms. No. TCAC-D-20-00473R2
O-H and C-H bond dissociations in non-phenyl and phenyl groups: A DFT study with dispersion and long-range corrections
Theoretical Chemistry Accounts

Dear Mr. Rusydi,

We are
pleased to tell you that your work has now been accepted for publication in Theoretical Chemistry Accounts.

Thank you for submitting your work to this journal.

With kind regards,
Dr. Ilaria Ciofini & Prof. Carlo Adamo
Editors-in-Chief
Theoretical Chemistry Accounts

—

****

Please note that this journal is a Transformative Journal (TJ). Authors may publish their research through the traditional subscription access route or make their paper open access through payment of an article-processing charge (APC). Find out more about Transformative Journals

Our flexible approach during the COVID-19 pandemic

If you need more time at any stage of the peer-review process, please do let us know. While our systems will continue to remind you of the original timelines, we aim to be as flexible as possible during the current pandemic.

This letter contains confidential information, is for your own use, and should not be forwarded to third parties.

Recipients of this email are registered users within the Editorial Manager database for this journal. We will keep your information on file to use in the process of submitting, evaluating and publishing a manuscript. For more information on how we use your personal details please see our privacy policy at https://www.springernature.com/production-privacy-policy. If you no longer wish to receive messages from this journal or you have questions regarding database management, please contact the Publication Office at the link below.

In compliance with data protection regulations, you may request that we remove your personal registration details at any time. (Use the following URL: https://www.editorialmanager.com/tcac/login.asp?a=r). Please contact the publication office if you have any questions.

6. Artikel Terbit

- Persiapan Terbit
- Persetujuan Terbit
- Artikel

Fwd: Proofs for your article in Theoretical Chemistry Accounts (2781)

1 pesan

Febdian Rusydi <rusydi@fst.unair.ac.id> 17 Juni 2021 07.04
Kepada: lusiasilfia@gmail.com

FYI

---------- Forwarded message ---------
From: <spr_corrections@springer.com>
Date: Wed, Jun 16, 2021 at 11:31 PM
Subject: Proofs for your article in Theoretical Chemistry Accounts (2781)
To: <rusydi@fst.unair.ac.id>

SPRINGER NATURE

Article Title : O—H and C—H bond dissociations in non-phenyl and phenyl groups: A DFT study with dispersion and long-range corrections

DOI : 10.1007/s00214-021-02781-6
TCAC-D-20-00473R2

Dear Author,

We are pleased to inform you that your paper is nearing publication. You can help us facilitate quick and accurate publication by using our e.Proofing system. The system will show you an HTML version of the article that you can correct online. In addition, you can view/download a PDF version for your reference.

As you are reviewing the proofs, please keep in mind the following:

- This is the only set of proofs you will see prior to publication.
- Only errors introduced during production process or that directly compromise the scientific integrity of the paper may be corrected.
- Any changes that contradict journal style will not be made.
- Any changes to scientific content (including figures) will require editorial review and approval.

Please check the author/editor names very carefully to ensure correct spelling, correct sequence of given and family names and that the given and family names have been correctly designated (NB the family name is highlighted in blue).

Please submit your corrections within 2 working days and make sure you fill out your response to any AUTHOR QUERIES raised during typesetting. Without your response to these queries, we will not be able to continue with the processing of your article for Online Publication.

Your article proofs are available at:

https://eproofing.springer.com/ePj/index/XRI3ED1ivjvrhghP3x4x00QIKQMBeT42oXRdm5LrRLsRxwKoNScPxBBqIJi4wJSYsG1zygmE9zyBOMIQ4IQ4nzK4-buA_cR8gx12Ry8kabE9r_S88t5eybA0AjC5XhHI

The URL is valid only until your paper is published online. It is for proof purposes only and may not be used by third parties.

Should you encounter difficulties with the proofs, please contact me.

We welcome your comments and suggestions. Your feedback helps us to improve the system.

Thank you very much.

Sincerely yours,

Springer Nature Correction Team

No. 6&7, 5th Street, Radhakrishnan Salai,
Mylapore, Chennai, Tamilnadu
India, Pincode 600 004
e-mail: spr_corrections@springer.com
Fax:

Regular Article

O—H and C—H bond dissociations in non-phenyl and phenyl groups: A DFT study with dispersion and long-range corrections

Lusia Silfia ~~Pulo~~ ~~Boli~~ Pulo Boli

Febdian Rusydi
Email : rusydi@fst.unair.ac.id

Vera Khoirunisa

Ira Puspitasari

Heni Rachmawati

Hermawan Kresno Dipojono

Department of Physics, Faculty of Science and Technology, Universitas Airlangga, Jl. Mulyorejo, Surabaya, 60115, Indonesia

Research Center for Quantum Engineering Design, Faculty of Science and Technology, Universitas Airlangga, Jl. Mulyorejo, Surabaya, 60115, Indonesia

Department of Engineering Physics, Faculty of Industrial Engineering, Institut Teknologi Bandung, Bandung, 40132, Indonesia

Engineering Physics Study Program, Institut Teknologi Sumatera, Jl. Terusan Ryacudu, Lampung Selatan, 35365, Indonesia

Information System Study Program, Faculty of Science and Technology, Universitas Airlangga, Jl. Mulyorejo, Surabaya, 60115, Indonesia

School of Pharmacy, Institut Teknologi Bandung, Jl. Ganesha 10, Bandung, 40132, Indonesia

Research Center for Nanoscience and Nanotechnology, Institut Teknologi Bandung, Jl. Ganesha 10, Bandung, 40132, Indonesia

Received: 28 December 2020 / Accepted: 15 May 2021

Abstract

Hydrogen atom transfer is one important reaction in biological system, in industry, and in atmosphere. The reaction is preluded by hydrogen bond dissociation. To gain a comprehensive understanding on the reaction, it is necessary to investigate how the current computational methods model hydrogen bond dissociation. As a starting point, we utilized density functional theory-based calculations to identify the effect of dispersion and long-range corrections on O—H and C—H dissociations in non-phenyl and phenyl groups. We employed five different methods, namely B3LYP, CAM-B3LYP (with long-range correction), M06-2X, and B3LYP and CAM-B3LYP with the D3 version of Grimme's dispersion. The results showed that for the case of O—H dissociation in two member of phenyl groups, namely phenol and catechol, the dispersion correction's effect was negligible, but the long-range correction's effect was significant. The significant effect was shown by the increasing of energy barrier and the shortening of O—H interatomic distance in the transition state. Therefore, we suggest one should consider the long-range correction in modeling hydrogen bond dissociation in phenolic compounds, namely phenol and catechol.

Keywords

Density functional theory
Dispersion correction
Energy
Long-range correction
Non-phenyl and phenyl groups
O—H and C—H dissociations

Supplementary Information

The online version contains supplementary material available at https://doi.org/10.1007/s00214-021-02781-6.

1. Introduction

Hydrogen atom transfer is one important reaction that occurs in various environments: the biological systems, the atmosphere, and the industry. In biological systems, the reaction takes place in lipid peroxidation formation [1, 2] and its prevention, [3, 4, 5, 6, 7, 8] as well as in free radicals formation [9]. In the atmosphere, the reaction involves hydroxyl radical (OH) and organic or inorganic materials [10, 11]. Meanwhile in industry, one way the reaction occurs is in the presence of a catalyst [12, 13]. Overall, the reaction has been a subject of experimental and computational studies. However, there is still a need to understand how the current computational methods can model hydrogen bond dissociation. This understanding will help to achieve a comprehensive insight into the hydrogen atom transfer reaction.

Numerous publications have reported the usage of computational methods based on density functional theory (DFT) to investigate hydrogen bond dissociation. One quantity describing the hydrogen bond dissociation is bond dissociation energy (BDE). In 1999, Barckholtz et al. reported the use of one DFT exchange-correlation (XC) functional, B3LYP, to predict C-H BDE of small aromatics. The predictions were in agreement with the available experimental values [14]. In the following years, the XC was used to predict the BDE of various bonds in small and large molecules [15, 16, 17]. On the other hand, other publications showed that B3LYP has low accuracy [18, 19, 20] but is reliable to predict the substituent effect such as in alkyl and peroxyl radicals [18]. In 2008, Zhao and Truhlar introduced XC from the Minnesota family, M06-2X. This XC has much-improved accuracy in predicting BDE [21]. M06-2X is reliable for various cases, such as predicting substituent effects on O-C and C-C BDE of lignin [22] and predicting BDE of polyphenols in various solvents [23]. The DFT used for the above prediction was unrestricted [15, 22]. In addition to B3LYP and M06-2X, Du et al. used CAM-B3LYP, which includes a long-range correction to B3LYP, in their calculations. They found that CAM-B3LYP underestimates O-CH3 BDE relative to experimental values. However, this XC has better performance for aromatic molecules than for non-aromatic molecules [24]. Even though many references have reported the use of various DFT XCs for predicting BDE, there is still limited references reported about the path taken by hydrogen atom during the bond dissociation. The use of XCs to model the path is necessary to gain insight into the hydrogen atom transfer reactions. Thus, the present work investigates the effect of dispersion and long-range corrections in O-H and C-H bond dissociations. The corrections have been integrated into DFT XCs. Therefore, it is necessary to use DFT to identify the effect of dispersion and long-range correction on O-H and C-H bond dissociations.

This work aims to study the effects of dispersion and long-range corrections on the O-H and C-H bond dissociations computationally. We utilize DFT with three functionals combined with the D3 version of Grimme's dispersion. The combination is five methods: B3LYP that has been used for chemical computation, CAM-B3LYP that includes a long-range correction, B3LYP-GD3 and CAM-B3LYP-GD3 which include Grimme's dispersion, and M06-2X that has a good performance for noncovalent interactions [25, 26, 27, 28]. The dissociation is designed to occur at O-H and C-H bonds of six non-phenyl and three phenyl groups. The phenyl groups containing O-H bonds are chosen to represent the phenolic compounds. To achieve the goal, we calculate bond dissociation energy and build hydrogen bond dissociation pathways using two techniques: a relaxed scan calculation and a geometry optimization in the ground and transition states. We have used these two techniques to study other chemical reactions [29, 30, 31, 32]. This study will answer the following question: What are the effects of the dispersion and long-range corrections on the O-H and C-H dissociations of non-phenyl and phenyl groups?

2. Computational models

2.1. Reaction model

Scheme 1 presents our model for the homolytic hydrogen bond dissociation. The reactant was R-H′ possessing O-H, or C-H, bond; the products were R· and a hydrogen atom (H′·). There were nine molecules of interest for R-H′, which were (a) hydroxyl, (b) methylidyne, (c) water, (d) methane, (e) methanol, (f) ethane, (g) toluene, (h) phenol, and (i) catechol.

Figure 1 presents the Kekulé structures of these molecules.

Scheme 1

The initial state [in.] and the final state [fi.] of the reaction model.

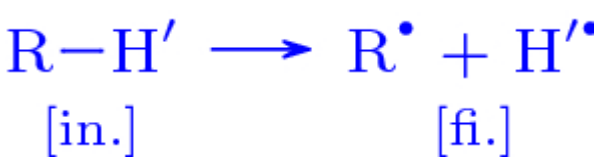

Fig. 1

Kekulé structures of the molecules of interest. The primed H was the dissociated hydrogen atom. For clarity in molecules (**g**)–(**i**), only dissociated hydrogen atom was shown, and carbon atoms were replaced by numbers

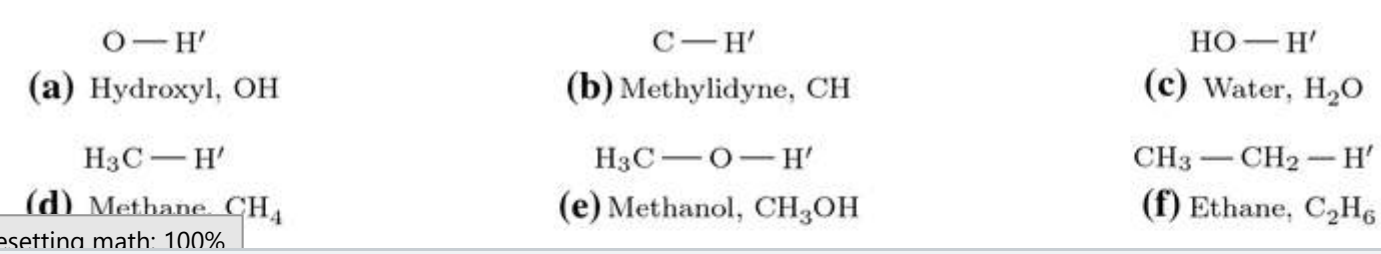

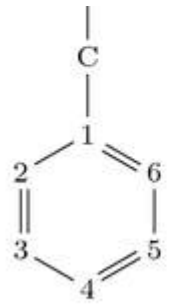

(g) Toluene, $C_6H_5CH_3$

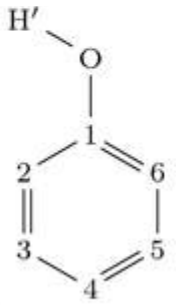

(h) Phenol, C_6H_5OH

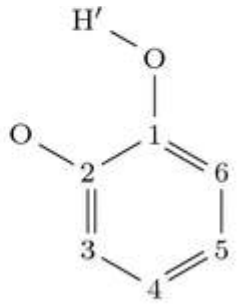

(i) Catechol, $C_6H_4(OH)_2$

2.2. DFT calculations

We performed computational techniques with the basis of DFT [33, 34]. We used 6-311++G(d,p) basis set with three different XCs; they were (1) B3LYP, (2) CAM-B3LYP, and (3) M06-2X which were implemented in Gaussian 16 software [35]. The first XC has become a standard functional for a geometry structure study, while the second XC has improved the long-range interaction of the first XC. The third XC has been parameterized, such that noncovalent interactions take into account. We applied the D3 version of Grimme's dispersion to accommodate the dispersion effect along the dissociation pathways. We combined the XCs and the dispersion into five different methods, as shown in Table 1. In addition to DFT, we used Natural Bond Orbital (NBO) calculations for the natural hybrid orbital and charge population analysis [36].

Table 1

List of methods used in the manuscript

M1	B3LYP
M2	B3LYP + GD3
M3	CAM-B3LYP
M4	CAM-B3LYP + GD3
M5	M06-2X

The procedure for DFT calculations is as follows. First, we validated that the three XCs were capable to obtain the spin-state and the geometry in the ground state. For this purpose, we chose hydroxyl and phenol because they represented molecules with odd and even number of electrons and because their experimental results were available. Second, we performed a geometry optimization to obtain the geometry of all molecules of interest in the ground state using the five calculation methods. To obtain BDE (D°) of hydrogen, we coupled DFT with frequency calculations. It resulted in the total electronic energy with thermal correction to enthalpy at 298.15 K in the ground state. D° was the enthalpy difference between the final and the initial states in Scheme 1. Third, we constructed the hydrogen bond dissociation pathways.

We employed two different computational techniques for the third DFT calculations procedure. The first technique was a relaxed scan calculation, where one hydrogen atom (with prime mark in Figure 1) left oxygen or carbon atom of $R^{\cdot}$ and let $R^{\cdot}$ relaxed. The increments were set to be 0.2 Å for all methods. The second one was based on the geometry optimization in the ground and transition states. We applied the first technique to the selected non-phenyl and phenyl groups. The value of D° that was affected and was not affected by dispersion and/or long-range corrections became the restriction in selecting molecules in the first technique. The first technique resulted in potential energy curve (PEC), and the dissociation pathway was visualized using a polar coordinate. We emphasized that the pathway that led to other than hydrogen bond dissociation would not be discussed further. The PEC that was affected by dispersion and/or long-range corrections became the restriction to select molecules in the second technique. The second technique yielded a dissociation pathway in energy level diagrams (ELD). We have successfully applied both techniques in our previous studies for bigger molecules [29, 30, 31, 32].

We excluded PEC results from M06-2X in the current study because it produced unreasonable results. We also noted that Mardirossian and Head-Gordon [37] reported a similar case. They highlighted that M06-2X poorly predicted the bond length of krypton dimer and benzene-silane dimer through their potential energy curves. We listed the symbols and acronyms in Table 2 to assist readers in getting familiar with them.

Table 2

List of symbols and acronyms used throughout the manuscript

Symbol/acronym	Description
D°	Bond dissociation energy
r	Distances between atoms
BDE	Bond dissociation energy
DFT	Density functional theory
ELD	Energy level diagram
	Intermediate state

Symbol/acronym	Description
PEC	Potential energy curve
TS	Transition state

XC	Exchange-correlation

3. Results and discussion

3.1. The ground state structures

Spin-state and geometry The geometry optimization using the three XCs obtained the doublet and singlet as the lowest in energy level for hydroxyl and phenol, respectively. On average, the doublet was 4.6 eV lower than the quartet (in hydroxyl), while the singlet was 4.2 eV lower than the triplet (in phenol). The doublet and the singlet were more stable compared to the quartet and the triplet. The results agree with the ground spin-states of hydroxyl and phenol reported in references [38, 39]. Furthermore, the selected geometrical parameters of hydroxyl and phenol in those spin-states were less than 0.017 Å and 1.4 degrees (see Table 3). The values were within the accuracy limit for DFT calculations [40]. Therefore, the three XCs were capable to obtain the correct ground state structure of the molecules with odd or even number of electrons. Based on these results, the same XCs were used to obtain the ground spin-state of other molecules with an odd and even numbers of electrons which were doublet and singlet, respectively.

Table 3

The discrepancy of calculated geometrical parameters of hydroxyl and phenol by (1) B3LYP, (2) CAM-B3LYP, and (3) M06-2X with respect to the experimental values [41]. The parameters were bond length (R, in Å) and bond angle (A, in degree). The parameter in (i) belongs to hydroxyl, while others belong to phenol

	Parameter	Expr.	(1)	(2)	(3)
(i)	R(O,H′)	0.970	+0.006	+0.005	+0.003
(ii)	R(O,H′)	0.956	+0.007	+0.005	+0.005
(iii)	R(C,C)av	1.397	− 0.003	− 0.009	-0.006
(iv)	R(1,O)	1.364	+0.006	0.000	− 0.001
(v)	R(4,H)	1.082	+0.001	+0.001	0.000
(vi)	R(5,H)	1.076	+0.008	+0.008	+0.008
(vii)	R(6,H)	1.084	+0.002	+0.001	+0.002
(viii)	A(1,O,H′)	109.0	+0.8	+1.0	+0.8

The dispersion and long-range corrections Table 4 presents O-H′ and C-H′ bond lengths of the obtained ground state geometry of all molecules of interest. The Cartesian coordinates of the ground state geometry were given in Table S1-S9 of Supplementary Information (SI). Calculation using the method with dispersion correction (M2 and M4) obtained the same bond length as the method without the correction (M1 and M3). The method with the long-range correction (M3) and the method parameterized with dispersion-like interaction (M5) obtained slightly shorter bond lengths (the negative values) than the method without the correction (M1). The results suggest the dispersion and the long-range corrections do not alter the ground state O-H′ and C-H′ bond lengths of our molecules of interest.

Table 4

The difference of calculated O-H′ and C-H′ bond lengths from M1 (Å). The label referred to Fig. 1

	Molecule	Bond	M1	M2	M3	M4	M5
(a)	Hydroxyl	O-H′	0.976	0.000	−0.002	−0.002	−0.004
(b)	Methylidyne	C-H′	1.127	0.000	−0.003	−0.003	−0.007
(c)	Water	O-H′	0.962	0.000	−0.001	−0.001	−0.003
(d)	Methane	C-H′	1.091	0.000	−0.001	−0.001	−0.002
(e)	Methanol	O-H′	0.961	0.000	−0.002	−0.002	−0.003
(f)	Ethane	C-H′	1.094	0.000	−0.001	−0.001	−0.002
(g)	Toluene	C-H′	1.094	0.000	−0.002	−0.002	−0.002
(h)	Phenol	O-H′	0.963	0.000	−0.002	−0.002	−0.002
(i)	Catechol	O-H′	0.962	0.000	−0.002	−0.002	−0.002

3.2. The bond dissociation energy

 the discrepancy of D° between the calculated and experimental values. Among all methods, the M5 method obtained

which suggested using the M5 method for D° calculations of molecules with singlet spin-state. Therefore, M06-2X functional is suitable for dealing with the hydrogen bond dissociation energy of molecules with singlet spin-state.

Table 5

The discrepancy of calculated D° with respect to the experimental values (kJ/mol) [41, 42]. The label referred to Fig. 1

	Molecule	Bond	Expr.	M1	M2	M3	M4	M5
(a)	Hydroxyl	O-H′	429.73	−1.1	−1.1	−0.8	−0.8	−9.2
(b)	Methylidyne	C-H′	338.4	+1.8	+1.8	−2.2	−2.2	−8.1
(c)	Water	O-H′	497.32	−17.1	−17.1	−14.0	−14.0	−11.7
(d)	Methane	C-H′	439.3	−8.3	−8.2	−7.1	−7.0	−6.1
(e)	Methanol	O-H′	440.2	−26.4	−25.2	−21.1	−20.3	−11.5
(f)	Ethane	C-H′	420.5	−8.9	−7.6	−6.8	−6.0	−3.4
(g)	Toluene	C-H′	375.5	−10.8	−9.1	−5.8	−4.7	+2.9
(h)	Phenol	O-H′	362.8	−16.0	−14.6	−9.6	−8.6	+6.7
(i)	Catechol	O-H′	342.3	−32.0	−29.9	−24.0	−22.5	−9.8

The discrepancies obtained by M2, M3, and M4 were varied compared to that obtained by M1. In all molecules [Table 5 (a)-(i)], M2 obtained 0.9 kJ/mol (in average) discrepancies higher than M1 did. Moreover, M4 obtained 0.6 kJ/mol (in average) discrepancies higher than M3 did. The results indicate that the dispersion correction does not alter the calculated D° of molecules with singlet and doublet spin-states. In hydroxyl and methylidyne [Table 5 (a) and (b)], M3 obtained 1.9 kJ/mol (in average) discrepancies lower than M1 did. Meanwhile, in other molecules [Table 5 (c)-(i)], M3 obtained 4.4 kJ/mol (in average) discrepancies higher than M1 did. The 4.4 kJ/mol is significant, which implies that the long-range correction is the reason for D° alteration of molecules with singlet spin-state. Thus, the long-range correction plays a role in altering D° of molecules with singlet spin-state but not the molecules with doublet spin-state.

Among seven molecules in Table 5 (c)-(i), the alteration of discrepancies from M1 to M3 on O-H′ bonds differed from that on C-H′ bonds. The seven molecules were in their singlet spin-state. For four molecules with O-H′ bonds, the discrepancies increased by 5.7 kJ/mol (on average) from M1 to M3. However, for three molecules with C-H′ bonds, the discrepancies only increased by 2.8 kJ/mol (in average) from M1 to M3. The increase on O-H′ bonds is more significant than on C-H′ bonds. It indicates that the long-range correction alters the calculated D° on O-H′ bond more than that on C-H′ bond of molecules with singlet spin-state.

The increase in the discrepancy on O-H′ bonds was not accompanied by bond length alteration but by O-H′ bond orbitals alteration. As discussed in Sect. 3.1, from M1 to M3, the ground state O-H′ bond length only altered by 0.002 Å. However, from M1 to M3, the O-H′ bond orbitals altered mainly in $(sp^{\lambda})_O$ hybrid orbitals (see Table S10 of the SI). According to the NBO calculations, the average percentage of alteration at $(sp^{\lambda})_O$ hybrid orbitals was 33 times more than that at $(sp^{\lambda})_C$ hybrid orbitals. Therefore, the long-range correction plays a role in altering the electron density in the O-H′ bond orbitals; hence the calculated D° of O-H′ bond increases.

3.3. The potential energy curve

Figure 2 shows the PECs of four selected molecules together with their respective polar coordinates. All methods yielded two types of PEC profiles. The first type was a PEC-like of dissociation diatomic molecules [Fig. 2(a)–2(b) left]. Region I described the dissociation process, and region II described H′· was already a free atom. All methods agreed one to each other. The second type was somewhat challenging to explain since not all methods agreed [Fig. 2(c)–2(d) left]. There was region III that contained barriers. PEC profiles in methylidyne and ethane were supportive results to the first type, while PEC profiles in hydroxyl and water were supportive results to the second type. Hence, they were placed in Supporting Information [Figure S1(a)–(b) and S1(c)–(d) left]. On the other hand, the polar coordinates show that the hydrogen bond dissociation pathways in methane [Fig. 2(a) right] are different from those in other molecules [Fig. 2(b)–2(d) right and Figure S1(c)–(d) right of the SI]. All methods were only agreed for methane. It implies that the corrections (long-range and dispersion) significantly affect the pathway in real space rather than in the PEC profile.

Fig. 2

PECs of C-H′ and O-H′ bond dissociations with their respective polar coordinates. The I, II, and III represented three different regions based on the similarity of events at each region. Angles in the polar coordinate were H-C-H′ in methane, 2–1–C-H′ in toluene, H-C-O-H′ in methanol, and 2–1–O-H′ in phenol (see Fig. 1). The initial angle was at zero degree, then deviated clockwise or counterclockwise. Particularly in methane, the clockwise represented inward deviation. **B1a**, **B1b**, **B2**, and **B3** in (d) represented first barrier obtained by M1 and M2, first barrier obtained by M3 and M4, second and third barrier obtained by all four methods, respectively

Overall, the PEC profiles of methanol and phenol [Fig. 2(c)–2(d) left] were explained as follows. In region III, methanol and phenol had

l had one, and phenol had at least three barriers. In both cases, M2 yielded a similar barrier height to M1 did. So did M4

different barrier height than M1 did. The results indicate that the long-range correction does alter the PEC profile of O-H′ dissociation. Therefore, the long-range correction plays a more significant role than the dispersion correction in the PEC profiles of O-H′ dissociation.

In detail, for phenol [Fig. 2(d)], the variation of PEC profiles was accompanied by the variation of dissociation pathways in the polar coordinate. Both variations occurred only at a certain O-H′ distance ($r_{O-H'}$) range. The PEC profile variation range was around 1.8–3 Å; while the pathway variation range was around 2–4 Å. In those ranges, M3 yielded a different profile and pathway than M1 did. Kamiya et al. [43] also obtained different profiles when using XCs with long-range correction in a system interacting through a van der Waals interaction (noncovalent interaction). Thus, the different profiles obtained by the long-range correction (M3) may be due to the presence of noncovalent interactions, particularly at a region with barriers. Therefore, in line with its role in O-H′ BDE, the long-range correction may play a role in the energy barrier of O-H′ dissociation.

Along the phenol dissociation pathway, M1 and M3 obtained different *r* at B1a, B1b, and B2 (See Table S11 of the SI). At B1a and B1b, atom H′· was located around atom O [See Figure S2 of the SI]. Here, M3 obtained shorter $r_{O-H'}$ at B1a than M1 did at B1b. Different than at B1a and B1b, at B2 atom H′· was located between atom 2 and atom 3. Here, M3 obtained shorter $r_{2-H'}$ and longer $r_{3-H'}$ than M1 did. The results indicate that the shortening and lengthening of *r* are due to the long-range correction.

The *r* alteration after the introduction of long-range correction was accompanied by atomic charges alteration. The NBO calculations showed that atom O, 2, and 3 [See Fig. 1(h)] were negatively charged while atom H′· was positively charged. At B1a, M3 yielded greater positive charge on atom H′· and greater negative charge on atom O than M1 did. It implies that the increasing coulombic attraction between atom O and H′· is the reason for the shortening of $r_{O-H'}$ at B1a. At B2, M3 obtained lesser positive charge on atom H′· and greater negative charge on atom 2 than M1 did. It indicates that the increasing coulombic attraction between atom 2 and H′· is the reason for the shortening of the $r_{2-H'}$. At this location, M3 obtained lesser negative charge on atom 3 than M1 did. It implies the increasing coulombic repulsion between atom 3 and H′· is the reason for the lengthening of the $r_{3-H'}$. Therefore, the Coulombic interactions play a role in the alteration of *r*.

3.4. The dissociation pathway

Figure 3 shows the O-H′ dissociation pathways of two selected molecules, phenol and catechol, in an ELD. For the case of phenol [Fig. 3(a)], each pathway had three transition states (TS) and three intermediate states (IS) as predicted earlier in Fig. 2(d)left; while for the case of catechol [Fig. 3(b)], each pathway had two TSs and two ISs. The experiment has observed the presence of IS1 in a photochemical reaction [44]. While a theoretical study reported IS1 and IS3 as two isomers of phenol [45]. Another theoretical study reported the first step in decomposition of catechol lead to IS4 [46]. The similarity between the molecules in the intermediate states with the previous studies indicates the possibility of hydrogen migration before O-H′ dissociation occurred.

Fig. 3

Energy level diagram for O-H′ dissociation pathways of two selected molecules. R1, R2, P1, and P2 represent phenol, catechol, product of phenol dissociation, and product of catechol dissociation. While TS and IS stand for transition state and intermediate state. The TSs were shown with the selected interatomic distances (unit in Å)

The dissociation pathways in phenol and catechol showed that all methods obtained the same relative electronic energy order in each TS. The order for both cases was M1 ≈ M2 < M3 ≈ M4 < M5. For the case of phenol, the average difference between the energy obtained by methods with long-range correction (M3 and M4) and methods without the correction (M1 and M2) was 0.16 eV. Similarly, for the case of catechol, the average difference was 0.14 eV. The differences are significant. It was aligned with the PEC profile difference [Fig. 2(d)left] after the long-range correction was introduced, particularly at the region with barriers. The results imply that the long-range correction predicts the dissociation is more difficult at a region where the noncovalent interaction may be present. Therefore, the correction indeed plays a role in the energy barrier of O-H′ dissociation.

Methods with long-range correction (M3 and M4) obtained shorter *r* than methods without the correction did in the TS structures. For the case of phenol, the $r_{O-H'}$ and $r_{3-H'}$ shortened by 0.01 Å on average. The shortening was also similar to the case of catechol. The 0.01 Å is significant compared to the O-H′ bond length shortening in the ground state of phenol and catechol [Table 4(h) and (i)]. Thus, the shortening confirms the shortening of *r* along the dissociation pathway discussed in Subsection 3.3. For this reason, the long-range correction indeed plays a role in *r* in the transition state.

Methods with the long-range correction (M3 and M4) obtained similar relative electronic energy to M5 did in the TSs. The average differences of relative electronic energy obtained by those methods were 0.07 for phenol and 0.06 for catechol. These values are very small which indicate the similarity of transition state according to those methods. Therefore, CAM-B3LYP and M06-2X predict comparable transition state of O-H′ dissociation.

Overall, all methods showed consistent performances on the BDE calculations and O-H′ dissociation pathways prediction. For the BDE calculations, the methods obtained the D° of O-H′ bonds in all molecules increased in the following order: M1 ≈ M2 < M3 ≈ M4 < M5. The increase of D° after the presence of long-range correction in CAM-B3LYP (M3) was in agreement with the study by Chan et al. [47] For the pathways prediction, the methods obtained variation of pathways in phenol and catechol dissociation. The variations were identified by the alteration in energy barriers and $r_{O-H'}$ in the TS. The energy barrier increased in the same order as the increase in D° of O-H′ bonds. This result validates the study by Peach et al. [48] that showed increasing barrier height when using CAM-B3LYP

The shortening due to the long-range correction (M3) was in agreement with our previous study [31]. The results show the significance of this research: the use of long-range correction in CAM-B3LYP affects the $r_{O-H'}$ in TS. On the other hand, the M06-2X used in this study predicted the highest D° and energy barrier. The D° was similar to the experimental observation. Its developer suggested the functional for applications involving main group thermochemistry, kinetics, and noncovalent interactions [21, 28].

4. Conclusion

We have studied the effects of dispersion and long-range corrections on O-H and C-H dissociations of non-phenyl and phenyl groups. The effects were identified through bond dissociation energy and dissociation pathways. We summarized that the dispersion correction had negligible effects on the O-H and C-H bond dissociation energies and the non-phenyl and phenyl groups dissociation pathways. While the long-range correction in CAM-B3LYP had a minor effect on the O-H bond dissociation energy and a significant effect on the O-H dissociation pathways. We found that the long-range correction increased the bond dissociation energy of the O-H bond of non-phenyl and phenyl groups in their singlet states by 5.7 kJ/mol. We argued that the increase was due to the alteration of electron density in the O-H bond orbitals. However, the dissociation energy was still far from the experimental results. The significant effects of the long-range correction on the O-H dissociation pathways occurred in two members of phenyl groups, namely phenol and catechol. The effects were identified as follows. First, the correction shortened the O-H distances in the transition states by 0.01 Å, on average. Second, the correction increased the energy barrier by 0.16 eV (in phenol) and 0.14 eV (in catechol), on average. Overall, our results support other theoretical studies on the increasing energy barrier due to the long-range correction. Accordingly, we suggest that one should consider the long-range correction when studying hydrogen bond dissociation in phenolic compounds, such as phenol and catechol.

Publisher's Note

Acknowledgements

Authors thank to Rizka Nur Fadilla (Universitas Airlangga, Indonesia) and Prof. Azizan Ahmad (University Kebangsaan Malaysia, Malaysia) for the insightful discussions. LSPB is grateful for the doctoral scholarship by Lembaga Pengelola Dana Pendidikan (LPDP). All calculations using Gaussian 16 software are performed at Riven Cluster, the high-performance computing facility in Research Center for Quantum Engineering Design, Universitas Airlangga, Indonesia.

Author Contributions

F.R. contributed to conceptualization; L.S.P.B, H.R., and I.P. contributed to formal analysis; L.S.P.B and V.K. were involved in investigation; F.R. and L.S.P.B contributed to methodology; I.P. provided the resources; L.S.P.B contributed to writing—original draft preparation; F.R. and H.K.D contributed to writing—review and editing. All authors have read and agreed to the published version of the manuscript.

Declarations

Funding This work was supported by Universitas Airlangga under grant scheme Riset Kolaborasi Mitra Luar Negeri 2019 no. 1148/UN3.14/LT/2019 and by Direktorat Riset dan Pengabdian Masyarakat, Deputi Bidang Penguatan Riset dan Pengembangan Kementerian Riset dan Teknologi/Badan Riset dan Inovasi Nasional, Republik Indonesia under grant scheme Penelitian Dasar Unggulan Perguruan Tinggi (PDUPT) 2020 no. 1288r/I1.C06/PL/2020.

Conflict of Interest The authors have no conflicts of interest to declare that are relevant to the content of this article.

Availability of Data and Materials All data analyzed during this study are included in this published article and its supplementary information file.

Code Availability Not Applicable.

Supplementary Information

Below is the link to the electronic supplementary material.

Supplementary file 1 (PDF 811kb)

References

1. Zielinski ZAM, Pratt DA (2017) J Org Chem 82(6):2817–2825

2. Yin H, Porter NA (2011) Chem Rev 111(10):5944–5972

3. Shang Y, Zhou H, Li X, Zhou J, Chen K (2019) New J Chem 43:15736–15742

4. Vo QV, Nam PC, Bay MV, Thong NM, Cuong ND, Mechler A (2018) Sci Rep 8:12361

5. Xue Y, Zheng Y, An L, Dou Y, Liu Y (2014) Food Chem 151:198–206

7. Galano A, Alvarez-Diduk R, Ramirez-Silva MT, Alarcon-Angeles G, Rojas-Hernandez A (2009) Chem Phys 363:13–23

8. Jovanovic SV, Steenken S, Boone CW, Simic MG (1999) J Am Chem Soc 121:9677–9681

9. Wang Y-N, Eriksson LA (2001) Theor Chem Acc 106:158–162

10. Mallick S, Sarkar S, Bandyopadhyay B, Kumar P (2018) J Phys Chem A 122(1):350–363

11. Kumar M, Sinha A, Francisco JS (2016) Acc Chem Res 49(5):877–883

12. Liang F, Zhong W, Xiang L, Mao L, Xu Q, Kirk SR, Yin D (2019) J Catal 378:256–269

13. Asgari P, Hua Y, Bokka A, Thiamsiri C, Prasitwatcharakorn W, Karedath A, Chen X, Sardar S, Yum K, Leem G, Pierce BS, Nam K, Gao J, Jeon J (2019) Nat Catal 2:164–173

14. Barckholtz C, Barckholtz TA, Hadad CM (1999) J Am Chem Soc 121(3):491–500

15. Wang L, Yang F, Zhao X, Li Y (2019) Food Chem 275:339–345

16. Nantasenamat C, Isarankura-Na-Ayudhya C, Naenna T, Prachayasittikul V (2008) J Mol Graph Model 27:188–196

17. Zhang H-Y, Sun Y-M, Wang X-L (2003) Chem Eur J 9:502–508

18. Brinck T, Lee H-N, Jonsson M (1999) J Phys Chem 103:7094–7104

19. Izgorodina EI, Coote ML, Radom L (2005) J Phys Chem A 109:7558–7566

20. Izgorodina EI, Brittain DRB, Hodgson JL, Krenske EH, Lin CY, Namazian M, Coote ML (2007) J Phys Chem A 111:10754–10768

21. Zhao Y, Truhlar DG (2008) J Phys Chem A 112:1095–1099

22. Beste A, Buchanan AC III (2009) J Org Chem 74(7):2837–2841

23. Zheng Y-Z, Fu Z-M, Deng G, Guo R, Chen D-F (2020) Phytochemistry 178:112454

24. Du T, Quina FH, Tunega D, Zhang J, Aquino AJA (2020) Theor Chem Acc 139:75

25. Yanai T, Tew DP, Handy NC (2004) Chem Phys Lett 393:51–57

26. Grimme S, Antony J, Ehrlich S, Krieg H (2010) J Chem Phys 132:154104

27. Becke AD (1993) J Chem Phys 98:5648

28. Zhao Y, Truhlar DG (2008) Theor Chem Acc 120:215–241

29. Rusydi F, Madinah R, Puspitasari I, Mark-Lee WF, Ahmad A, Rusydi A (2020). Biochem Mol Biol Educ. https://doi.org/10.1002/bmb.21433

30. Fadilla RN, Rusydi F, Aisyah ND, Khoirunisa V, Dipojono HK, Ahmad F, Mudasir, Puspitasari I (2020) Molecules 25: 670

31. Rusydi F, Aisyah ND, Fadilla RN, Dipojono HK, Ahmad F, Mudasir, Puspitasari I, Rusydi A (2019) Heliyon 5: e02409

32. Fadilla RN, Aisyah ND, Dipojono HK, Rusydi F (2017) Procedia Eng 170:113–118

33. Hohenberg P, Kohn W (1964) Phys Rev 136:B864

ham LJ (1965) Phys Rev 140:A1133

35. Frisch M J, Trucks G W, Schlegel H B,Scuseria G E, Robb M A, Cheeseman J R, Scalmani G, Barone V,Petersson G A, Nakatsuji H, Li X, Caricato M, Marenich A V,Bloino J, Janesko B G, Gomperts R, Mennucci B, Hratchian H P, Ortiz JV, Izmaylov A F, Sonnenberg J L, Williams-Young D,Ding F, Lipparini F, Egidi F, Goings J, Peng B, Petrone A,Henderson T, Ranasinghe D, Zakrzewski V G, Gao J, Rega N,Zheng , Liang W, Hada M, Ehara M, Toyota K, Fukuda R,Hasegawa J, Ishida M, Nakajima T, Honda Y, Kitao O, Nakai H,Vreven T, Throssell K, Montgomery J A, Jr., Peralta J E,Ogliaro F, Bearpark M J, Heyd J J, Brothers E N, Kudin K N, Staroverov VN, Keith T A, Kobayashi R, Normand J,Raghavachari K, Rendell A P, Burant JC, Iyengar S S, Tomasi J,Cossi M, Millam JM, Klene M, Adamo C, Cammi R,Ochterski J W, Martin R L, Morokuma K, Farkas O, Foresman J B, andFox D J (2013) Gaussian 16, Revision C.01, Gaussian, Inc.,Wallingford CT

36. Glendening ED, Reed AE, Carpenter JE, Weinhold F Nbo version 3.1

37. Mardirossian N, Head-Gordon M (2016) J Chem Theory Comput 12:4303–4325

38. Jones DB, da Silva GB, Neves RFC, Duque HV, Chiari L, de Oliveira EM, Lopes MCA, da Costa RF, Varella MTN, Bettega MHF, Lima MAP, Brunger MJ (2014) J Chem Phys 141:074314

39. Huber KP, Herzberg G (1979) Molecular spectra and moelcular structure IV constants of diatomic molecules. Springer, US, p 508

40. Young DC, Computational chemistry: A practical guide for applying techniques to real-world problems. Wiley, New York, 2001, Chp. 16, Page 138

41. Haynes WM (2014) CRC Handbook of Chemistry and Physics, 95th ed., CRC Press, Boca Rotan, Chp.9

42. Lucarini M, Pedulli GF, Guerra M (2004) Chem Eur J 10:933–939

43. Kamiya M, Tsuneda T, Hirao K (2002) J Chem Phys 117:6010

44. Parker K, Davis SR (1999) J Am Chem Soc 121:4271–4277

45. Zhu L, Bozzelli JW (2003) J Phys Chem A 107:3696–3703

46. Altarawneh M, Dlugogorski BZ, Kennedy EM, Mackie J (2010) J Phys Chem A 114:1060–1067

47. Chan B, Morris M, Radom L (2011) Aust J Chem 64:394–402

48. Peach MJG, Helgaker T, Salek P, Keal TW, Lutnæs OB, Tozer DJ, Handyd NC (2006) Phys Chem Chem Phys 8:558–562

Licence to Publish

SPRINGER NATURE

Journal Name:	Theoretical Chemistry Accounts	(the 'Journal')
Manuscript Number:	TCAC-D-20-00473R2	
Proposed Title of Article:	O—H and C—H bond dissociations in non-phenyl and phenyl groups: A DFT study with dispersion and long-range corrections	
Author(s) [Please list all named Authors]:	Febdian Rusydi, Lusia Silfia Pulo Boli, Vera Khoirunisa, Ira Puspitasari, Heni Rachmawati, Hermawan Kresno Dipojono	(the 'Author')
Corresponding Author Name:	Febdian Rusydi	

1 Publication

Springer-Verlag GmbH, DE (the 'Licensee') will consider publishing this article, including any supplementary information and graphic elements therein (e.g. illustrations, charts, moving images) (the 'Article').
Headings are for convenience only.

2 Grant of Rights

In consideration of the Licensee evaluating the Article for publication, the Author grants the Licensee the exclusive (except as set out in clauses 3, 4 and 5a) iv) and sub-licensable right, unlimited in time and territory, to copy-edit, reproduce, publish, distribute, transmit, make available and store the Article, including abstracts thereof, in all forms of media of expression now known or developed in the future, including pre- and reprints, translations, photographic reproductions and extensions.

Furthermore, to enable additional publishing services, such as promotion of the Article, the Author grants the Licensee the right to use the Article (including the use of any graphic elements on a stand-alone basis) in whole or in part in electronic form, such as for display in databases or data networks (e.g. the Internet), or for print or download to stationary or portable devices. This includes interactive and multimedia use as well as posting the Article in full or in part or its abstract on social media, and the right to alter the Article to the extent necessary for such use. The Licensee may also let third parties share the Article in full or in part or its abstract on social media and may in this context sub-license the Article and its abstract to social media users. Author grants to Licensee the right to re-license Article metadata without restriction (including but not limited to author name, title, abstract, citation, references, keywords and any additional information as determined by Licensee).

If the Article is rejected by the Licensee and not published, all rights under this agreement shall revert to the Author.

3 Self Archiving

Author is permitted to self-archive a preprint and the accepted manuscript version of their Article.

a) A preprint is the version of the Article before peer-review has taken place ("Preprint"). Prior to acceptance for publication, Author retains the right to make a Preprint of their Article available on any of the following: their own personal, self-maintained website; a legally compliant Preprint server such as but not limited to arXiv and bioRxiv. Once the Article has been published, the Author should update the acknowledgement and provide a link to the definitive version on the publisher's website: "This is a preprint of an article published in [insert journal title]. The final authenticated version is available online at: https://doi.org/[insert DOI]"

b) The accepted manuscript version, by industry standard called the "Author's Accepted Manuscript" ("AAM") is the version accepted for publication in a journal following peer review but prior to copyediting and typesetting that can be made available under the following conditions:
(i) Author retains the right to make an AAM of the Article available on their own personal, self-maintained website immediately on acceptance, (ii) Author retains the right to make an AAM of the Article available for public release on any of the following 12 months after first publication ("Embargo Period"): their employer's internal website; their institutional and/or funder repositories; AAMs may also be deposited in such repositories immediately on acceptance, provided that they are not made publicly available until after the Embargo Period.

An acknowledgement in the following form should be included, together with a link to the published version on the publisher's website: "This is a post-peer-review, pre-copyedit version of an article published in [insert journal title]. The final authenticated version is available online at:

http://dx.doi.org/[insert DOI]".

4 Reuse Rights

Author retains the following non-exclusive rights for the published version provided that, when reproducing the Article or extracts from it, the Author acknowledges and references first publication in the Journal according to current citation standards. In any event the acknowledgement should contain as a minimum, "First published in [Journal name, volume, page number, year] by Springer Nature".

a) to reuse graphic elements created by the Author and contained in the Article, in presentations and other works created by them;

b) the Author and any academic institution where they work at the time may reproduce the Article for the purpose of course teaching (but not for inclusion in course pack material for onward sale by libraries and institutions);

c) to reuse the published version of the Article or any part in a thesis written by the same Author , and to make a copy of that thesis available in a repository of the Author(s)' awarding academic institution, or other repository required by the awarding academic institution. An acknowledgement should be included in the citation: "Reproduced with permission from Springer Nature"; and

d) to reproduce, or to allow a third party to reproduce the Article, in whole or in part, in any other type of work (other than thesis) written by the Author for distribution by a publisher after an embargo period of 12 months.

5 Warranties & Representations

Author warrants and represents that:

a)

i. the Author is the sole copyright owner or has been authorised by any additional copyright owner(s) to grant the rights defined in clause 2,
ii. the Article does not infringe any intellectual property rights (including without limitation copyright, database rights or trade mark rights) or other third party rights and no licence from or payments to a third party are required to publish the Article,
iii. the Article has not been previously published or licensed,
iv. if the Article contains materials from other sources (e.g. illustrations, tables, text quotations), Author has obtained written permissions to the extent necessary from the copyright holder(s), to license to the Licensee the same rights as set out in clause 2 and has cited any such materials correctly;

b) all of the facts contained in the Article are according to the current body of research true and accurate;
c) nothing in the Article is obscene, defamatory, violates any right of privacy or publicity, infringes any other human, personal or other rights of any person or entity or is otherwise unlawful and that informed consent to publish has been obtained for all research participants;
d) nothing in the Article infringes any duty of confidentiality which Author might owe to anyone else or violates any contract, express or implied, of Author. All of the institutions in which work recorded in the Article was created or carried out have authorised and approved such research and publication; and
e) the signatory who has signed this agreement has full right, power and authority to enter into this agreement on behalf of all of the Authors.

6 Cooperation

a) Author shall cooperate fully with the Licensee in relation to any legal action that might arise from the publication of the Article, and the Author shall give the Licensee access at reasonable times to any relevant accounts, documents and records within the power or control of the Author. Author agrees that the distributing entity is intended to have the benefit of and shall have the right to enforce the terms of this agreement.
b) Author authorises the Licensee to take such steps as it considers necessary at its own expense in the Author's name(s) and on their behalf if the Licensee believes that a third party is infringing or is likely to infringe copyright in the Article including but not limited to initiating legal proceedings.

7 Author List

Changes of authorship, including, but not limited to, changes in the corresponding author or the sequence of authors, are not permitted after acceptance of a manuscript.

8 Corrections

Author agrees that the Licensee may retract the Article or publish a correction or other notice in relation to the Article if the Licensee considers in its reasonable opinion that such actions are appropriate from a legal, editorial or research integrity perspective.

9 Governing Law

This agreement shall be governed by, and shall be construed in accordance with, the laws of the Federal

Republic of Germany. The courts of Berlin, Germany shall have the exclusive jurisdiction.

Springer-Verlag GmbH, DE, Heidelberger Platz 3, 14197 Berlin, Germany
v.2.3 - (05_2021)-SVGmbH DE

Theoretical Chemistry Accounts (2021) 140:94
https://doi.org/10.1007/s00214-021-02781-6

REGULAR ARTICLE

O—H and C—H bond dissociations in non-phenyl and phenyl groups: A DFT study with dispersion and long-range corrections

Lusia Silfia Pulo Boli[2,3] · Febdian Rusydi[1,2] · Vera Khoirunisa[2,4] · Ira Puspitasari[2,5] · Heni Rachmawati[6,7] · Hermawan Kresno Dipojono[3]

Received: 28 December 2020 / Accepted: 15 May 2021

Abstract

Hydrogen atom transfer is one important reaction in biological system, in industry, and in atmosphere. The reaction is preluded by hydrogen bond dissociation. To gain a comprehensive understanding on the reaction, it is necessary to investigate how the current computational methods model hydrogen bond dissociation. As a starting point, we utilized density functional theory-based calculations to identify the effect of dispersion and long-range corrections on O—H and C—H dissociations in non-phenyl and phenyl groups. We employed five different methods, namely B3LYP, CAM-B3LYP (with long-range correction), M06-2X, and B3LYP and CAM-B3LYP with the D3 version of Grimme's dispersion. The results showed that for the case of O—H dissociation in two member of phenyl groups, namely phenol and catechol, the dispersion correction's effect was negligible, but the long-range correction's effect was significant. The significant effect was shown by the increasing of energy barrier and the shortening of O—H interatomic distance in the transition state. Therefore, we suggest one should consider the long-range correction in modeling hydrogen bond dissociation in phenolic compounds, namely phenol and catechol.

Keywords Density functional theory · Dispersion correction · Energy · Long-range correction · Non-phenyl and phenyl groups · O—H and C—H dissociations

1 Introduction

Hydrogen atom transfer is one important reaction that occurs in various environments: the biological systems, the atmosphere, and the industry. In biological systems, the reaction takes place in lipid peroxidation formation [1, 2] and its prevention, [3–8] as well as in free radicals formation [9]. In the atmosphere, the reaction involves hydroxyl radical (OH) and organic or inorganic materials [10, 11]. Meanwhile in industry, one way the reaction occurs is in the presence of a catalyst [12, 13]. Overall, the reaction has been a subject of experimental and computational studies. However, there is still a need to understand how the current computational methods can model hydrogen bond dissociation. This understanding will help to achieve a comprehensive insight into the hydrogen atom transfer reaction.

Numerous publications have reported the usage of computational methods based on density functional theory (DFT) to investigate hydrogen bond dissociation. One quantity describing the hydrogen bond dissociation is bond dissociation energy (BDE). In 1999, Barckholtz et al. reported the use of one DFT exchange-correlation (XC) functional,

✉ Febdian Rusydi
rusydi@fst.unair.ac.id

1 Department of Physics, Faculty of Science and Technology, Universitas Airlangga, Jl. Mulyorejo, Surabaya 60115, Indonesia

2 Research Center for Quantum Engineering Design, Faculty of Science and Technology, Universitas Airlangga, Jl. Mulyorejo, Surabaya 60115, Indonesia

3 Department of Engineering Physics, Faculty of Industrial Engineering, Institut Teknologi Bandung, Bandung 40132, Indonesia

4 Engineering Physics Study Program, Institut Teknologi Sumatera, Jl. Terusan Ryacudu, Lampung Selatan 35365, Indonesia

5 Information System Study Program, Faculty of Science and Technology, Universitas Airlangga, Jl. Mulyorejo, Surabaya 60115, Indonesia

6 School of Pharmacy, Institut Teknologi Bandung, Jl. Ganesha 10, Bandung 40132, Indonesia

7 Research Center for Nanoscience and Nanotechnology, Institut Teknologi Bandung, Jl. Ganesha 10, Bandung 40132, Indonesia

Published online: 21 June 2021

B3LYP, to predict C-H BDE of small aromatics. The predictions were in agreement with the available experimental values [14]. In the following years, the XC was used to predict the BDE of various bonds in small and large molecules [15–17]. On the other hand, other publications showed that B3LYP has low accuracy [18–20] but is reliable to predict the substituent effect such as in alkyl and peroxyl radicals [18]. In 2008, Zhao and Truhlar introduced XC from the Minnesota family, M06-2X. This XC has much-improved accuracy in predicting BDE [21]. M06-2X is reliable for various cases, such as predicting substituent effects on O-C and C-C BDE of lignin [22] and predicting BDE of polyphenols in various solvents [23]. The DFT used for the above prediction was unrestricted [15, 22]. In addition to B3LYP and M06-2X, Du et al. used CAM-B3LYP, which includes a long-range correction to B3LYP, in their calculations. They found that CAM-B3LYP underestimates O-CH3 BDE relative to experimental values. However, this XC has better performance for aromatic molecules than for non-aromatic molecules [24]. Even though many references have reported the use of various DFT XCs for predicting BDE, there is still limited references reported about the path taken by hydrogen atom during the bond dissociation. The use of XCs to model the path is necessary to gain insight into the hydrogen atom transfer reactions. Thus, the present work investigates the effect of dispersion and long-range corrections in O-H and C-H bond dissociations. The corrections have been integrated into DFT XCs. Therefore, it is necessary to use DFT to identify the effect of dispersion and long-range correction on O-H and C-H bond dissociations.

This work aims to study the effects of dispersion and long-range corrections on the O-H and C-H bond dissociations computationally. We utilize DFT with three functionals combined with the D3 version of Grimme's dispersion. The combination is five methods: B3LYP that has been used for chemical computation, CAM-B3LYP that includes a long-range correction, B3LYP-GD3 and CAM-B3LYP-GD3 which include Grimme's dispersion, and M06-2X that has a good performance for noncovalent interactions [25–28]. The dissociation is designed to occur at O-H and C-H bonds of six non-phenyl and three phenyl groups. The phenyl groups containing O-H bonds are chosen to represent the phenolic compounds. To achieve the goal, we calculate bond dissociation energy and build hydrogen bond dissociation pathways using two techniques: a relaxed scan calculation and a geometry optimization in the ground and transition states. We have used these two techniques to study other chemical reactions [29–32]. This study will answer the following question: What are the effects of the dispersion and long-range corrections on the O-H and C-H dissociations of non-phenyl and phenyl groups?

2 Computational models

2.1 Reaction model

Scheme 1 presents our model for the homolytic hydrogen bond dissociation. The reactant was R-H′ possessing O-H, or C-H, bond; the products were R· and a hydrogen atom (H′·). There were nine molecules of interest for R-H′, which were (a) hydroxyl, (b) methylidyne, (c) water, (d) methane, (e) methanol, (f) ethane, (g) toluene, (h) phenol, and (i) catechol.

$$\underset{\text{[in.]}}{R{-}H'} \longrightarrow \underset{\text{[fi.]}}{R^{\bullet}} + H'^{\bullet}$$

Scheme 1 The initial state [in.] and the final state [fi.] of the reaction model.

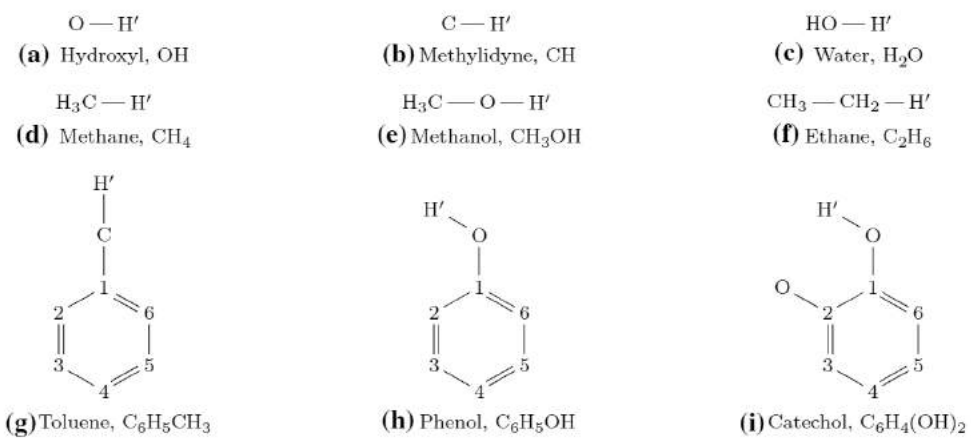

Fig. 1 Kekulé structures of the molecules of interest. The primed H was the dissociated hydrogen atom. For clarity in molecules (g)–(i), only dissociated hydrogen atom was shown, and carbon atoms were replaced by numbers

Table 1 List of methods used in the manuscript

M1	B3LYP
M2	B3LYP + GD3
M3	CAM-B3LYP
M4	CAM-B3LYP + GD3
M5	M06-2X

Figure 1 presents the Kekulé structures of these molecules.

2.2 DFT calculations

We performed computational techniques with the basis of DFT [33, 34]. We used 6-311++G(d,p) basis set with three different XCs; they were (1) B3LYP, (2) CAM-B3LYP, and (3) M06-2X which were implemented in Gaussian 16 software [35]. The first XC has become a standard functional for a geometry structure study, while the second XC has improved the long-range interaction of the first XC. The third XC has been parameterized, such that noncovalent interactions take into account. We applied the D3 version of Grimme's dispersion to accommodate the dispersion effect along the dissociation pathways. We combined the XCs and the dispersion into five different methods, as shown in Table 1. In addition to DFT, we used Natural Bond Orbital (NBO) calculations for the natural hybrid orbital and charge population analysis [36].

The procedure for DFT calculations is as follows. First, we validated that the three XCs were capable to obtain the spin-state and the geometry in the ground state. For this purpose, we chose hydroxyl and phenol because they represented molecules with odd and even number of electrons and because their experimental results were available. Second, we performed a geometry optimization to obtain the geometry of all molecules of interest in the ground state using the five calculation methods. To obtain BDE ($D°$) of hydrogen, we coupled DFT with frequency calculations. It resulted in the total electronic energy with thermal correction to enthalpy at 298.15 K in the ground state. $D°$ was the enthalpy difference between the final and the initial states in Scheme 1. Third, we constructed the hydrogen bond dissociation pathways.

We employed two different computational techniques for the third DFT calculations procedure. The first technique was a relaxed scan calculation, where one hydrogen atom (with prime mark in Figure 1) left oxygen or carbon atom of R· and let R· relaxed. The increments were set to be 0.2 Å for all methods. The second one was based on the geometry optimization in the ground and transition states. We applied the first technique to the selected non-phenyl and phenyl groups. The value of $D°$ that was affected and was not affected by dispersion and/or long-range corrections became the restriction in selecting molecules in the first technique. The first technique resulted in potential energy curve (PEC), and the dissociation pathway was visualized using a polar coordinate. We emphasized that the pathway that led to other than hydrogen bond dissociation would not be discussed further. The PEC that was affected by dispersion and/or long-range corrections became the restriction to select molecules in the second technique. The second technique yielded a dissociation pathway in energy level diagrams (ELD). We have successfully applied both techniques in our previous studies for bigger molecules [29–32].

We excluded PEC results from M06-2X in the current study because it produced unreasonable results. We also noted that Mardirossian and Head-Gordon [37] reported a similar case. They highlighted that M06-2X poorly predicted the bond length of krypton dimer and benzene-silane dimer through their potential energy curves. We listed the symbols and acronyms in Table 2 to assist readers in getting familiar with them.

3 Results and discussion

3.1 The ground state structures

Spin-state and geometry The geometry optimization using the three XCs obtained the doublet and singlet as the lowest in energy level for hydroxyl and phenol, respectively. On average, the doublet was 4.6 eV lower than the quartet (in hydroxyl), while the singlet was 4.2 eV lower than the triplet (in phenol). The doublet and the singlet were more stable compared to the quartet and the triplet. The results agree with the ground spin-states of hydroxyl and phenol reported in references [38, 39]. Furthermore, the selected geometrical parameters of hydroxyl and phenol in those spin-states were less than 0.017 Å and 1.4 degrees (see Table 3). The values were within the accuracy limit for DFT calculations [40].

Table 2 List of symbols and acronyms used throughout the manuscript

Symbol/acronym	Description
$D°$	Bond dissociation energy
r	Distances between atoms
BDE	Bond dissociation energy
DFT	Density functional theory
ELD	Energy level diagram
IS	Intermediate state
NBO	Natural Bond Orbital
PEC	Potential energy curve
TS	Transition state
XC	Exchange-correlation

Table 3 The discrepancy of calculated geometrical parameters of hydroxyl and phenol by (1) B3LYP, (2) CAM-B3LYP, and (3) M06-2X with respect to the experimental values [41]. The parameters were bond length (R, in Å) and bond angle (A, in degree). The parameter in (i) belongs to hydroxyl, while others belong to phenol

	Parameter	Expr.	(1)	(2)	(3)
(i)	R(O,H′)	0.970	+0.006	+0.005	+0.003
(ii)	R(O,H′)	0.956	+0.007	+0.005	+0.005
(iii)	R(C,C)av	1.397	− 0.003	− 0.009	-0.006
(iv)	R(1,O)	1.364	+0.006	0.000	− 0.001
(v)	R(4,H)	1.082	+0.001	+0.001	0.000
(vi)	R(5,H)	1.076	+0.008	+0.008	+0.008
(vii)	R(6,H)	1.084	+0.002	+0.001	+0.002
(viii)	A(1,O,H′)	109.0	+0.8	+1.0	+0.8

Therefore, the three XCs were capable to obtain the correct ground state structure of the molecules with odd or even number of electrons. Based on these results, the same XCs were used to obtain the ground spin-state of other molecules with an odd and even numbers of electrons which were doublet and singlet, respectively.

The dispersion and long-range corrections Table 4 presents O-H′ and C-H′ bond lengths of the obtained ground state geometry of all molecules of interest. The Cartesian coordinates of the ground state geometry were given in Table S1-S9 of Supplementary Information (SI). Calculation using the method with dispersion correction (M2 and M4) obtained the same bond length as the method without the correction (M1 and M3). The method with the long-range correction (M3) and the method parameterized with dispersion-like interaction (M5) obtained slightly shorter bond lengths (the negative values) than the method without the correction (M1). The results suggest the dispersion and the long-range corrections do not alter the ground state O-H′ and C-H′ bond lengths of our molecules of interest.

3.2 The bond dissociation energy

Table 5 presents the discrepancy of $D°$ between the calculated and experimental values. Among all methods, the M5 method obtained $D°$ the closest to the experimental values for molecules with singlet spin-state. The results supported the work of Zhao and Truhlar [21], which suggested using the M5 method for $D°$ calculations of molecules with singlet spin-state. Therefore, M06-2X functional is suitable for dealing with the hydrogen bond dissociation energy of molecules with singlet spin-state.

The discrepancies obtained by M2, M3, and M4 were varied compared to that obtained by M1. In all molecules

Table 4 The difference of calculated O-H′ and C-H′ bond lengths from M1 (Å). The label referred to Fig. 1

	Molecule	Bond	M1	M2	M3	M4	M5
(a)	Hydroxyl	O-H′	0.976	0.000	−0.002	−0.002	−0.004
(b)	Methylidyne	C-H′	1.127	0.000	−0.003	−0.003	−0.007
(c)	Water	O-H′	0.962	0.000	−0.001	−0.001	−0.003
(d)	Methane	C-H′	1.091	0.000	−0.001	−0.001	−0.002
(e)	Methanol	O-H′	0.961	0.000	−0.002	−0.002	−0.003
(f)	Ethane	C-H′	1.094	0.000	−0.001	−0.001	−0.002
(g)	Toluene	C-H′	1.094	0.000	−0.002	−0.002	−0.002
(h)	Phenol	O-H′	0.963	0.000	−0.002	−0.002	−0.002
(i)	Catechol	O-H′	0.962	0.000	−0.002	−0.002	−0.002

Table 5 The discrepancy of calculated $D°$ with respect to the experimental values (kJ/mol) [41, 42]. The label referred to Fig. 1

	Molecule	Bond	Expr.	M1	M2	M3	M4	M5
(a)	Hydroxyl	O-H′	429.73	−1.1	−1.1	−0.8	−0.8	−9.2
(b)	Methylidyne	C-H′	338.4	+1.8	+1.8	−2.2	−2.2	−8.1
(c)	Water	O-H′	497.32	−17.1	−17.1	−14.0	−14.0	−11.7
(d)	Methane	C-H′	439.3	−8.3	−8.2	−7.1	−7.0	−6.1
(e)	Methanol	O-H′	440.2	−26.4	−25.2	−21.1	−20.3	−11.5
(f)	Ethane	C-H′	420.5	−8.9	−7.6	−6.8	−6.0	−3.4
(g)	Toluene	C-H′	375.5	−10.8	−9.1	−5.8	−4.7	+2.9
(h)	Phenol	O-H′	362.8	−16.0	−14.6	−9.6	−8.6	+6.7
(i)	Catechol	O-H′	342.3	−32.0	−29.9	−24.0	−22.5	−9.8

[Table 5 (a)-(i)], M2 obtained 0.9 kJ/mol (in average) discrepancies higher than M1 did. Moreover, M4 obtained 0.6 kJ/mol (in average) discrepancies higher than M3 did. The results indicate that the dispersion correction does not alter the calculated $D°$ of molecules with singlet and doublet spin-states. In hydroxyl and methylidyne [Table 5 (a) and (b)], M3 obtained 1.9 kJ/mol (in average) discrepancies lower than M1 did. Meanwhile, in other molecules [Table 5 (c)-(i)], M3 obtained 4.4 kJ/mol (in average) discrepancies higher than M1 did. The 4.4 kJ/mol is significant, which implies that the long-range correction is the reason for $D°$ alteration of molecules with singlet spin-state. Thus, the long-range correction plays a role in altering $D°$ of molecules with singlet spin-state but not the molecules with doublet spin-state.

Among seven molecules in Table 5 (c)-(i), the alteration of discrepancies from M1 to M3 on O-H′ bonds differed from that on C-H′ bonds. The seven molecules were in their singlet spin-state. For four molecules with O-H′ bonds, the discrepancies increased by 5.7 kJ/mol (on average) from M1 to M3. However, for three molecules with C-H′ bonds, the discrepancies only increased by 2.8 kJ/mol (in average) from M1 to M3. The increase on O-H′ bonds is more significant than on C-H′ bonds. It indicates that the long-range correction alters the calculated $D°$ on O-H′ bond more than that on C-H′ bond of molecules with singlet spin-state.

The increase in the discrepancy on O-H′ bonds was not accompanied by bond length alteration but by O-H′ bond orbitals alteration. As discussed in Sect. 3.1, from M1 to M3, the ground state O-H′ bond length only altered by 0.002 Å. However, from M1 to M3, the O-H′ bond orbitals altered mainly in $(sp^{\lambda})_O$ hybrid orbitals (see Table S10 of the SI). According to the NBO calculations, the average percentage of alteration at $(sp^{\lambda})_O$ hybrid orbitals was 33 times more than that at $(sp^{\lambda})_C$ hybrid orbitals. Therefore, the long-range correction plays a role in altering the electron density in the O-H′ bond orbitals; hence the calculated $D°$ of O-H′ bond increases.

3.3 The potential energy curve

Figure 2 shows the PECs of four selected molecules together with their respective polar coordinates. All methods yielded two types of PEC profiles. The first type was a PEC-like of dissociation diatomic molecules [Fig. 2(a)–2(b) left]. Region I described the dissociation process, and region II described H′· was already a free atom. All methods agreed one to each other. The second type was somewhat challenging to explain since not all methods agreed [Fig. 2(c)–2(d) left]. There was region III that contained barriers. PEC profiles in methylidyne and ethane were supportive results to the first type, while PEC profiles in hydroxyl and water were supportive results to the second type. Hence, they were placed in Supporting Information [Figure S1(a)–(b) and S1(c)–(d) left]. On the other hand, the polar coordinates show that the hydrogen bond dissociation pathways in methane [Fig. 2(a) right] are different from those in other molecules [Fig. 2(b)–2(d) right and Figure S1(c)–(d) right of the SI]. All methods were only agreed for methane. It implies that the corrections (long-range and dispersion) significantly affect the pathway in real space rather than in the PEC profile.

Overall, the PEC profiles of methanol and phenol [Fig. 2(c)–2(d) left] were explained as follows. In region III, methanol and phenol had barriers; methanol had one, and phenol had at least three barriers. In both cases, M2 yielded a similar barrier height to M1 did. So did M4 and M3. It means the dispersion correction does not alter the PEC profile of O-H′ dissociation. However, in both cases, M3 yielded a different barrier height than M1 did. The results indicate that the long-range correction does alter the PEC profile of O-H′ dissociation. Therefore, the long-range correction plays a more significant role than the dispersion correction in the PEC profiles of O-H′ dissociation.

In detail, for phenol [Fig. 2(d)], the variation of PEC profiles was accompanied by the variation of dissociation pathways in the polar coordinate. Both variations occurred only at a certain O-H′ distance ($r_{O–H'}$) range. The PEC profile variation range was around 1.8–3 Å; while the pathway variation range was around 2–4 Å. In those ranges, M3 yielded a different profile and pathway than M1 did. Kamiya et al. [43] also obtained different profiles when using XCs with long-range correction in a system interacting through a van der Waals interaction (noncovalent interaction). Thus, the different profiles obtained by the long-range correction (M3) may be due to the presence of noncovalent interactions, particularly at a region with barriers. Therefore, in line with its role in O-H′ BDE, the long-range correction may play a role in the energy barrier of O-H′ dissociation.

Along the phenol dissociation pathway, M1 and M3 obtained different r at B1a, B1b, and B2 (See Table S11 of the SI). At B1a and B1b, atom H′· was located around atom O [See Figure S2 of the SI]. Here, M3 obtained shorter $r_{O–H'}$ at B1a than M1 did at B1b. Different than at B1a and B1b, at B2 atom H′· was located between atom 2 and atom 3. Here, M3 obtained shorter $r_{2–H'}$ and longer $r_{3–H'}$ than M1 did. The results indicate that the shortening and lengthening of r are due to the long-range correction.

The r alteration after the introduction of long-range correction was accompanied by atomic charges alteration. The NBO calculations showed that atom O, 2, and 3 [See Fig. 1(h)] were negatively charged while atom H′· was positively charged. At B1a, M3 yielded greater positive charge on atom H′· and greater negative charge on atom O than M1 did. It implies that the increasing coulombic attraction between atom O and H′· is the reason for the shortening of $r_{O–H'}$ at B1a. At B2, M3 obtained lesser positive charge on

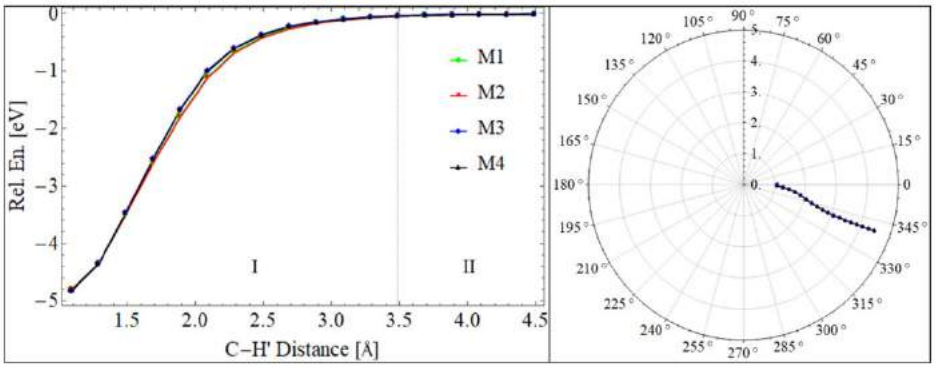

(a) PEC (left) and polar coordinate (right) of methane.

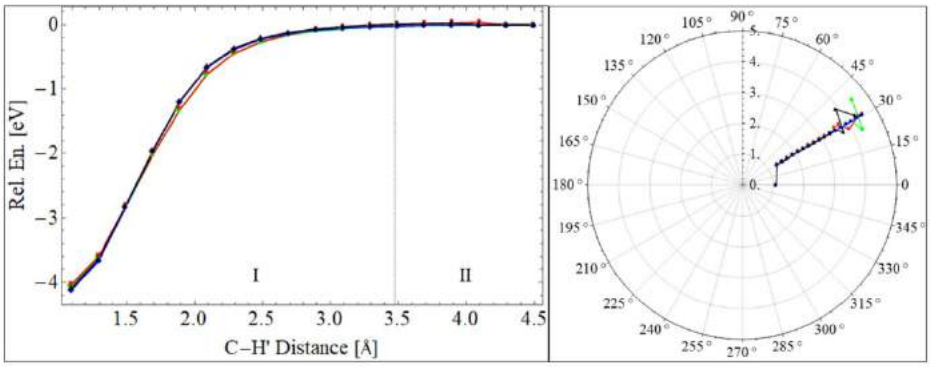

(b) PEC (left) and polar coordinate (right) of toluene.

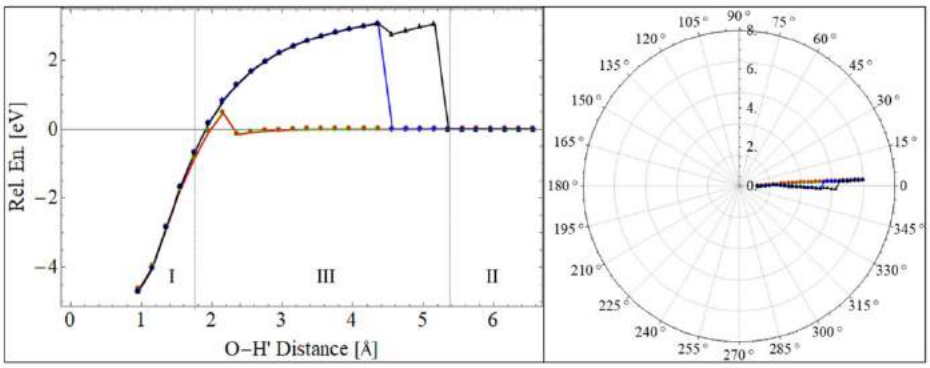

(c) PEC (left) and polar coordinate (right) of methanol.

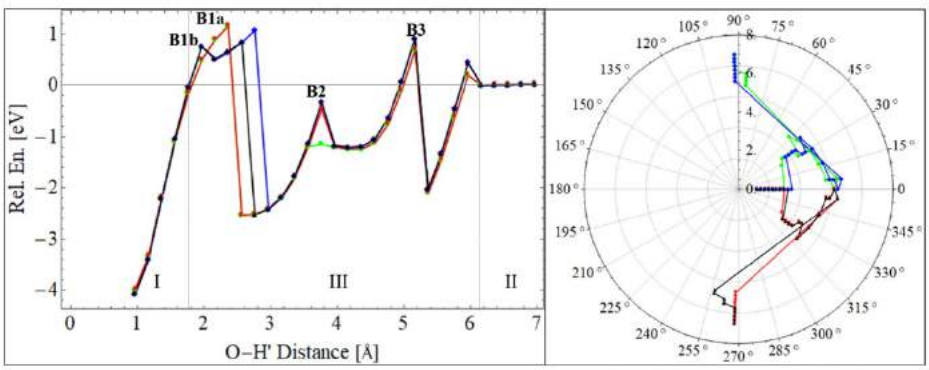

(d) PEC (left) and polar coordinate (right) of phenol.

Fig. 2 PECs of C-H′ and O-H′ bond dissociations with their respective polar coordinates. The I, II, and III represented three different regions based on the similarity of events at each region. Angles in the polar coordinate were H-C-H′ in methane, 2–1–C-H′ in toluene, H-C-O-H′ in methanol, and 2–1–O-H′ in phenol (see Fig. 1). The initial angle was at zero degree, then deviated clockwise or counterclockwise. Particularly in methane, the clockwise represented inward deviation. **B1a**, **B1b**, **B2**, and **B3** in (d) represented first barrier obtained by M1 and M2, first barrier obtained by M3 and M4, second and third barrier obtained by all four methods, respectively

atom H′ and greater negative charge on atom 2 than M1 did. It indicates that the increasing coulombic attraction between atom 2 and H′ is the reason for the shortening of the $r_{2-H'}$. At this location, M3 obtained lesser negative charge on atom 3 than M1 did. It implies the increasing coulombic repulsion between atom 3 and H′ is the reason for the lengthening of the $r_{3-H'}$. Therefore, the Coulombic interactions play a role in the alteration of r.

3.4 The dissociation pathway

Figure 3 shows the O-H′ dissociation pathways of two selected molecules, phenol and catechol, in an ELD. For the case of phenol [Fig. 3(a)], each pathway had three transition states (TS) and three intermediate states (IS) as predicted earlier in Fig. 2(d)left; while for the case of catechol [Fig. 3(b)], each pathway had two TSs and two ISs. The experiment has observed the presence of IS1 in a photochemical reaction [44]. While a theoretical study reported IS1 and IS3 as two isomers of phenol [45]. Another theoretical study reported the first step in decomposition of catechol lead to IS4 [46]. The similarity between the molecules in the intermediate states with the previous studies indicates the possibility of hydrogen migration before O-H′ dissociation occurred.

The dissociation pathways in phenol and catechol showed that all methods obtained the same relative electronic energy order in each TS. The order for both cases was M1 ≈ M2 < M3 ≈ M4 < M5. For the case of phenol, the average difference between the energy obtained by methods with long-range correction (M3 and M4) and methods without the correction (M1 and M2) was 0.16 eV. Similarly, for the case of catechol, the average difference was 0.14 eV. The differences are significant. It was aligned with the PEC profile difference [Fig. 2(d)left] after the long-range correction

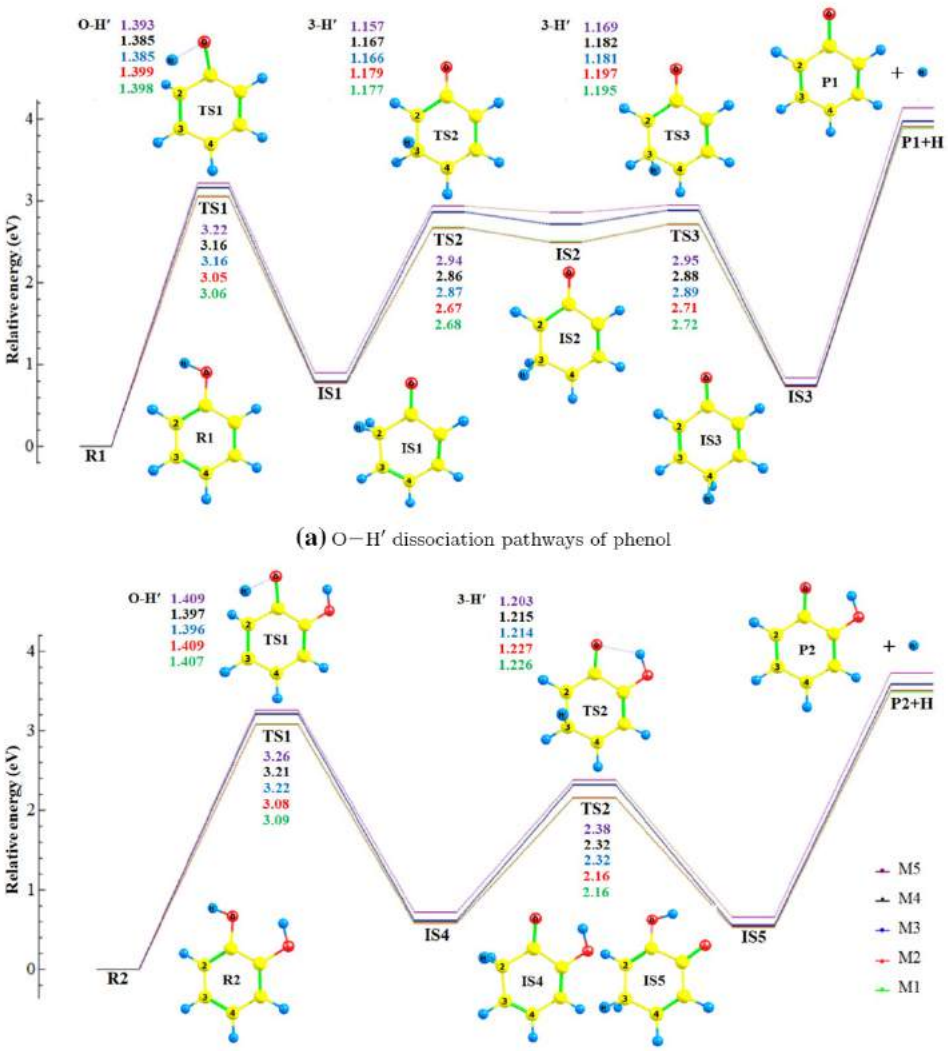

Fig. 3 Energy level diagram for O-H′ dissociation pathways of two selected molecules. R1, R2, P1, and P2 represent phenol, catechol, product of phenol dissociation, and product of catechol dissociation. While TS and IS stand for transition state and intermediate state. The TSs were shown with the selected interatomic distances (unit in Å)

was introduced, particularly at the region with barriers. The results imply that the long-range correction predicts the dissociation is more difficult at a region where the noncovalent interaction may be present. Therefore, the correction indeed plays a role in the energy barrier of O-H′ dissociation.

Methods with long-range correction (M3 and M4) obtained shorter r than methods without the correction did in the TS structures. For the case of phenol, the $r_{O-H'}$ and $r_{3-H'}$ shortened by 0.01 Å on average. The shortening was also similar to the case of catechol. The 0.01 Å is significant compared to the O-H′ bond length shortening in the ground state of phenol and catechol [Table 4(h) and (i)]. Thus, the shortening confirms the shortening of r along the dissociation pathway discussed in Subsection 3.3. For this reason, the long-range correction indeed plays a role in r in the transition state.

Methods with the long-range correction (M3 and M4) obtained similar relative electronic energy to M5 did in the TSs. The average differences of relative electronic energy obtained by those methods were 0.07 for phenol and 0.06 for catechol. These values are very small which indicate the similarity of transition state according to those methods. Therefore, CAM-B3LYP and M06-2X predict comparable transition state of O-H′ dissociation.

Overall, all methods showed consistent performances on the BDE calculations and O-H′ dissociation pathways prediction. For the BDE calculations, the methods obtained the $D°$ of O-H′ bonds in all molecules increased in the following order: M1 ≈ M2 < M3 ≈ M4 < M5. The increase of $D°$ after the presence of long-range correction in CAM-B3LYP (M3) was in agreement with the study by Chan et al. [47] For the pathways prediction, the methods obtained variation of pathways in phenol and catechol dissociation. The variations were identified by the alteration in energy barriers and $r_{O-H'}$ in the TS. The energy barrier increased in the same order as the increase in $D°$ of O-H′ bonds. This result validates the study by Peach et al. [48] that showed increasing barrier height when using CAM-B3LYP compared to B3LYP. The increasing energy barriers was accompanied by the shortening of $r_{O-H'}$ as follows: M1 ≈ M2 > M3 ≈ M4. The shortening due to the long-range correction (M3) was in agreement with our previous study [31]. The results show the significance of this research: the use of long-range correction in CAM-B3LYP affects the $r_{O-H'}$ in TS. On the other hand, the M06-2X used in this study predicted the highest $D°$ and energy barrier. The $D°$ was similar to the experimental observation. Its developer suggested the functional for applications involving main group thermochemistry, kinetics, and noncovalent interactions [21, 28].

4 Conclusion

We have studied the effects of dispersion and long-range corrections on O-H and C-H dissociations of non-phenyl and phenyl groups. The effects were identified through bond dissociation energy and dissociation pathways. We summarized that the dispersion correction had negligible effects on the O-H and C-H bond dissociation energies and the non-phenyl and phenyl groups dissociation pathways. While the long-range correction in CAM-B3LYP had a minor effect on the O-H bond dissociation energy and a significant effect on the O-H dissociation pathways. We found that the long-range correction increased the bond dissociation energy of the O-H bond of non-phenyl and phenyl groups in their singlet states by 5.7 kJ/mol. We argued that the increase was due to the alteration of electron density in the O-H bond orbitals. However, the dissociation energy was still far from the experimental results. The significant effects of the long-range correction on the O-H dissociation pathways occurred in two members of phenyl groups, namely phenol and catechol. The effects were identified as follows. First, the correction shortened the O-H distances in the transition states by 0.01 Å, on average. Second, the correction increased the energy barrier by 0.16 eV (in phenol) and 0.14 eV (in catechol), on average. Overall, our results support other theoretical studies on the increasing energy barrier due to the long-range correction. Accordingly, we suggest that one should consider the long-range correction when studying hydrogen bond dissociation in phenolic compounds, such as phenol and catechol.

Supplementary Information The online version contains supplementary material available at https://doi.org/10.1007/s00214-021-02781-6.

Acknowledgements Authors thank to Rizka Nur Fadilla (Universitas Airlangga, Indonesia) and Prof. Azizan Ahmad (University Kebangsaan Malaysia, Malaysia) for the insightful discussions. LSPB is grateful for the doctoral scholarship by Lembaga Pengelola Dana Pendidikan (LPDP). All calculations using Gaussian 16 software are performed at Riven Cluster, the high-performance computing facility in Research Center for Quantum Engineering Design, Universitas Airlangga, Indonesia.

Author Contributions F.R. contributed to conceptualization; L.S.P.B, H.R., and I.P. contributed to formal analysis; L.S.P.B and V.K. were involved in investigation; F.R. and L.S.P.B contributed to methodology; I.P. provided the resources; L.S.P.B contributed to writing—original draft preparation; F.R. and H.K.D contributed to writing—review and editing. All authors have read and agreed to the published version of the manuscript.

Declarations

Funding This work was supported by Universitas Airlangga under grant scheme Riset Kolaborasi Mitra Luar Negeri 2019 no. 1148/UN3.14/LT/2019 and by Direktorat Riset dan Pengabdian Masyarakat, Deputi Bidang Penguatan Riset dan Pengembangan Kementerian Riset dan Teknologi/Badan Riset dan Inovasi Nasional, Republik Indone-

sia under grant scheme Penelitian Dasar Unggulan Perguruan Tinggi (PDUPT) 2020 no. 1288r/I1.C06/PL/2020.

Conflict of Interest The authors have no conflicts of interest to declare that are relevant to the content of this article.

Availability of Data and Materials All data analyzed during this study are included in this published article and its supplementary information file.

Code Availability Not Applicable.

References

1. Zielinski ZAM, Pratt DA (2017) J Org Chem 82(6):2817–2825
2. Yin H, Porter NA (2011) Chem Rev 111(10):5944–5972
3. Shang Y, Zhou H, Li X, Zhou J, Chen K (2019) New J Chem 43:15736–15742
4. Vo QV, Nam PC, Bay MV, Thong NM, Cuong ND, Mechler A (2018) Sci Rep 8:12361
5. Xue Y, Zheng Y, An L, Dou Y, Liu Y (2014) Food Chem 151:198–206
6. Iuga C, Alvarez-Idaboy JR, Russo N (2012) J Org Chem 12:3868–3877
7. Galano A, Alvarez-Diduk R, Ramirez-Silva MT, Alarcon-Angeles G, Rojas-Hernandez A (2009) Chem Phys 363:13–23
8. Jovanovic SV, Steenken S, Boone CW, Simic MG (1999) J Am Chem Soc 121:9677–9681
9. Wang Y-N, Eriksson LA (2001) Theor Chem Acc 106:158–162
10. Mallick S, Sarkar S, Bandyopadhyay B, Kumar P (2018) J Phys Chem A 122(1):350–363
11. Kumar M, Sinha A, Francisco JS (2016) Acc Chem Res 49(5):877–883
12. Liang F, Zhong W, Xiang L, Mao L, Xu Q, Kirk SR, Yin D (2019) J Catal 378:256–269
13. Asgari P, Hua Y, Bokka A, Thiamsiri C, Prasitwatcharakorn W, Karedath A, Chen X, Sardar S, Yum K, Leem G, Pierce BS, Nam K, Gao J, Jeon J (2019) Nat Catal 2:164–173
14. Barckholtz C, Barckholtz TA, Hadad CM (1999) J Am Chem Soc 121(3):491–500
15. Wang L, Yang F, Zhao X, Li Y (2019) Food Chem 275:339–345
16. Nantasenamat C, Isarankura-Na-Ayudhya C, Naenna T, Prachayasittikul V (2008) J Mol Graph Model 27:188–196
17. Zhang H-Y, Sun Y-M, Wang X-L (2003) Chem Eur J 9:502–508
18. Brinck T, Lee H-N, Jonsson M (1999) J Phys Chem 103:7094–7104
19. Izgorodina EI, Coote ML, Radom L (2005) J Phys Chem A 109:7558–7566
20. Izgorodina EI, Brittain DRB, Hodgson JL, Krenske EH, Lin CY, Namazian M, Coote ML (2007) J Phys Chem A 111:10754–10768
21. Zhao Y, Truhlar DG (2008) J Phys Chem A 112:1095–1099
22. Beste A, Buchanan AC III (2009) J Org Chem 74(7):2837–2841
23. Zheng Y-Z, Fu Z-M, Deng G, Guo R, Chen D-F (2020) Phytochemistry 178:112454
24. Du T, Quina FH, Tunega D, Zhang J, Aquino AJA (2020) Theor Chem Acc 139:75
25. Yanai T, Tew DP, Handy NC (2004) Chem Phys Lett 393:51–57
26. Grimme S, Antony J, Ehrlich S, Krieg H (2010) J Chem Phys 132:154104
27. Becke AD (1993) J Chem Phys 98:5648
28. Zhao Y, Truhlar DG (2008) Theor Chem Acc 120:215–241
29. Rusydi F, Madinah R, Puspitasari I, Mark-Lee WF, Ahmad A, Rusydi A (2020). Biochem Mol Biol Educ. https://doi.org/10.1002/bmb.21433
30. Fadilla RN, Rusydi F, Aisyah ND, Khoirunisa V, Dipojono HK, Ahmad F, Mudasir, Puspitasari I (2020) Molecules 25: 670
31. Rusydi F, Aisyah ND, Fadilla RN, Dipojono HK, Ahmad F, Mudasir, Puspitasari I, Rusydi A (2019) Heliyon 5: e02409
32. Fadilla RN, Aisyah ND, Dipojono HK, Rusydi F (2017) Procedia Eng 170:113–118
33. Hohenberg P, Kohn W (1964) Phys Rev 136:B864
34. Kohn W, Sham LJ (1965) Phys Rev 140:A1133
35. Frisch MJ, Trucks GW, Schlegel HB,Scuseria GE, Robb MA, Cheeseman JR, Scalmani G, Barone V,Petersson GA, Nakatsuji H, Li X, Caricato M, Marenich AV,Bloino J, Janesko BG, Gomperts R, Mennucci B, Hratchian HP, Ortiz JV, Izmaylov AF, Sonnenberg JL, Williams-Young D,Ding F, Lipparini F, Egidi F, Goings J, Peng B, Petrone A,Henderson T, Ranasinghe D, Zakrzewski VG, Gao J, Rega N, Zheng, Liang W, Hada M, Ehara M, Toyota K, Fukuda R,Hasegawa J, Ishida M, Nakajima T, Honda Y, Kitao O, Nakai H,Vreven T, Throssell K, Montgomery JA, Jr., Peralta J E,Ogliaro F, Bearpark MJ, Heyd JJ, Brothers EN, Kudin K N, Staroverov VN, Keith TA, Kobayashi R, Normand J, Raghavachari K, Rendell AP, Burant JC, Iyengar SS, Tomasi J, Cossi M, Millam JM, Klene M, Adamo C, Cammi R, Ochterski JW, Martin RL, Morokuma K, Farkas O, Foresman JB, Fox DJ (2013) Gaussian 16, Revision C.01, Gaussian, Inc., Wallingford CT
36. Glendening ED, Reed AE, Carpenter JE, Weinhold F Nbo version 3.1
37. Mardirossian N, Head-Gordon M (2016) J Chem Theory Comput 12:4303–4325
38. Jones DB, da Silva GB, Neves RFC, Duque HV, Chiari L, de Oliveira EM, Lopes MCA, da Costa RF, Varella MTN, Bettega MHF, Lima MAP, Brunger MJ (2014) J Chem Phys 141:074314
39. Huber KP, Herzberg G (1979) Molecular spectra and moelcular structure IV constants of diatomic molecules. Springer, US, p 508
40. Young DC, Computational chemistry: A practical guide for applying techniques to real-world problems. Wiley, New York, 2001, Chp. 16, Page 138
41. Haynes WM (2014) CRC Handbook of Chemistry and Physics, 95th ed., CRC Press, Boca Rotan, Chp.9
42. Lucarini M, Pedulli GF, Guerra M (2004) Chem Eur J 10:933–939
43. Kamiya M, Tsuneda T, Hirao K (2002) J Chem Phys 117:6010
44. Parker K, Davis SR (1999) J Am Chem Soc 121:4271–4277
45. Zhu L, Bozzelli JW (2003) J Phys Chem A 107:3696–3703
46. Altarawneh M, Dlugogorski BZ, Kennedy EM, Mackie J (2010) J Phys Chem A 114:1060–1067
47. Chan B, Morris M, Radom L (2011) Aust J Chem 64:394–402
48. Peach MJG, Helgaker T, Salek P, Keal TW, Lutnæs OB, Tozer DJ, Handyd NC (2006) Phys Chem Chem Phys 8:558–562